HAWAII'S FLOATING CITY

DEVELOPMENT PROGRAM

THEORETICAL INVESTIGATIONS AND OPTIMIZATION OF THE PLATFORM'S SEAKEEPING CHARACTERISTICS

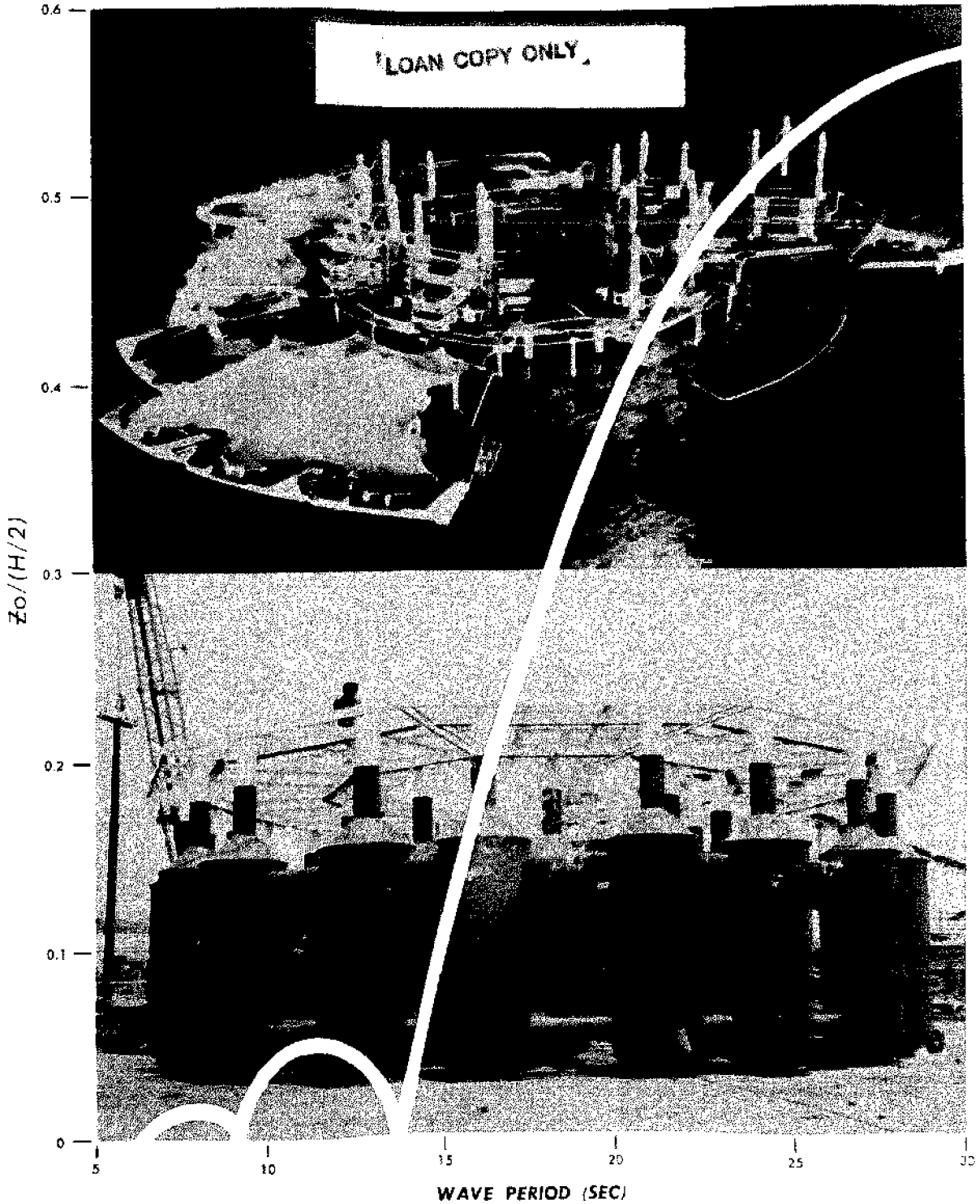

UNIHI - Sea Grant - CR-73-01

HAWAII'S FLOATING CITY

DEVELOPMENT PROGRAM

Technical Report No. 2

Theoretical Investigations and Optimization of the Platform's Seakeeping Characteristics

by

Ludwig H. Seidl, Ph.D.
Department of Ocean Engineering
University of Hawaii

May, 1973

for

National Sea Grant Program
National Oceanic and Atmospheric Administration
U.S. Department of Commerce
Rockville, Maryland 20852

Principal Investigators:

John P. Craven
Dean, Marine Programs
University of Hawaii

Joe A. Hanson
Chief Scientist
System Sciences Division
Oceanic Institute

This work is a result of research sponsored by NOAA Office of Sea Grant, Department of Commerce, under Grant #2-35245. The U.S. Government is authorized to produce and distribute reprints for governmental purposes notwithstanding any copyright notation that may appear hereon.

ACKNOWLEDGEMENTS

Dr. Ludwig H. Seidl, Associate Professor of Ocean Engineering, accomplished the research described herein under contract to the Oceanic Institute. Dr. Seidl is, of course, also the author of this volume. He was assisted in the research by James M. Smith

ABSTRACT

This report of Hawaii's Floating City preliminary engineering work presents the methods and findings of the initial theoretical investigations of the floating platform's seakeeping characteristics. It also provides recommendations for design refinements that will minimize platform motions and acceleration forces in the seaways expected to prevail at the proposed installation site.

Since single column heave response is of high importance, this facet is explored in detail first. Then equations of motion in six degrees of freedom are developed for a 3-column single module of the ten-module core-ring of the city and finally for the 30-column core-ring in its entirety. These equations have been expressed in FORTRAN IV and mathematical simulations for various configurations in regular and irregular seas run on an IBM 360/65 computer.

TABLE OF CONTENTS

I.	INTRODUCTION	1
II.	ENVIRONMENT	3
	A. Winds	3
	B. Currents	4
	C. Waves	4
III.	METHOD	4
IV.	SINGLE COLUMN INVESTIGATIONS	5
	A. Fundamental Equations of Motion	6
	B. Non-faired (Two Cylinder) Column Configuration	8
	C. Faired Column Configuration	18
	D. Faired Column Configuration with Connecting Cylinders	22
	E. Faired Configuration with Connecting Cylinders and Bottom Flange	26
	F. Variations of Draft	30
	G. Artificially Induced Added Mass	30
V.	MODULE	36
	A. Hydrostatics	36
	B. Response Operators in Six Degrees of Freedom	39
VI.	CORE-RING	51
	A. Hydrostatics	51
	B. Response Operators	61
	C. Response Operators for Existing Configuration	61
	D. Response Operators for Alternate Column Configuration	65
	E. Motions in Irregular Seas	71
	1. Ocean Wave Spectra	71
	2. Statistical Analysis	73
	3. Results	74

F. Limits of Perceptibility of Motion 85
G. Response Operators for the 1:20 Scale Model 89

VII. FINDINGS AND CONCLUSIONS 99

VIII. RECOMMENDATIONS FOR FUTURE RESEARCH 99

I. INTRODUCTION

During the spring and summer of 1971 a Hawaii State supported committee composed of architects, engineers, biologists and behavioral scientists derived the basic configuration of Hawaii's Floating City. The concept and its derivation are discussed in the First Annual Report of the program, August 31, 1972. The underbody configuration of this platform is essentially a rigidly interconnected cluster of spar buoys which we term "columns" supporting both a deck structure and moderate-height, multi-story buildings. This basic configuration is represented by the photograph of the 1:20 scale model of the core-ring of the city shown in Figure 1. The relationship of the waterborne 1:20 scale model to the air/sea interface is shown in Figure 2.

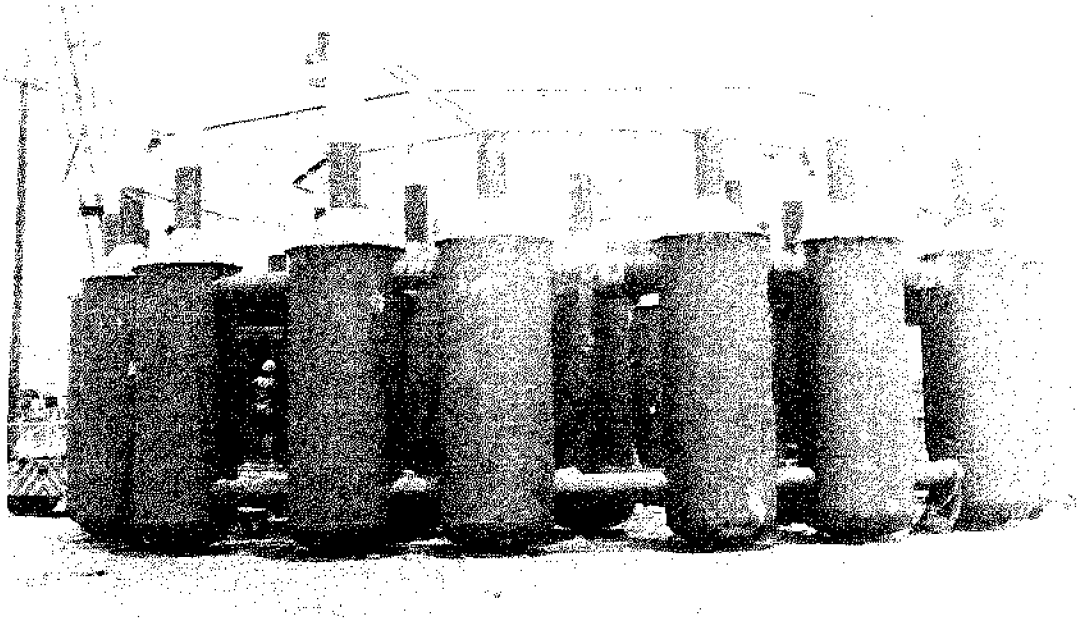

Fig. 1 1:20 scale model of the ten-module core-ring of Hawaii's proposed Floating City

This investigation has accepted the spar buoy cluster concept as a hypothesis. The task, then, is to determine the feasibility of this approach as well as to optimize it for maximum stability, economy, and safety in the winds, waves, and currents expected to prevail at the proposed installation site approximately three to five miles off the leeward shore of the island of

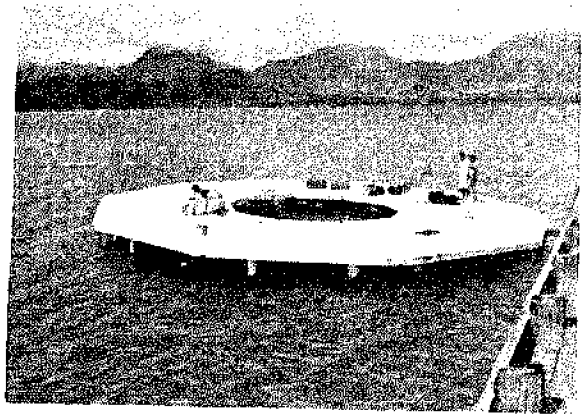

Fig. 2 The 1:20 scale model afloat at design water line (DWL) in Kaneohe Bay, Hawaii

Oahu. Thus, this theoretical investigation restricts its scope to the feasibility and optimization of the underbody design for the seaways to be expected at that site[1].

Some observations seem appropriate at this point. First, the design concept considered here lies somewhere between that of the single spar buoy and the mobile, semi-submersible platform employed in many modern off-shore drilling rigs. Second, the requirement for underbody drag reduction in the platform under investigation is much less severe than with the mobile oil rig for, while Hawaii's floating city must combat moderate currents and move short distances at times, it will not be necessary to propel it over long distances within economic time and fuel consumption limits. Third, motion and acceleration minimization are of prime importance if the city is to be a pleasant habitat for a wide variety of humans. Fourth, though we must eventually explore the theoretical behavior of the platform in various damaged conditions, time and resource limitations restricted the Phase I theoretical investigations to the intact condition of the core-ring only. Lastly, one must recognize that the theoretical tools available today are at best imprecise in their ability to define real platform motions in real complex wave trains. Therefore, confidence in theoretical results can only be achieved by calibrating them with full-sized or scaled empirical results. For this project, such calibrations will be obtained through the 1:150 and 1:20 scale model tests to be described in Technical Report No. 3, along with the test results and comparison with theoretical results.

With the above in mind, the following problem statement is offered: "Given the basic spar buoy cluster configuration of the city underbody, derive the optimum configuration. This platform must provide a high degree of stability in expected seaways and its buoyancy requirement is to be determined by the sum of fixed and live weight of the whole city. Intact

---

[1]See Technical Report No. 1 by M. St. Denise for a full treatment of the winds, waves, and currents to be expected at the installation site.

stability requirements are defined by criteria limiting the maximum static angle of heel due to wind and current loads, as well as off-center weights and forces. Furthermore, vertical, lateral, and rotational displacements and accelerations must remain within limits which will insure human comfort at any location in the city and, of course, must not exceed the limits for structural integrity of buildings above the main deck. Maximum allowable acceleration, then, is set at 0.015 g in any direction at any point in the structure."

This problem was attacked as described below. Numerical calculations were accomplished on an IBM Model 360-65 computer. FORTRAN IV was the program compilation language employed. Computer program documentation and program listings are available from the Oceanic Institute.

II. ENVIRONMENT

The city is to be located three to five miles off the leeward shore of the island of Oahu in the Hawaiian Archipelago in approximately 600 meters of water. Latitude and longitude are 21° 15' N and 157° 50' W respectively. Trade winds prevail much of each year but are broken by periods of calm and southerly "Kona" winds. Tropical storms and hurricanes are infrequent and of short duration. Currents in this area appear to be tide-dominated and so show strong directional reversals. Long period swells enter the area from a northerly direction in winter and from a southerly direction in summer. The northerly swells are frequently refracted around Oahu. Shorter period waves of considerable size are, of course, generated by storm conditions. The following summary defines the environmental conditions to which the design is directed. Technical Report No. 1, in which these data are developed, emphasizes that no long term recordings have been conducted at the site itself. Therefore, all data are extrapolated from the nearest appropriate site of recordation to the proposed floating city site.

A. Winds

Technical Report No. 1 divides the wind question into trade and "Kona" winds on the one hand and cyclonic storm winds on the other.

1. Trade and Kona Winds

The highest mean wind intensity recorded is 22-27 knots and occurs a total of only 1.3% of the year. Short term peak intensities are defined as the greatest one minute averages recorded over a reference period

of one month. The highest value recorded is 53 knots. Finally, peak gust intensity recorded at Honolulu International Airport (in 1959) was 58 knots.

Long term trend of mean wind intensity corresponding to a 100 year return period has been set at 39 knots with a 50% probability that the figure will be exceeded. The long term trend of peak wind intensity with the same conditions has been set at 62 knots. A gross estimate of the long term trend of gust intensity is 68 knots.

2. Kona Storms and Tropical Cyclones

The peak expected instantaneous value is approximately 125 knots and peak sustained value is approximately 80 knots.

B. Currents

Coupling of the wind, tide and global circulation components of the highly complex current patterns observed in nearby areas yields an expectation of maximum surface current velocity in the realm of 175 cm/sec with a 100 year return period. The tidal component appears to be nearly 60% of the total, so directions as well as velocities may be expected to vary with depth.

C. Waves

The figures derived in Technical Report No. 1 lead to an expectation that the floating city will be exposed to waves having a significant height of 4-12 ft and a period of 5-8 sec for 90-95% of the time during the summer months. Waves of the same sort will prevail slightly more than half the time during the winter months and will be interspersed with some dominance of 1-4 ft southern swells with periods ranging from 14-22 sec as well as Kona storm waves of 10-15 ft having periods of 8-10 sec about 10% of the time during the winter.

Infrequent wave height maxima are taken to be approximately 50 ft with periods in the realm of 16 sec. These figures are based on a 1000 year return period and, of course, would occur only during intense cyclonic activity.

III. METHOD

The core-ring platform which is the object of this investigation is a radially symmetrical ring of identical floating support columns which are essentially spar buoys. There are ten columns equally spaced in the inner ring

and twenty arranged in equidistant pairs in the outer ring. All columns are connected at their tops by a rigid deck and at the upper and lower extremities of their maximum dimensions by rather sizable horizontal tubes forming rigid connections with the columns themselves; the entire structure forming a rigid truss.

However, it is impractical for a variety of reasons to build this entire structure as a unit. Therefore, the design concept features modularity. There are ten modules in the present engineering concept of the core-ring. Each of these subtends 36° and is supported by three columns, one at the narrow inner edge and two at the broad outer edge.

It is necessary, of course, to investigate all six possible motions of the core-ring (surge, sway, heave, roll, pitch, and yaw). However, floating platforms such as the individual modules themselves or the core-ring in its entirety must be recognized as spar buoy clusters in which the heave response of the individual and coupled buoys (columns) is an important or dominant factor in the determination of roll and pitch of the total platform. Therefore, considerable attention is devoted to the heave response of an individual column.

Next it must be recognized that the individual modules must be seaworthy in moderate seas if they are to exist by themselves for even short periods of time and that they must also be quite stable in light to moderate seas if their assembly into the core-ring is to prove feasible. Thirdly, since assembly of the entire ring will take time, the partially assembled ring will be required to withstand possibly heavy seas with safety if not absolute stability. Lastly, the ultimate objective, of course, is to derive (within economic limits) an underbody configuration for the core-ring that will exhibit minimum motions and accelerations under all conditions.

Therefore, this investigation proceeds from the responses of an individual column, optimizing heave response, through investigations of the resultant behavior of platforms having multiple columns in six degrees of freedom and finally examines the expected behavior of the core-ring itself in six degrees of freedom in both regular and irregular seas.

IV. SINGLE COLUMN INVESTIGATIONS

The motion of the entire core-ring is to be determined in six degrees of freedom, i.e., surge, sway, heave, roll, pitch, and yaw. Of these, the most important motion is the heaving motion. This is true because the large lateral dimension of the ring dictates that its pitching and rolling motions will be generated mainly by heaving forces of the columns. Too, and for obvious reasons, it is easier and less expensive to establish the heaving characteristics of a single column than those of the entire ring, or even one

module. One can reason that, since all columns are to be identical, minimizing heave response of a single column should lead to modules and a core-ring with minimum response in heave also; and, with certain limitations, minimum pitch and roll too. With this justification, the heaving motion of a single column has been investigated to a considerable extent. This section develops the fundamental equations of motion of a single column and then explores (1) non-faired (two-cylinder) column configurations, (2) faired column configurations, (3) faired column configurations with horizontal struts attached, (4) configuration (3) with a bottom flange added, (5) the effects of varying draft, and (6) the effects of artificially increased hydrodynamic mass.

A. Fundamental Equations of Motion

The equation of motion of a single column (spar buoy) is given by

$$m\ddot{z} = m_h\ddot{r} + (b_s + b_f)\,|\dot{r}|\,\dot{r} + N_z\dot{r} + cr \qquad \text{(IV.1)}$$

where

$r = r(t)$ = relative vertical displacement between buoy and water

$$r(t) = \xi(t) - z(t)$$

$$\xi(t) = \frac{H}{2} e^{kz} \cos(kx - \quad t)$$

b_s = coefficient for skin friction drag

b_f = coefficient for form drag

N_z = coefficient for damping due to wave generation

The above equation is non-linear in the damping term. However, damping is not very important for tuning factors of $\lambda \geq 1.5$; and the columns are designed for a natural period longer than that of the longest wave to be expected. It will therefore suffice to linearize the equation by determining an equivalent damping term. As a criterion for equivalence the condition of equivalent work of the dissipative force per quarter cycle of the system's motion can be applied intuitively. Thus,

$$\int_0^{\frac{\pi}{2\omega}} (b_s + b_f)\,\dot{r}^2\,dr = \int_0^{\frac{\pi}{2\omega}} b\,\dot{r}\,dr \qquad \text{(IV.2)}$$

Assuming a harmonic solution

$$r = r_o \cos(\sigma t + \epsilon)$$

we obtain

$$b = \frac{8}{3\pi}(b_s + b_f)\, r_o \sigma \qquad \text{(IV.3)}$$

The linearized equation of motion is hence

$$m\ddot{z} = m_h \ddot{r} + b\dot{r} + N_z \dot{r} + c\, r \qquad \text{(IV.4)}$$

The proposed column configuration shows two main discontinuities with respect to vertical flow, namely, the conical transition from the small to the large cylinder, and the semi-ellipsoidal bottom end cap. The inertial force on the right hand side of the above equation, $(m_h \cdot \ddot{r})$ has therefore to be rewritten as a sum of the products of several added masses and their corresponding relative accelerations. This also will allow the wave inertial forces acting on the horizontal cylinders to be included. Of course, similar arguments hold for the drag forces too. Hence,

$$m\ddot{z} = \sum_i (m_h)_i \ddot{r}_i + \sum_i b_i \dot{r}_i + N_z r + c\, r \qquad \text{(IV.5)}$$

where the sums are over the number of discontinuities and appendages, protrusions, flanges and horizontal cylinders, with

$$r_i(t) = \xi_i(t) - z(t)$$

$$= \frac{H}{2} e^{-kl_i} \cos\sigma t - z(t) = \xi_{o,i} \cos\sigma t - z(t)$$

$$\dot{r}_i(t) = -\frac{H}{2} e^{-kl_i}\, \sigma \sin\sigma t - z(t) = -\sigma \xi_{o,i} \sin\sigma t - z(t)$$

$$\ddot{r}_i(t) = -\frac{H}{2} e^{-kl_i}\, \sigma^2 \cos\sigma t - z(t) = -\sigma^2 \xi_{o,i} \cos\sigma t - z(t)$$

l_i = distance of station below DWL

We obtain then,

$$(m + \sum_i (m_h)_i)\ddot{z} + (\sum_i b_i + N_z)\dot{z} + c\, z = F_i + F_v + F_d \qquad \text{(IV.6)}$$

where

$$F_i = -\sigma^2 (\Sigma_i (m_h)_i \ \xi_{o,i}) \cos\sigma t$$

$$F_v = -\sigma (\Sigma_i b_i \ \xi_{o,i}) \sin\sigma t$$

$$F_d = \rho g \Sigma_i \ (A_i \ \xi_{o,i}) \cos\sigma t$$

where A_i is the i- area (horizontal projection), having positive sign, if its area is facing down. Inspection of the three force terms (inertia, drag, and displacement) reveals that inertia and drag forces are ninety degrees out of phase and do not change sign with variances in wave frequency. The wave displacement force, however, because of the term $\Sigma_i A_i \ \xi_{o,i}$ may change sign with variances in wave frequency. Therefore we have here a tool which may be employed to develop a column shape that could yield a zero wave displacement force for a particular wave frequency. The term displacement force is derived from the fact that this force component is created by the displacement of water particles. It could also be called dynamic elevation head since it pertains to the pressure variation which occurs as the water surface rises and falls with the passage of each wave.

It is worth noting that, for a column stabilized platform with relatively small horizontal connecting cylinders (as the one under discussion), the wave displacement force is the dominating force.

B. Non-faired (Two Cylinder) Column Configurations

Good insight into the problem discussed above can be obtained by investigating the dynamics of a simple single column consisting of only two longitudinally joined cylinders of different diameters (Figure 3). The advantages of this simple configuration are: 1) the ease of constructing scale models, 2) a very short and inexpensive computer program, and 3) the limited number of parameters involved; all of which allow a quick and simple overview of the problem. Equation (IV.6) then reduces to

$$(m + \sum_{i=1}^{2} m_i) \ddot{z} + \sum_{i=1}^{2} b_i \dot{z} + c z = F_i + F_v + F_d \qquad \text{(IV.7)}$$

where

$$F_i = -\sigma^2 (\sum_{i=1}^{2} m_i \ \xi_{o,i}) \cos\sigma t$$

$$F_v = -\sigma (\sum_{i=1}^{2} b_i \ \xi_{o,i}) \sin\sigma t$$

$$F_d = \rho g (\sum_{i=1}^{2} A_i \ \xi_{o,i}) \cos\sigma t$$

and

Index 1 denotes the top of the larger cylinder
Index 2 denotes the bottom of the larger cylinder.

Hydrodynamic masses are derived by,

$$m_1 = \rho \, (C_{h_1}) \, \frac{2\pi}{3} (r_2^3 - r_1^3)$$

$$m_2 = \rho \, (C_{h_2}) \, \frac{2\pi}{3} \, (r_2^3)$$

Damping coefficients are

$$b_i = \frac{8}{3\pi} \, (b_s + b_f)_i \, \sigma \, r_{o,i}$$

where the coefficient for skin friction is given by

$$(b_s)_i = \frac{1}{2} \, \rho \, C_f S_i$$

$S_i \equiv$ wetted surface to be counted to station i.

The frictional coefficient is obtained by the ITTC formula

$$C_f = \frac{0.075}{\log_{10} R_e - 2.0} + 0.004$$

where

$$R_e = \frac{\bar{r}_i L}{\nu} \quad , \quad \bar{r}_i = \text{average velocity near station i}$$

The coefficient of form drag is

$$(b_f)_i = \frac{1}{2} \rho \, (C_D)_i \cdot A_i$$

$(C_D)_i$ drag coefficient for station i

A_i cross sectional area at station i

One small scale model was built to calibrate this simulation (Figure 4). Because of the limited water depth at the available model testing facility, bottom effects required inclusion in the theory. The wave velocity potential is given for intermediate water depth by

$$\phi \, (x, z, t) = - \frac{H}{2} \frac{g}{\sigma} \, \frac{\cosh k \, (z + d)}{\cosh k \, d} \, \sin \, (kx - \sigma t)$$

where d = water depth,

$$\dot{\xi}_1 = -\frac{\partial \phi}{\partial z} = \frac{H}{2}\sigma \frac{\sinh k(z+d)}{\sinh kd} \sin(kx - \sigma t)$$

$$\xi_i = \int \dot{\xi} dt = \frac{H}{2} \frac{\sinh k(z+d)}{\sinh kd} \cos(kx - \sigma t)$$

$$\ddot{\xi}_i = -\frac{H}{2}\sigma^2 \frac{\sinh k(z+d)}{\sinh kd} \cos(kx - \sigma t)$$

The natural frequency of oscillation is given by

$$\omega = \sqrt{\frac{c}{M + \sum m_i}} \quad \text{(rad/sec)}$$

and the natural period

$$T_{nat} = \frac{2\pi}{\omega} \quad \text{(sec)}$$

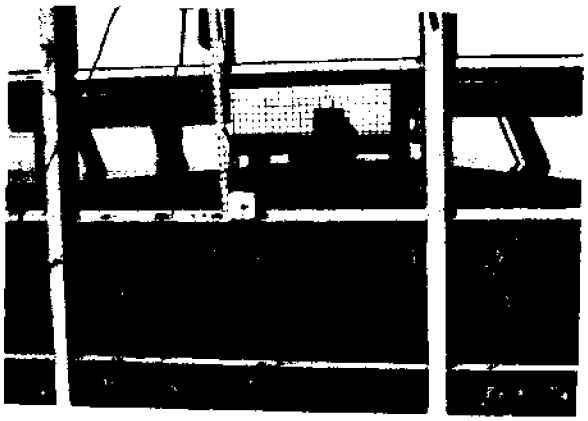

Fig. 4 Scale model of variation 6 of the non-faired column configuration in J.K.K. Look Laboratory wave flume.

Figure 3 depicts the variations of this configuration that were investigated. It will be noted that draft, volume, and the diameter of the upper cylinder were kept constant as the larger lower cylinder was varied. Figure 5 depicts the theory-derived unit amplitude responses in heave of the variations. The natural periods of oscillation are indicated in Figure 3. The calculations were carried out directly for the scale model size. The scale factor is 1:154 to the city's proposed full sized columns.

The most important result to be noted in Figure 5 is the zero response at wave frequencies slightly higher than the natural frequency. The exact position of the zero motion frequency (ω_c) is obtained from the frequency of zero wave force (Figure 6). The zero wave force is caused by cancelling net wave displacement and wave inertial forces. The net wave displacement force is the difference between the forces acting on the two horizontal control planes of the large cylinder. It is important to note that for all greater frequencies (i.e., $\sigma > \omega_c$), the inertial force and the wave displacement force have the same sign, i.e., they act in the same direction, namely,

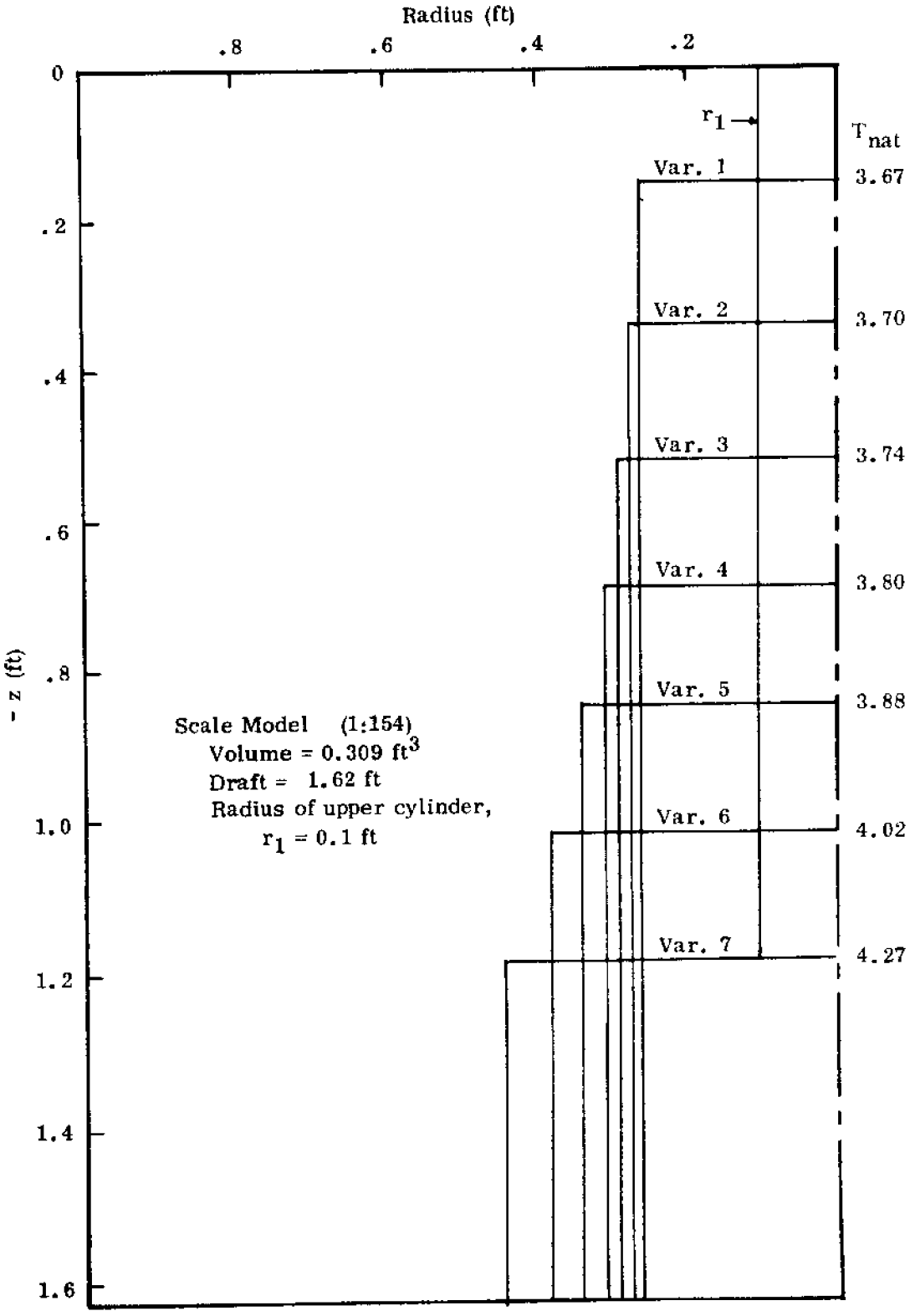

Fig. 3 Constant volume variations of the two-cylinder column configuration.

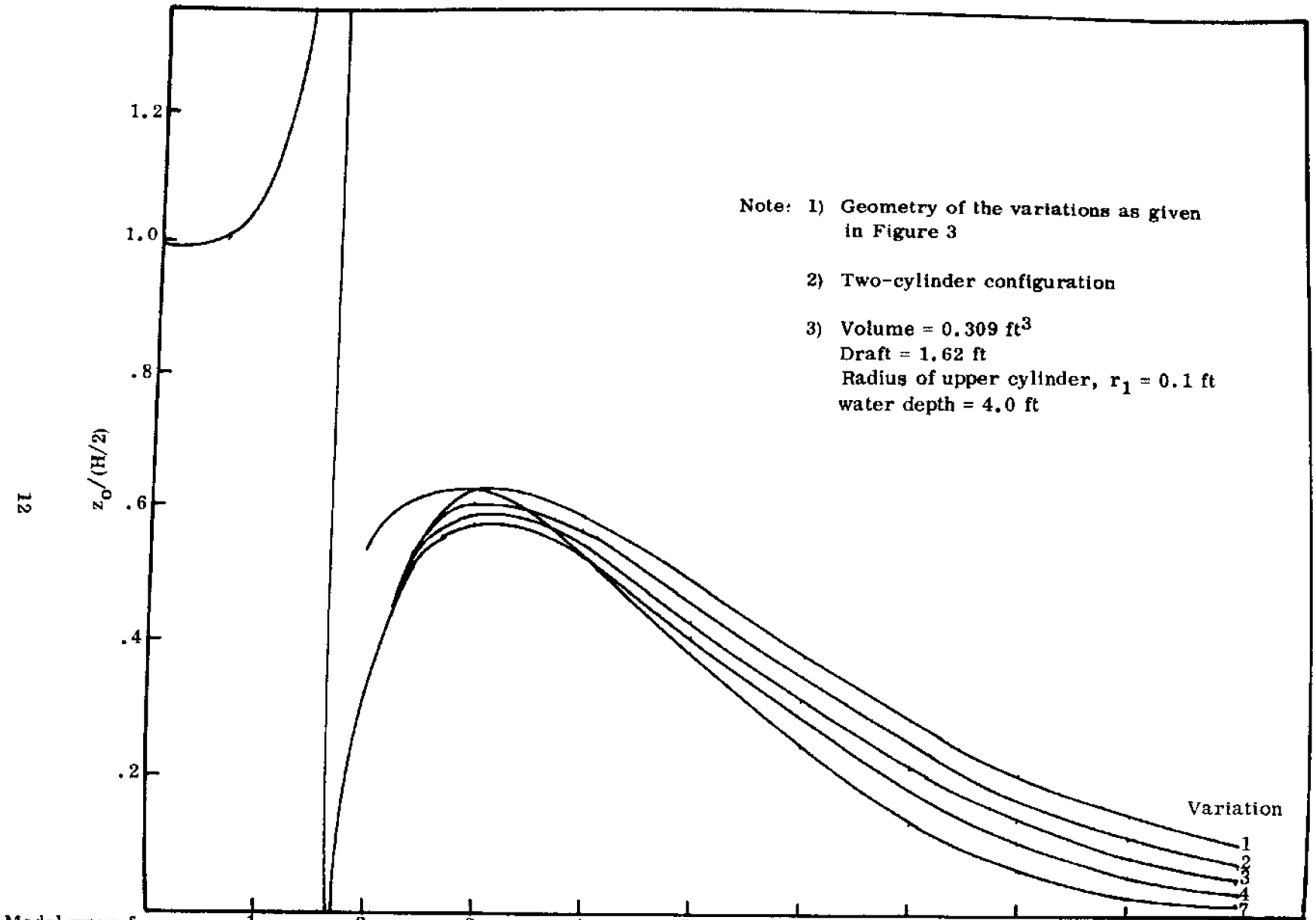

Model wave frequency	1	2	3	4	5	6	7	8	9	10 (rad/sec)
Model wave period	6.28	3.14	2.09	1.57	1.26	1.05	0.90	0.79	0.70	0.63
Full-scale wave period		38.5	25.6	19.4	15.4	12.8	11.0	9.7	8.6	7.7

Fig. 5 Unit amplitude response in heave of various non-faired single column configurations.

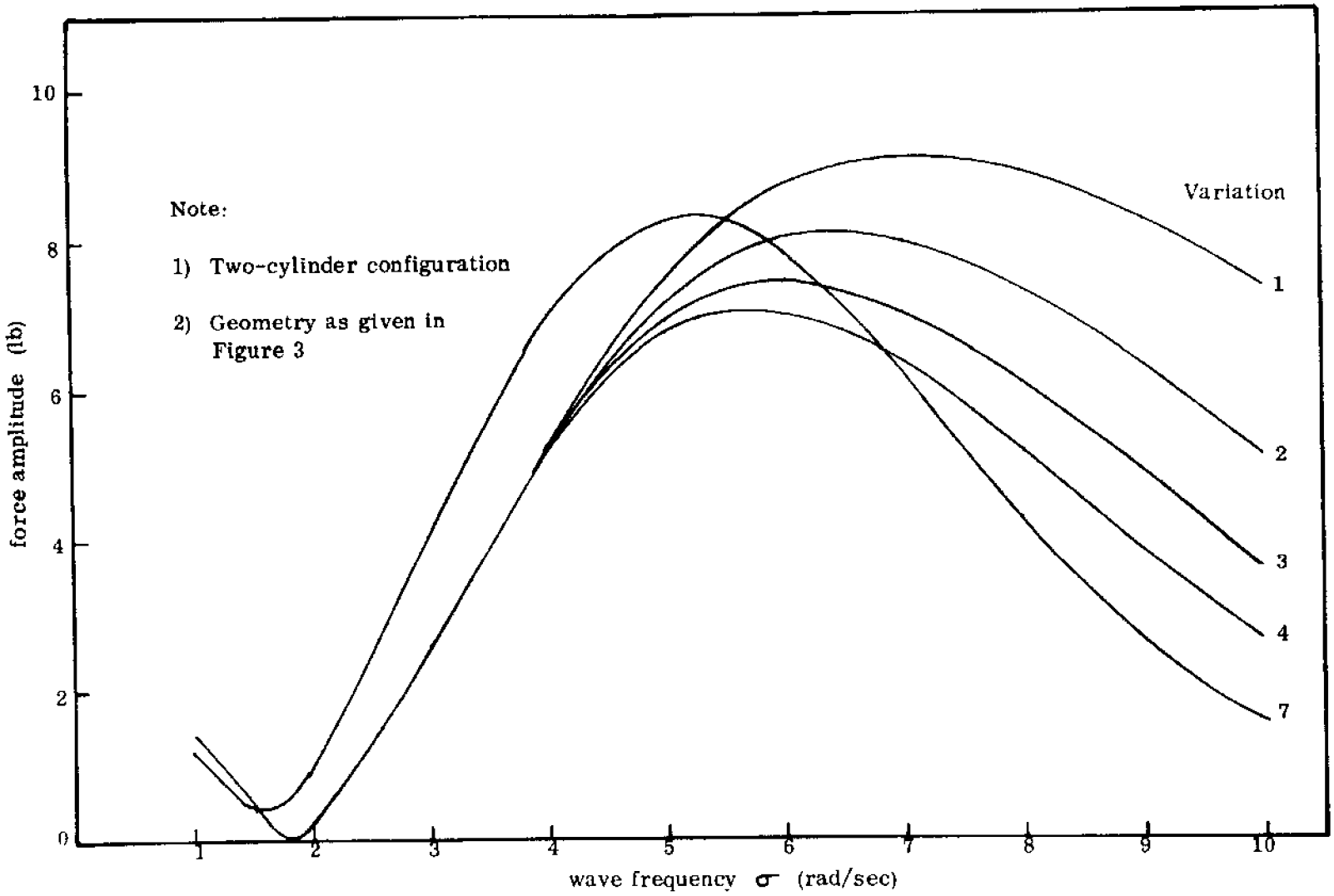

Fig. 6 Amplitudes of total wave force

downward at the instant when the wave crest is passing the buoy. In other words, the wave will not have the effect of lifting the column up as with surface ships, but rather of pushing the column down. To explain this in common terms, we find that the water motion and pressure fluctuation under a wave, which decrease rapidly with water depth, do not reach the bottom plane of the buoy, and therefore lack the upward pushing effect. Because the net wave displacement force and the inertial force act in the same direction, the application of flanges (damping plates) and the addition of the horizontal cylinders will only lead to an increase in wave force. Due to the increase in hydrodynamic mass the natural period will increase, however, and with it the tuning factor, which will lead to a decrease in the magnification factor. This will, however, still not outweigh the increase in inertial force, and the resulting motion will therefore increase.

The heaving motion will be in phase with the wave crest for frequencies larger than the zero motion frequency, because the wave force is 180 degrees out of phase and the column as a linear oscillator is about another 180 degrees out of phase with the wave force.

Figure 7 depicts a comparison of the theory against data points taken in scale model experiments carried out at the J.K.K. Look Laboratory. The natural period agreed perfectly. At resonance a maximum value of $z_o/(H/2) = 2.0$ was calculated and measured.

Figure 8 shows non-faired column variations of the same volume, but with the upper cylinder diameter increased to 0.24 feet. Figure 9 shows computed heave responses of these variations.

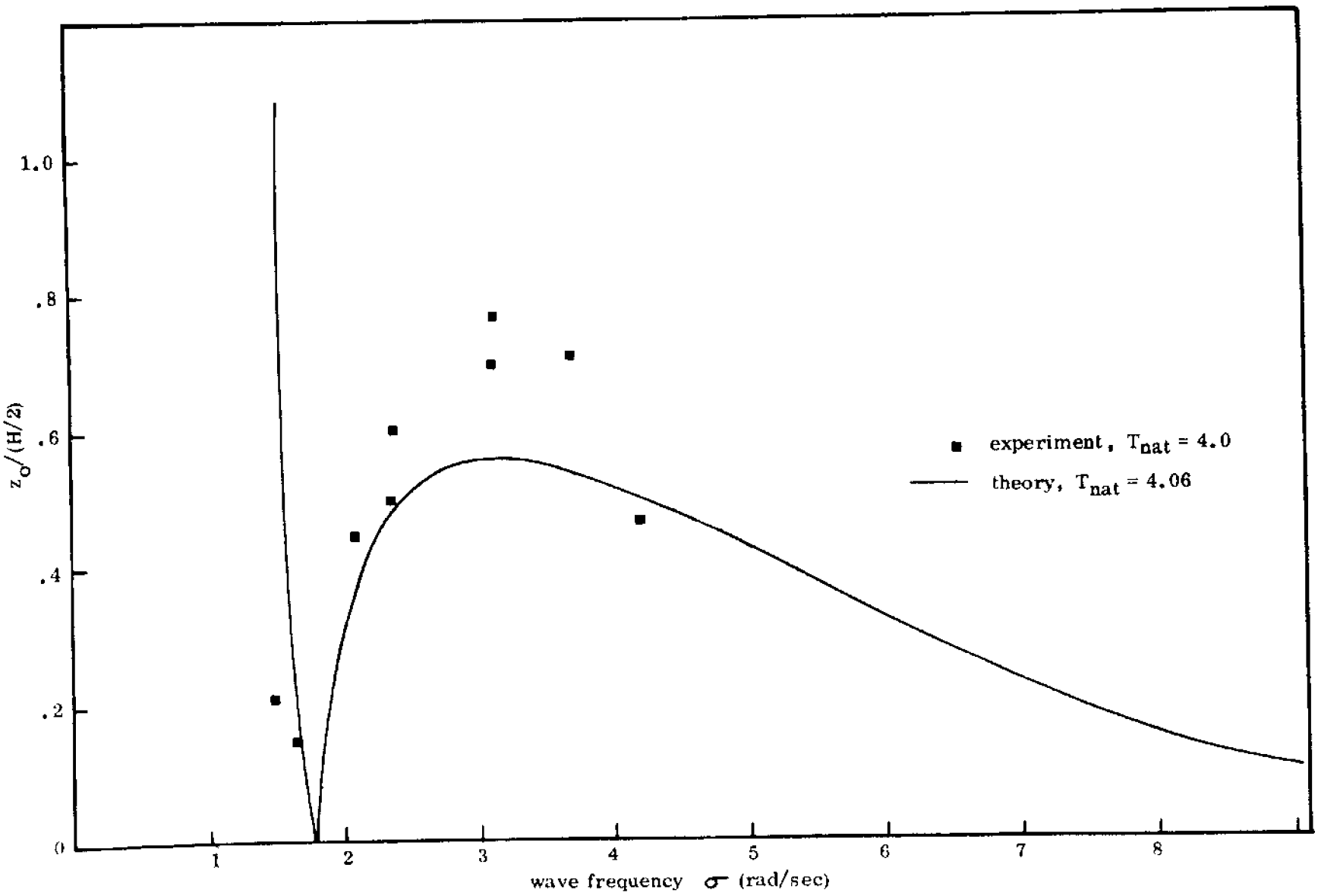

Fig. 7 Comparison between theory and experiment, unit amplitude response in heave

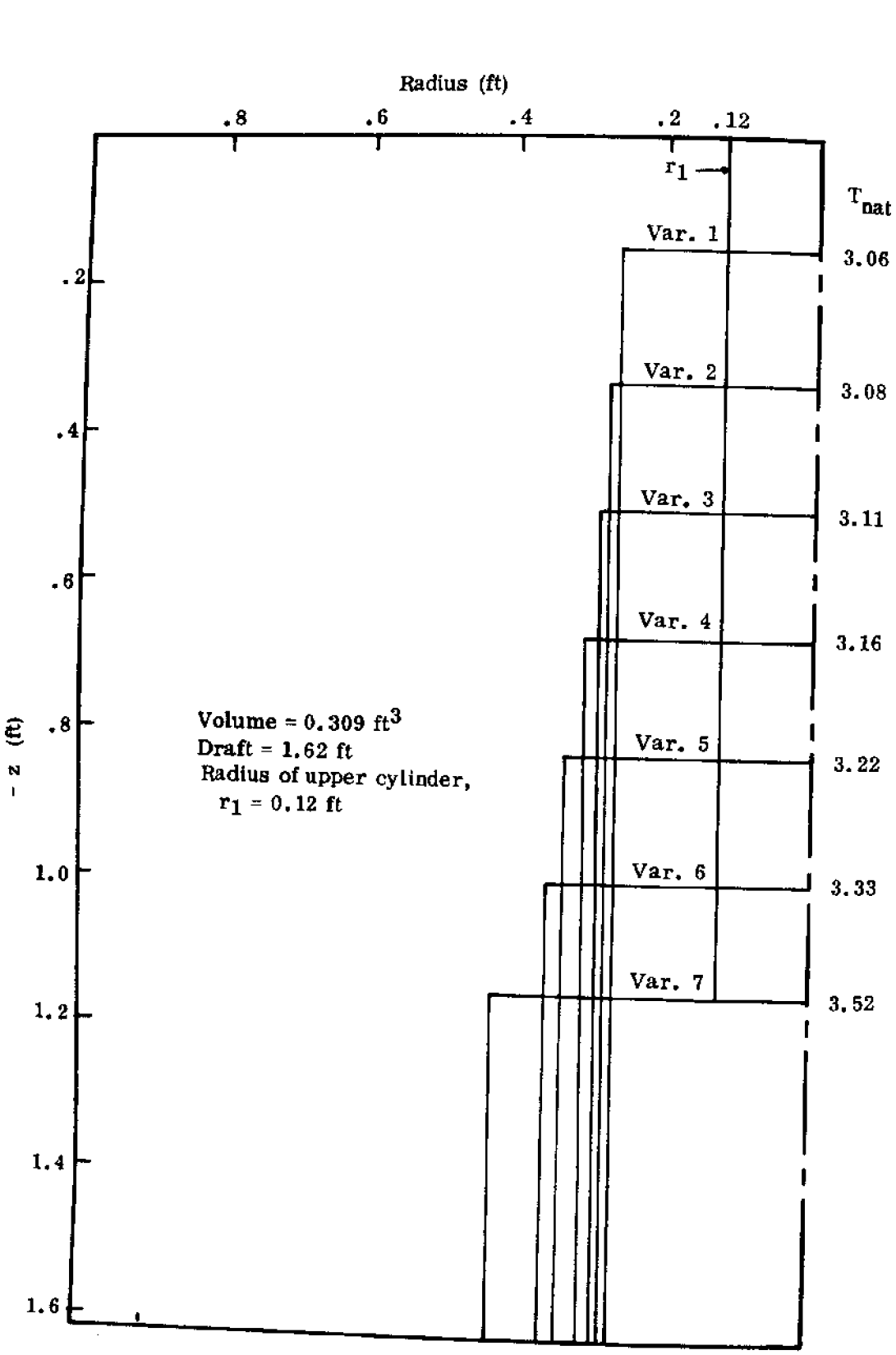

Fig. 8 Additional variations of two-cylinder column configuration.

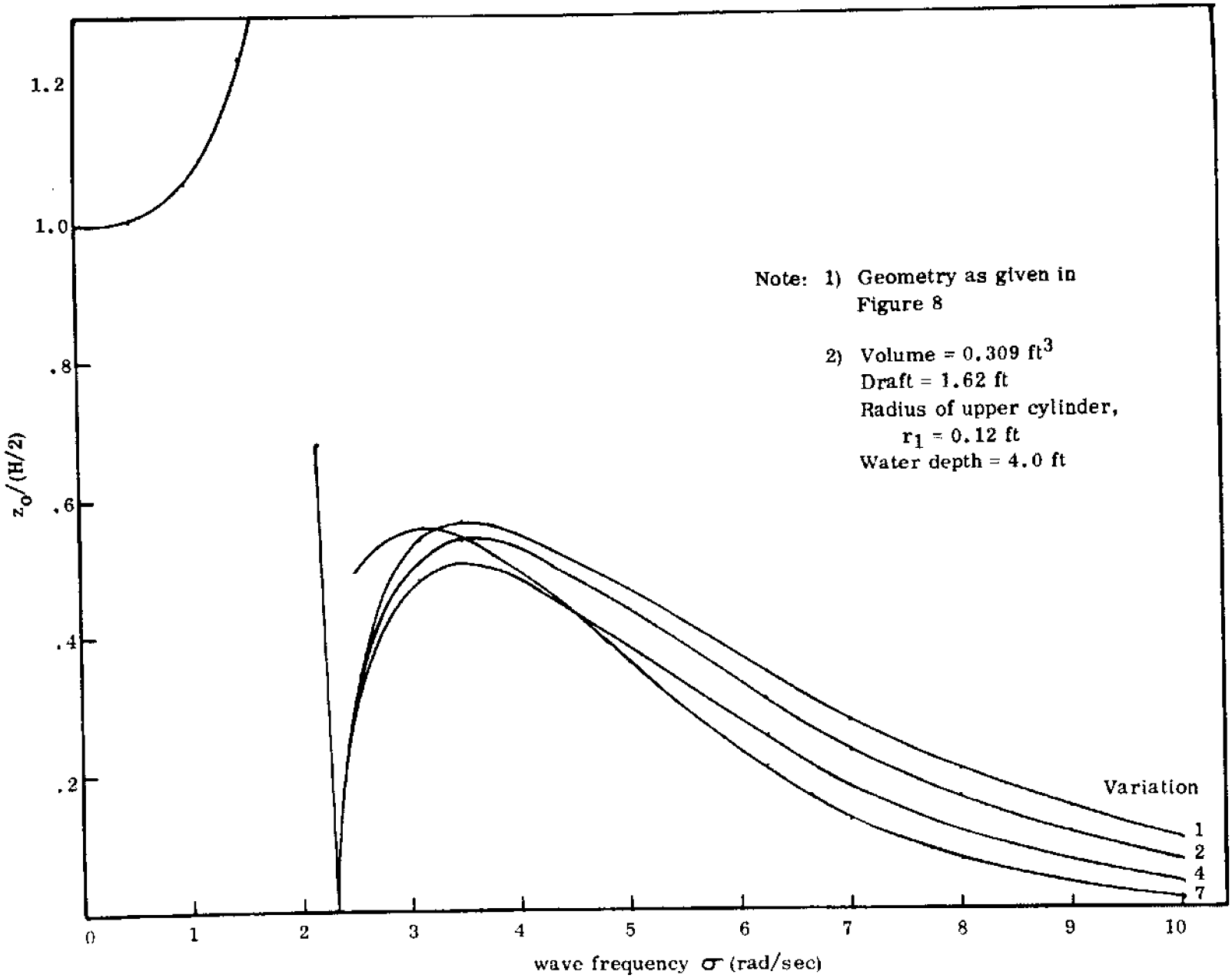

Fig. 9 Unit amplitude response in heave for additional variations of the two-cylinder column configuration

C. Faired Column Configuration

This configuration is somewhat more complicated than the non-faired case, though basically the same considerations hold. The computer program developed for the faired configuration is labeled HEAV3. Figure 10 depicts the variations of geometry that were investigated using HEAV3. As shown, the fairing consists of a cone on the top and a semi-ellipsoid added to the bottom of the large cylinder. Because of the fairing, damping has been greatly reduced from the previous two cylinder case. This leads to a difficulty in the model testing procedure, as it now takes considerably longer for the so-called transient motion to die out and so, for the column to attain steady state motion. Figure 11 depicts the calculated response operators for five variations of the column geometry given in Figure 10. It can be seen that this variation of geometry does not affect the response characteristics very greatly. It would seem from this, then, that the designer can be given rather free hand to base the shape of a column on other than hydrodynamic considerations. The corresponding inertial and total wave forces are given in Figure 12. It indicates that the two are acting in-phase for most frequencies. As expected, the contribution of inertial force to the total force is greatest for variation 5.

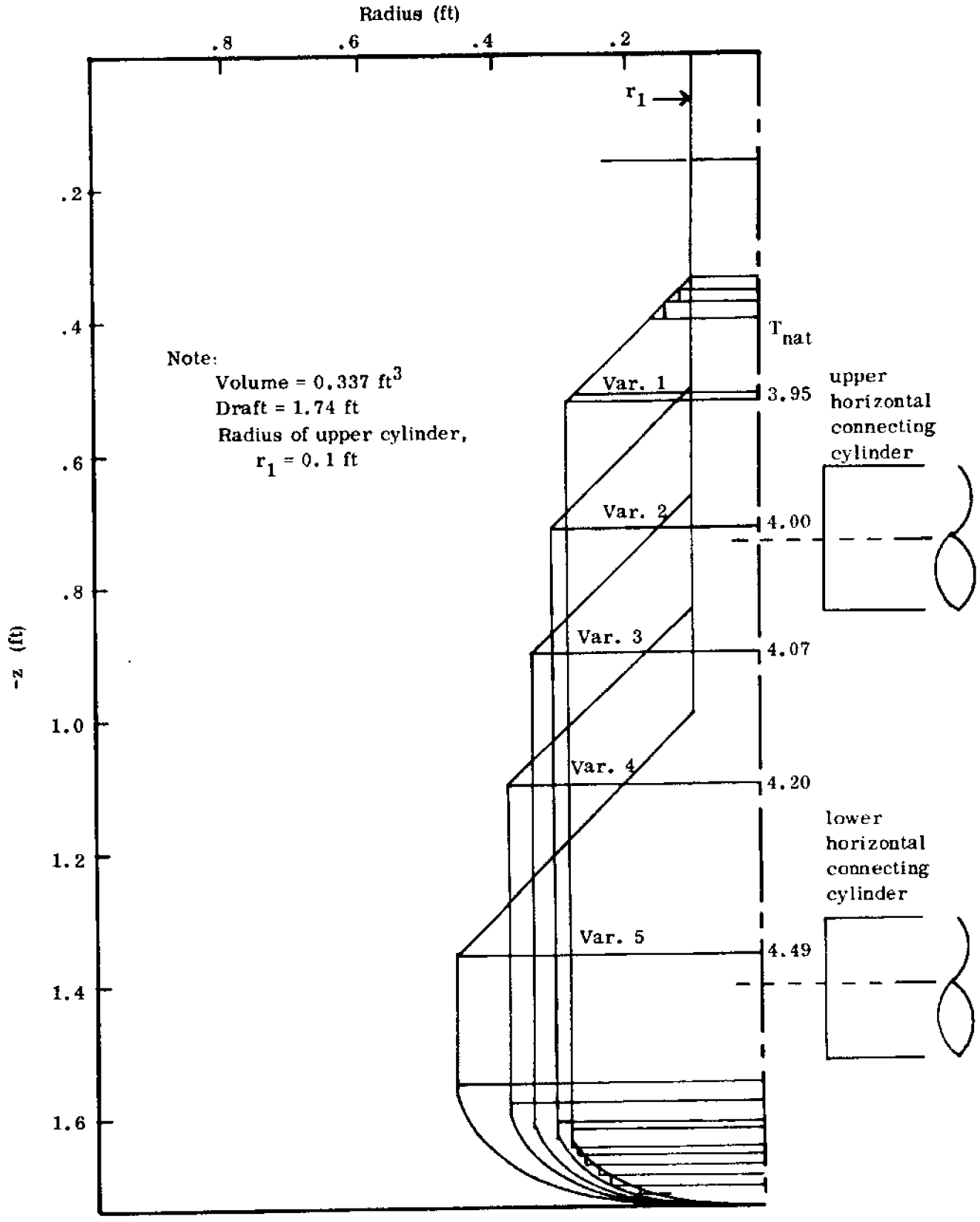

Fig. 10 Variations of faired column configuration

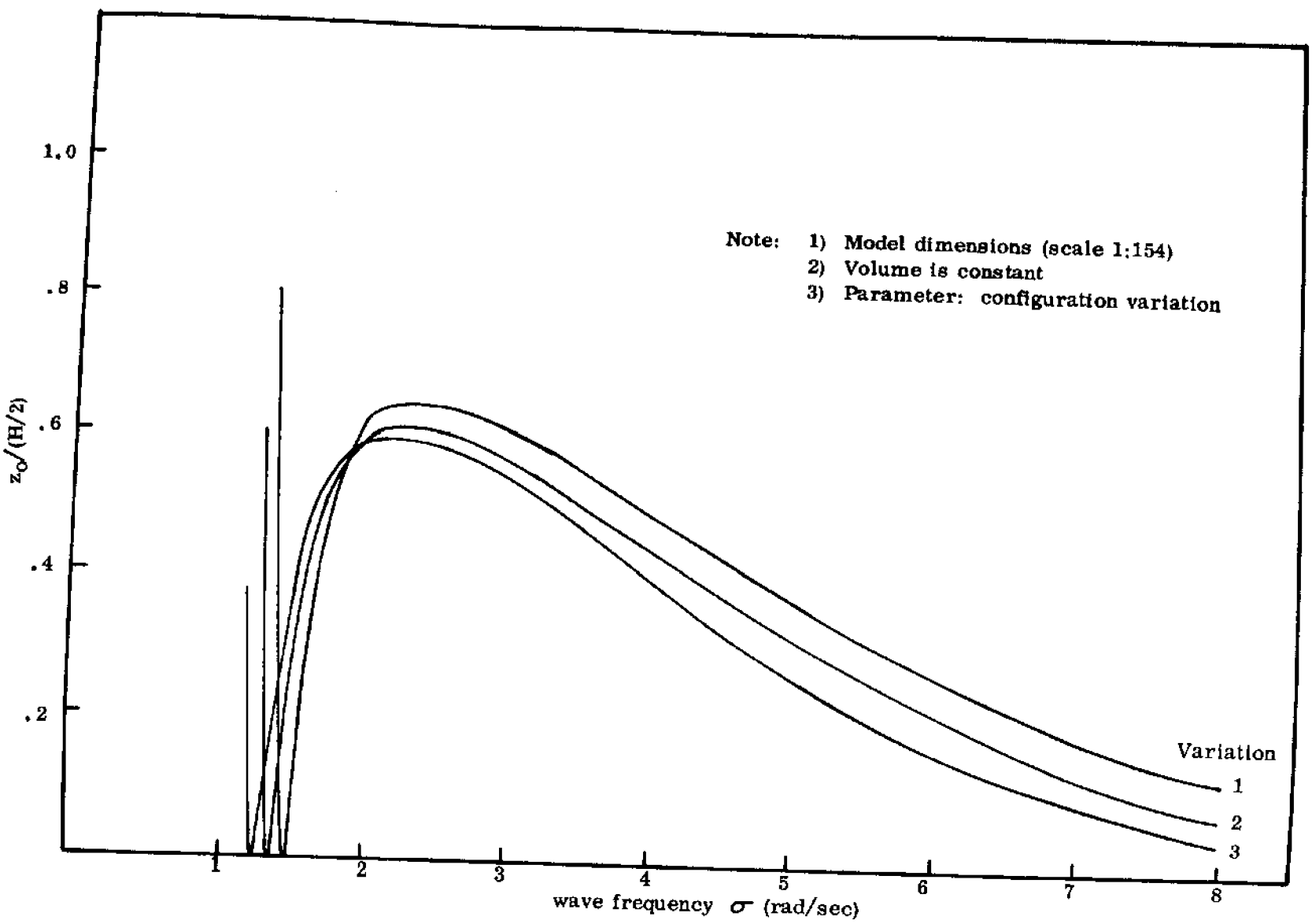

Fig. 11 Unit amplitude response in heave, variation of configuration defined in Fig. 10

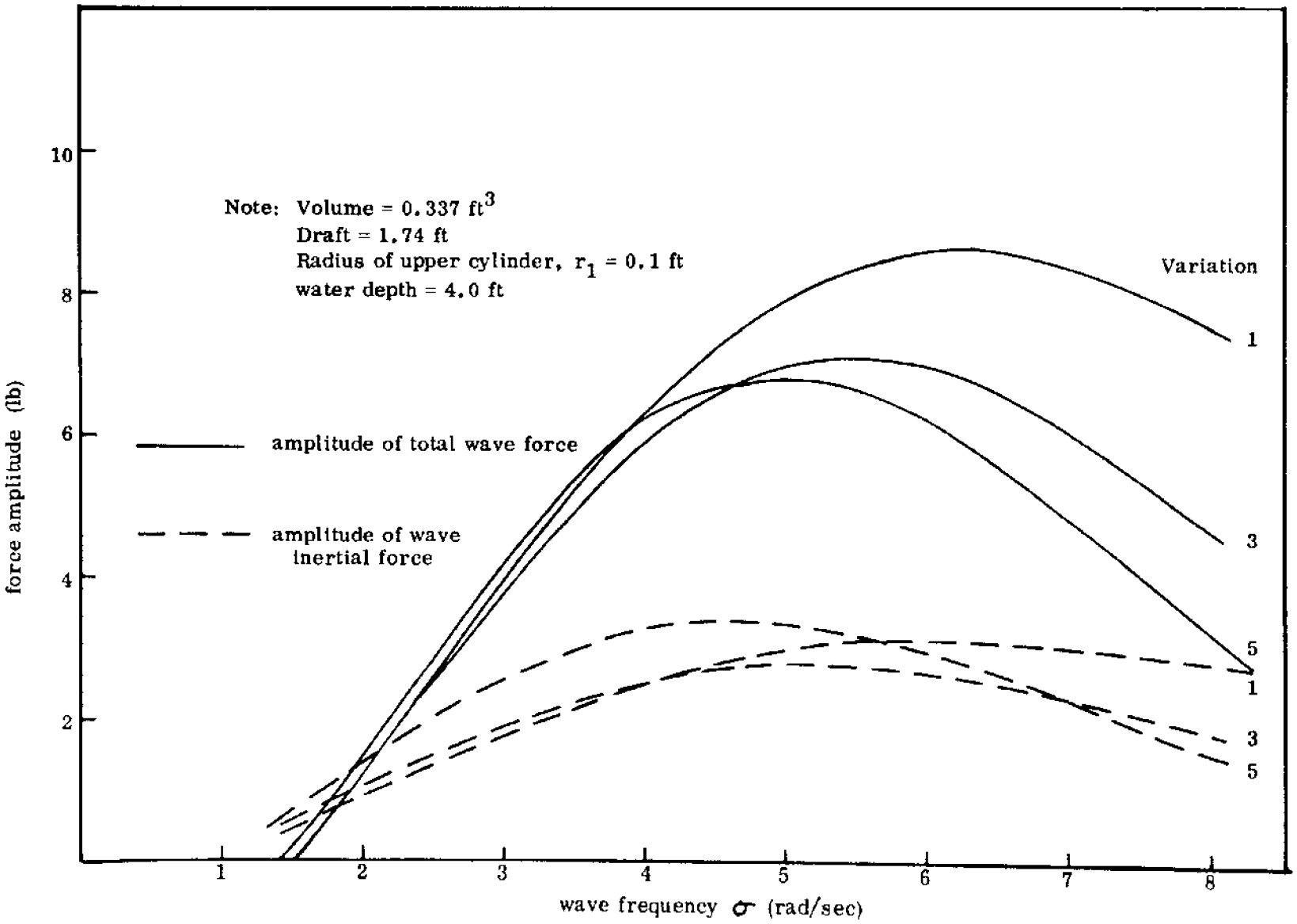

Fig. 12 Wave forces acting on Figure 10 variations (no horizontal connectors)

D. Faired Column Configuration with Connecting Cylinders

An equivalent portion of the horizontal connecting cylinders of a module (triad) was added at the locations indicated on the right of Figure 10 (1.5 diameters below the top and above the bottom of the large cylinder, respectively). The diameter of these horizontal cylinders was assumed to correspond to 30 ft in full scale. Motion calculations were carried out for a matrix of the same five configurations (Figure 10) but, with each configuration, also varying the upper diameter from 0.20 to 0.36 ft. Figure 13 depicts the variation of wave forces with geometry, in particular that of variation 1, varying the radius of the upper cylinder as parameter r_1. Here the points of cancelling wave displacement forces and the frequencies of almost zero total wave force are seen to be highly dependent on the upper cylinder diameter. Figure 14 depicts the corresponding response operators, showing very clearly the frequency of zero motion. Increasing the upper diameter appears to reduce motions in shorter period waves significantly; however, the natural frequency is increased as a second result. Thus, excessive increases in upper cylinder diameter would bring natural frequency within the frequency range of long swells. To reduce the natural frequency, one might add a flange at the bottom of the large cylinder (see E. below). This would increase the added mass in heave.

The influence of limited water depth is shown in Figure 15. It has therefore to be kept in mind that the 1:154 scale model tests at the J.K. Look Laboratory were carried out with a 4 ft water depth while the model depth corresponding to the 1800 ft depth at the planned location of the city would be 11.7 ft. The limited depth in the model tank is felt, however, only by waves with a frequency less than 4 rad/sec.

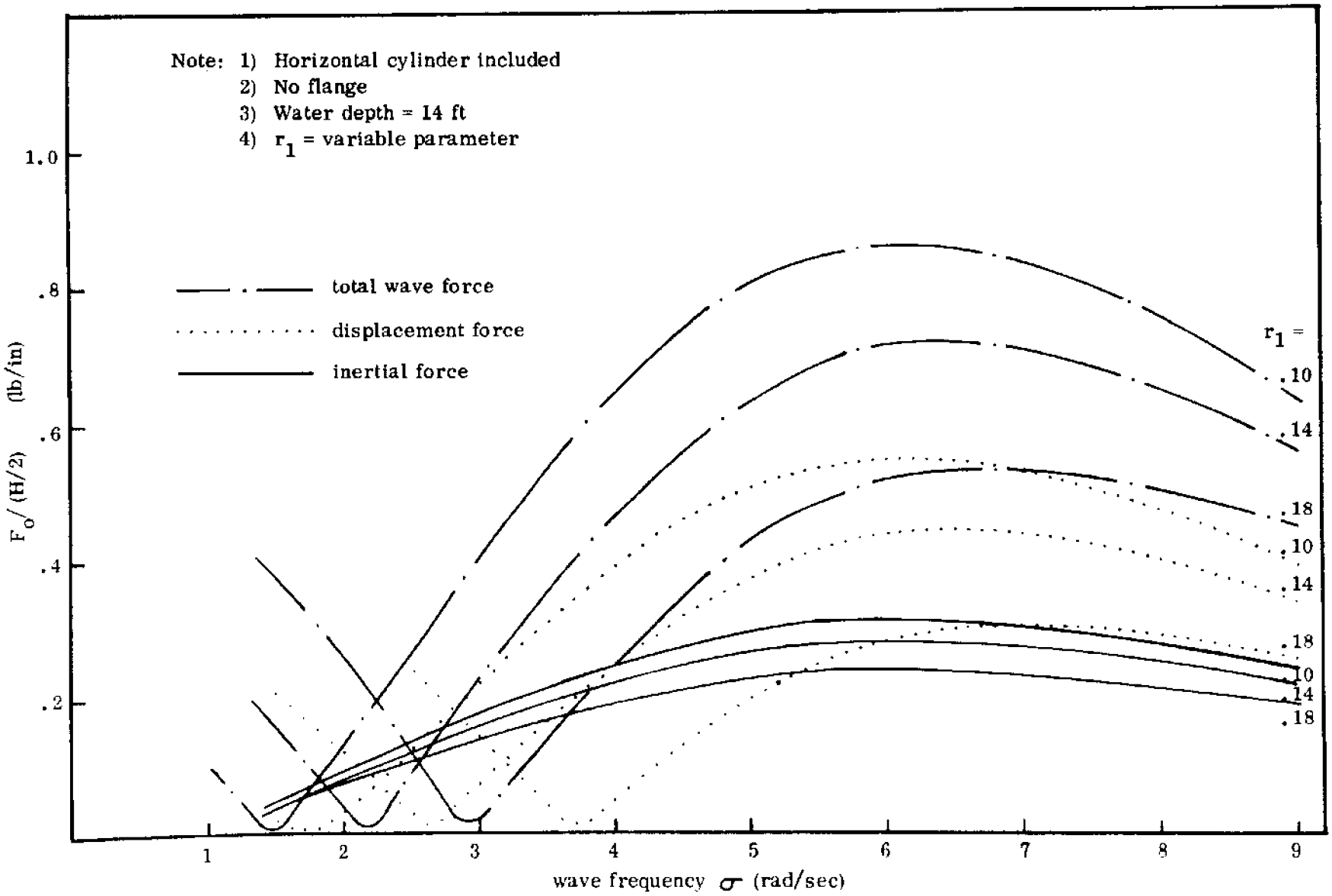

Fig. 13 Variation of wave forces with changes in r_1 for Figure 10 variation 1

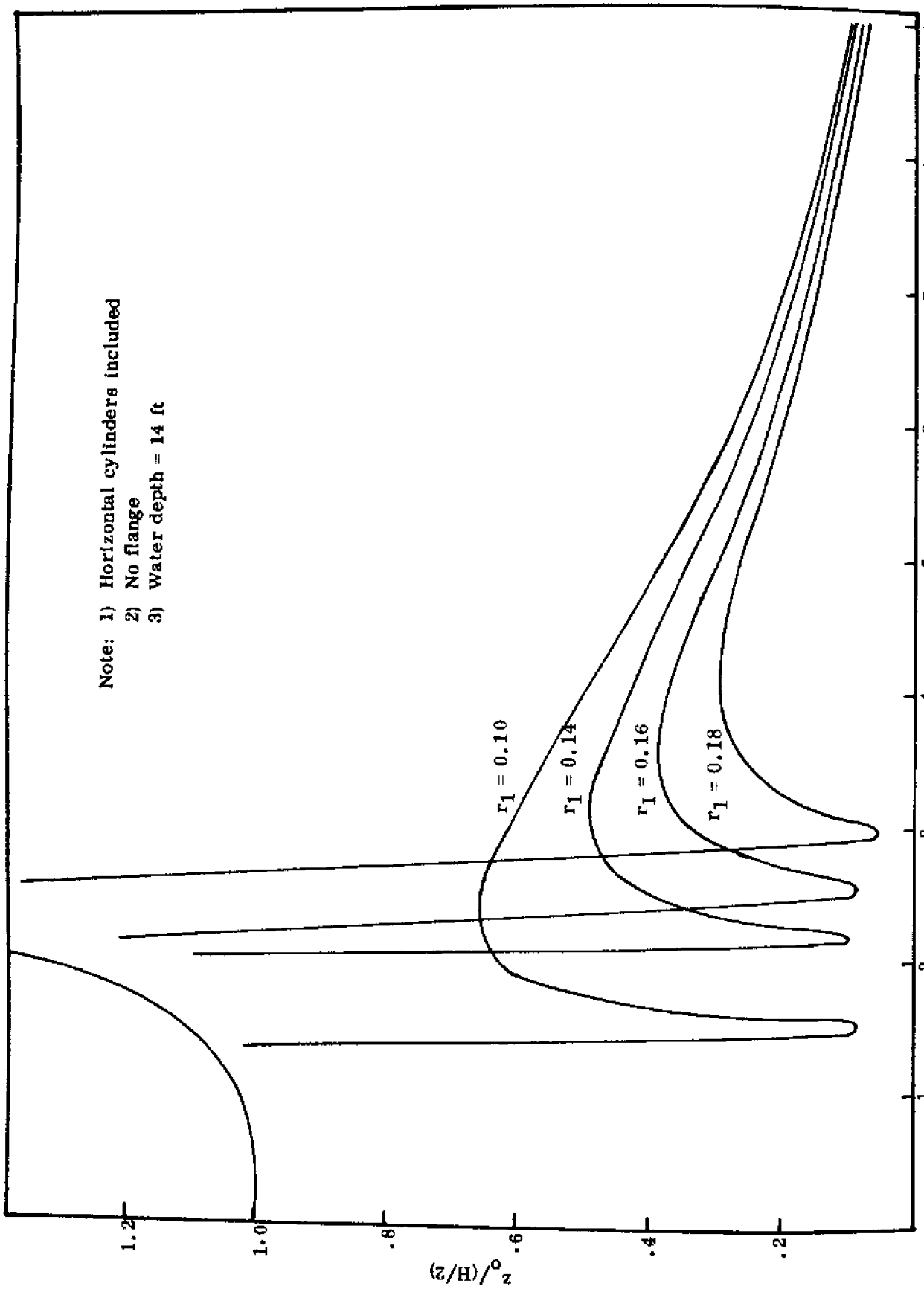

Fig. 14 Unit amplitude response in heave for Figure 10, variation 1 with changing r_1

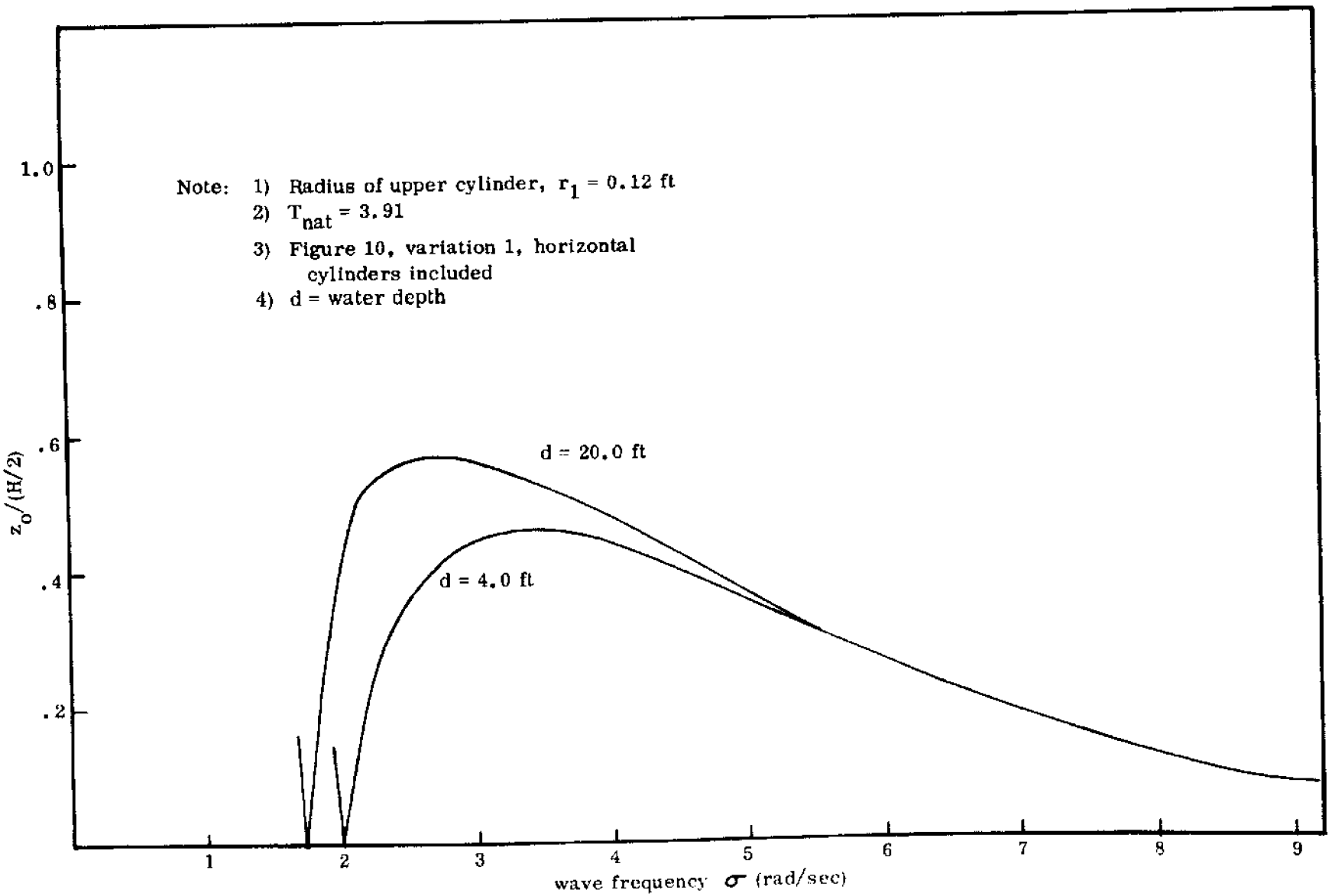

Fig. 15 Influence of water depth on heaving motion

E. Faired Configuration with Connecting Cylinders and Bottom Flange

First the effect of such a flange on the wave inertial force is investigated. Figure 16 depicts the variation of wave inertial force with width of flange, and it is seen that the inertial force is affected significantly, while the wave displacement force remains unchanged. Hence the point of cancelling inertial and displacement force changes. The corresponding response operators are depicted in Figure 17. We see, then, that increase in flange width increase the motion response for wave frequencies greater than the column's zero motion frequency, but that the natural frequency (and with it the occurrence of resonance) simultaneously moves toward lower frequencies. Figure 18 is analogous but pertains to a Figure 10, variation 1 column with an upper radius of 0.18 ft. It is interesting to note that the response characteristics of the column with 0.18 ft upper radius and 0.1364 (21 ft, full scale) flange appears to become the same as that of a column with 0.16 upper radius and a 0.0195 (3 ft, full scale) flange. The corresponding natural periods are also in agreement. It thus appears that, should overriding design considerations (such as damage control) dictate the use of a larger upper diameter, bottom flanges may be added to obtain a longer natural period.

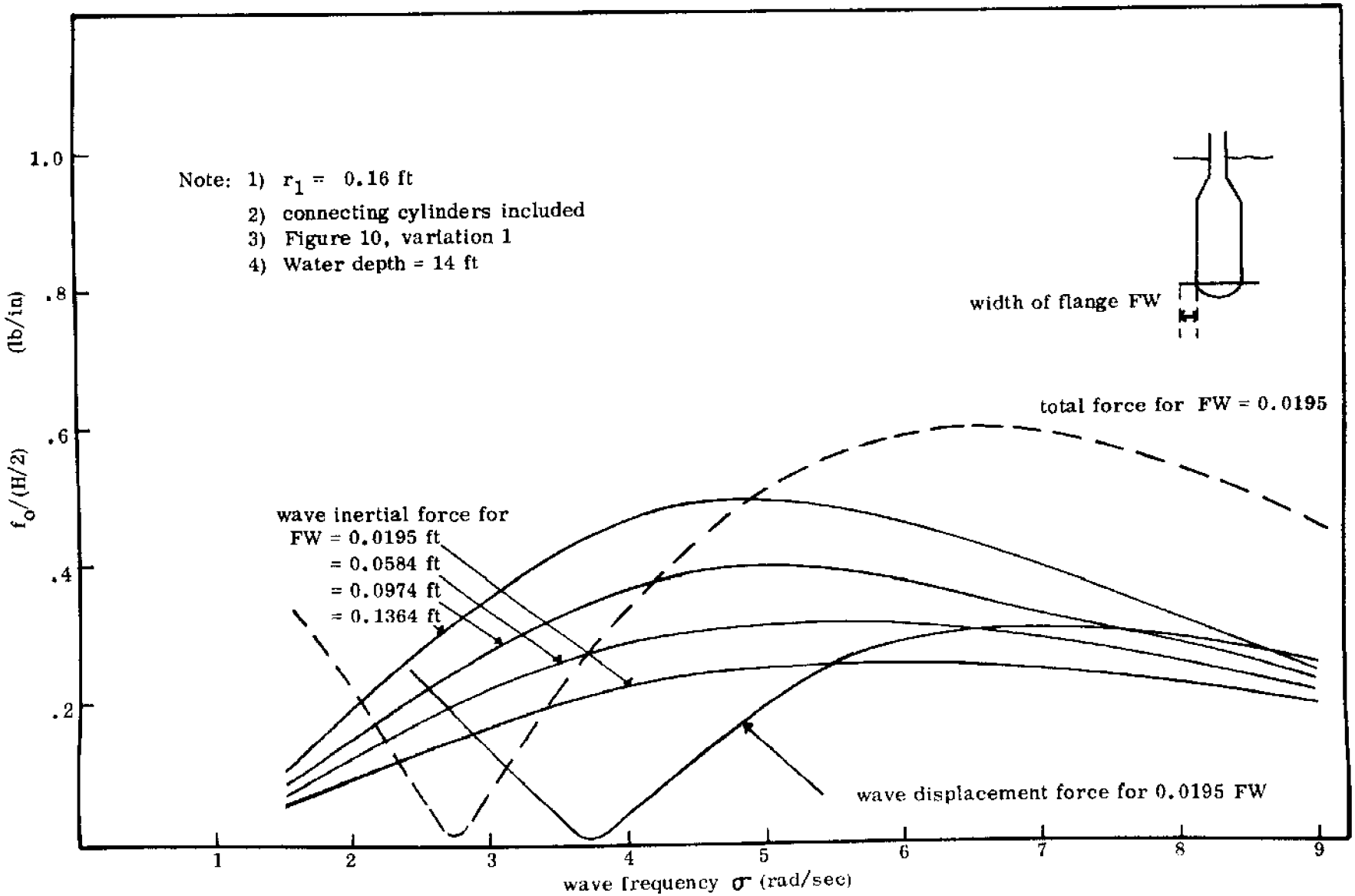

Fig. 16 Variation of wave inertial force with width of flange

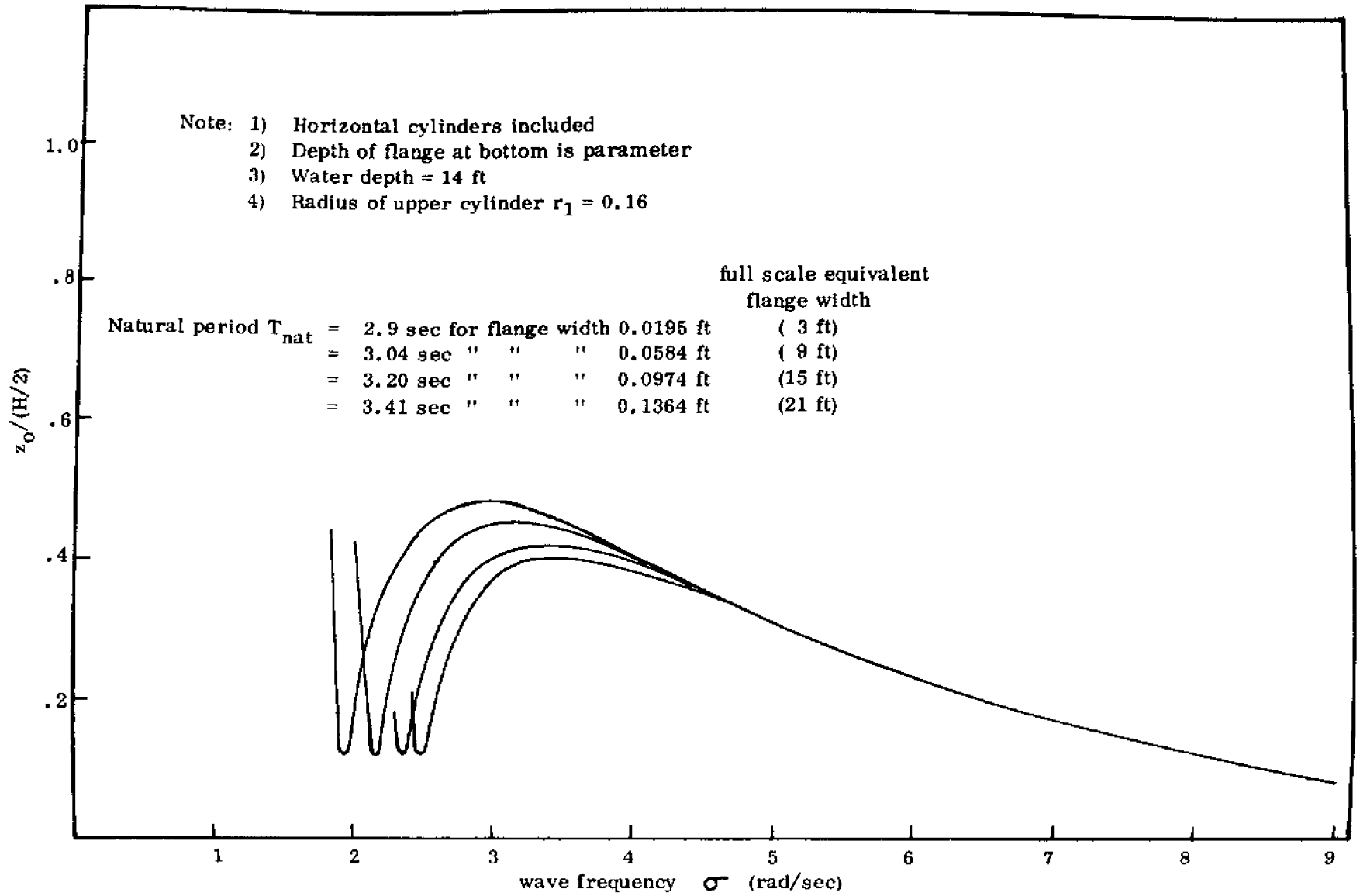

Fig. 17 Unit amplitude response in heave for Figure 10 variation 1 with flanges added

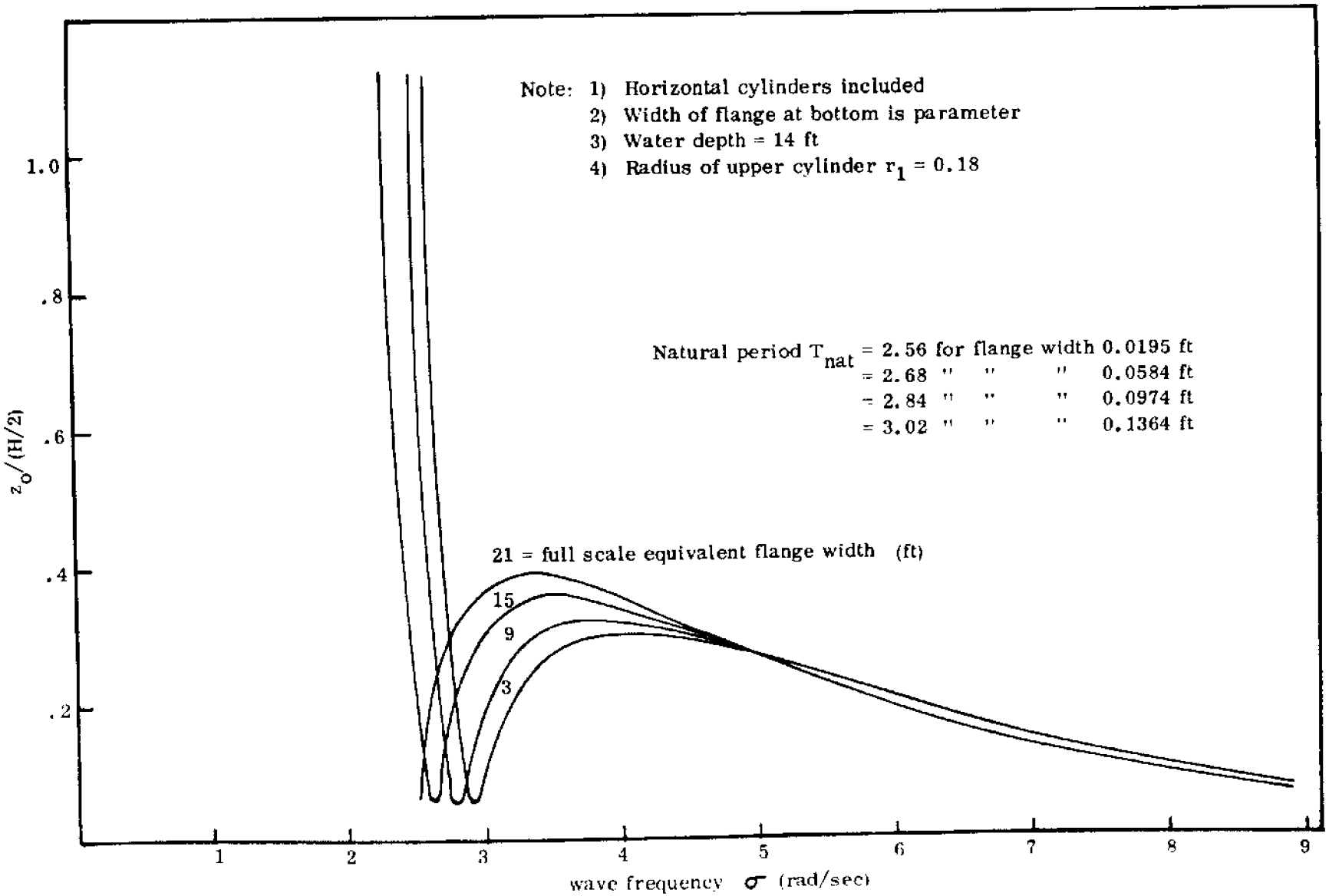

Fig. 18 Unit amplitude response in heave for Figure 10, variation 1 with bottom flange.

F. Variations of Draft

In all the previous variations of the sectional geometry of a column, the draft and the volume were kept constant. Now the draft is varied from H = 1.16 to H = 3.77 ft. The calculations were carried out for upper cylinder diameters of 0.32 and 0.36 ft respectively. Only these relatively large upper cylinder diameters were assumed because the effect of reduction in draft was of prime interest. So the diameter of the large cylinder must increase, and with it the wave inertial force. Therefore, a larger wave displacement force is needed to offset the inertial force. Hence, the larger upper cylinder diameter. The increased added mass (increasing as the third power of the large cylinder diameter) will also yield a low natural frequency in spite of the increased restoring coefficient resulting from the larger upper cylinder diameters of 0.32 and 0.36 ft, respectively. The resulting response operators are depicted in Figures 19 and 20. No bottom flanges were used in these cases.

G. Artificially Induced Added Mass

The effect of a large artificially induced added mass was studied as a conclusion to the single column investigation. Such added mass can be generated through the use of flanges as discussed in Section E, or by some suitable grillage work at the bottom of the cylinder. To counteract the considerable inertial forces to be assumed, the upper cylinder diameter was increased first to 0.36 and then to 0.40 ft (55.4 and 61.6 ft, full scale). The grillage work was assumed to be located first at a depth of 2.40 ft (370 ft, full scale) and then at 3.00 ft (462 ft, full scale). The grillage was assumed to be of such dimensions as to achieve an added mass of 1, 2, 3, and 4 fold over the basic mass of the whole column. Figures 21 and 22 depict the computed optimum response operators. All other combinations of size of grillage and/or depth of submergence yielded larger responses.

Finally, the heaving response of columns having even further increased upper cylinder diameter, namely 0.44 ft (67.8 ft, full scale) and 0.48 ft (73.9 ft, full scale) was calculated. A grillage or artificial reef of induced added mass equal to the basic mass of the column was used. These response operators are depicted in Figure 23.

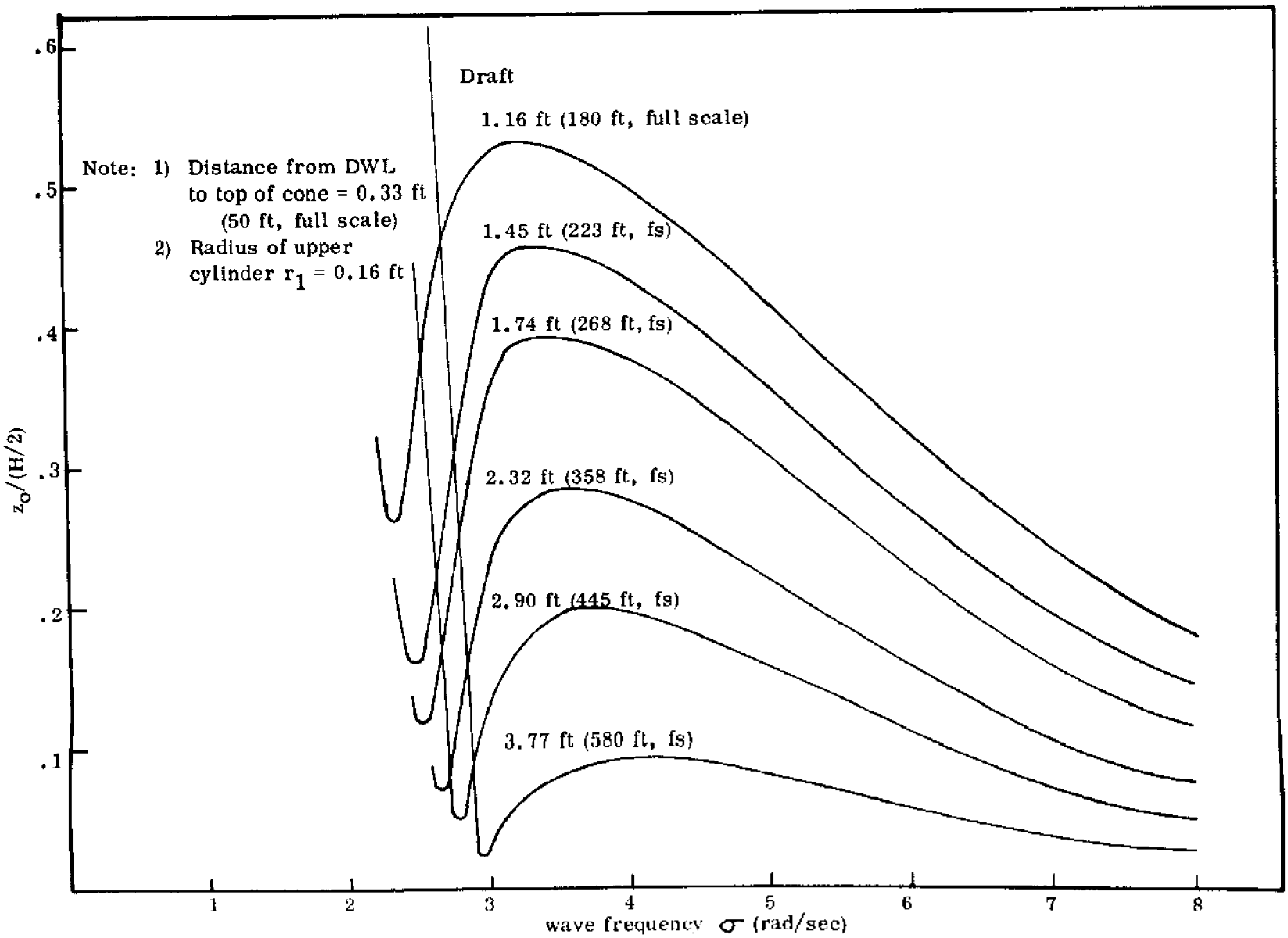

Fig. 19 Unit amplitude response in heave with variation of draft for r_1 = 0.16 ft.

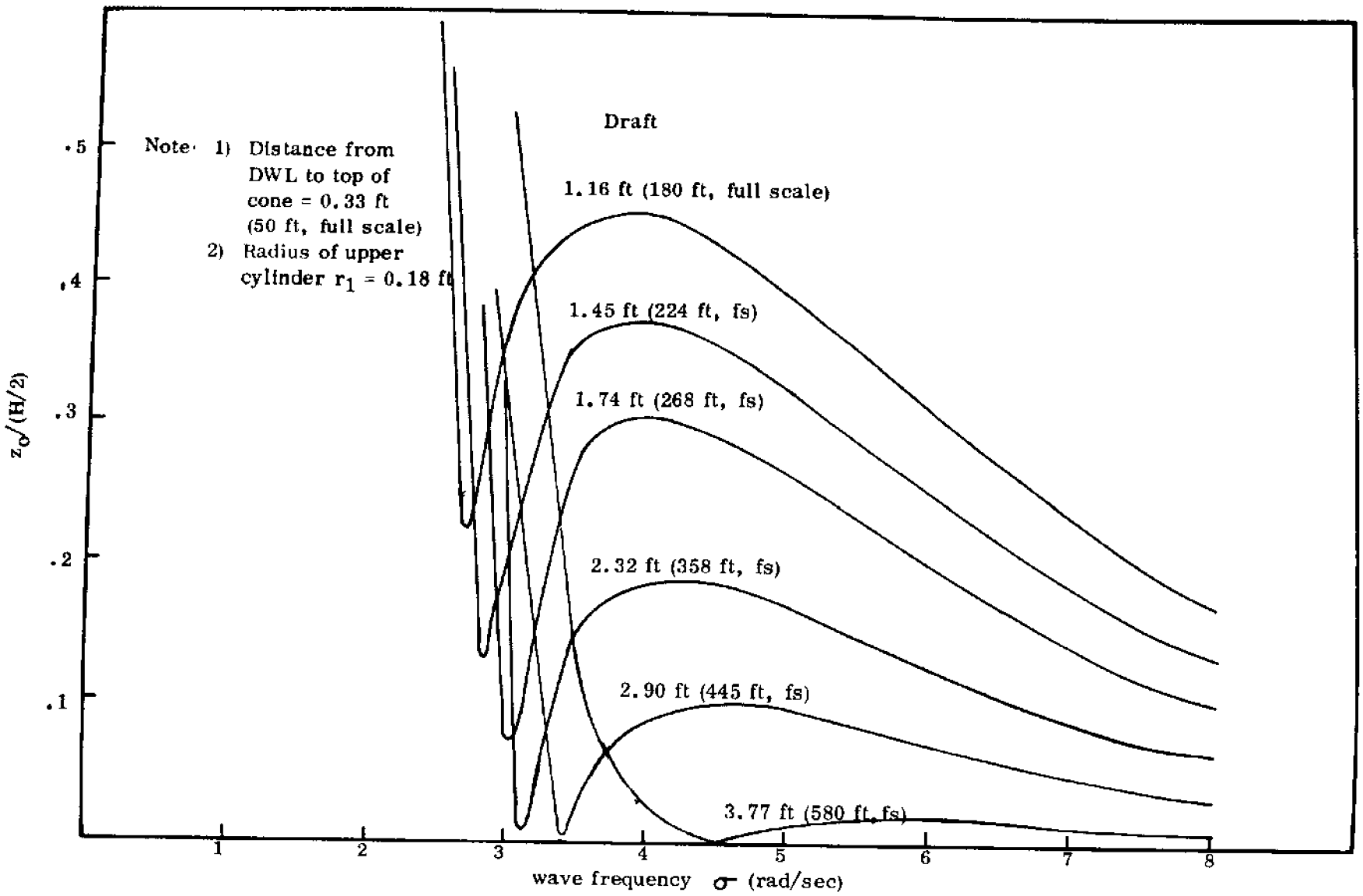

Fig. 20 Unit amplitude response in heave with variation of draft for r_1 = 0.18 ft.

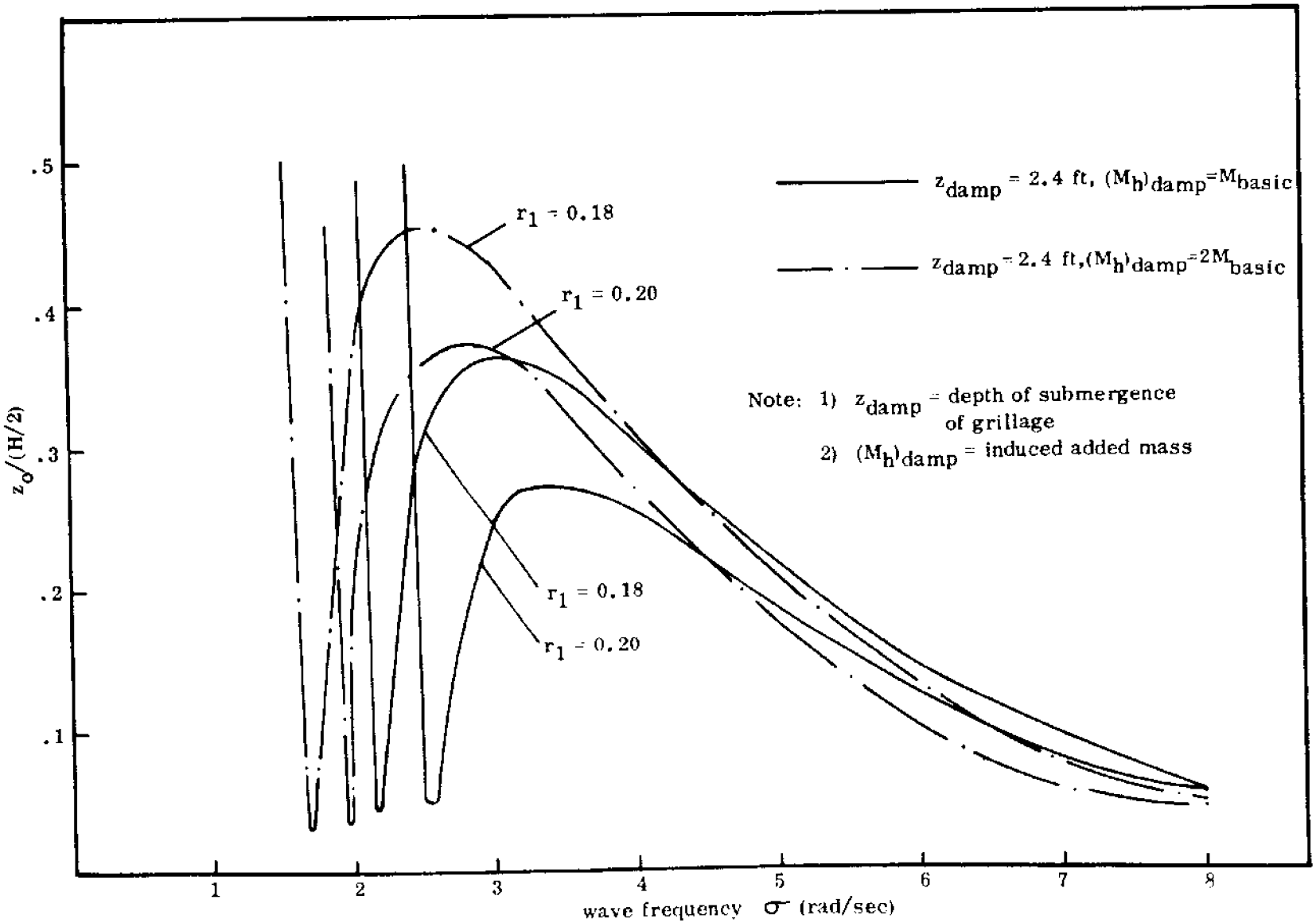

Fig. 21 Unit amplitude response in heave for artificially induced mass and increased upper cylinder diameter.

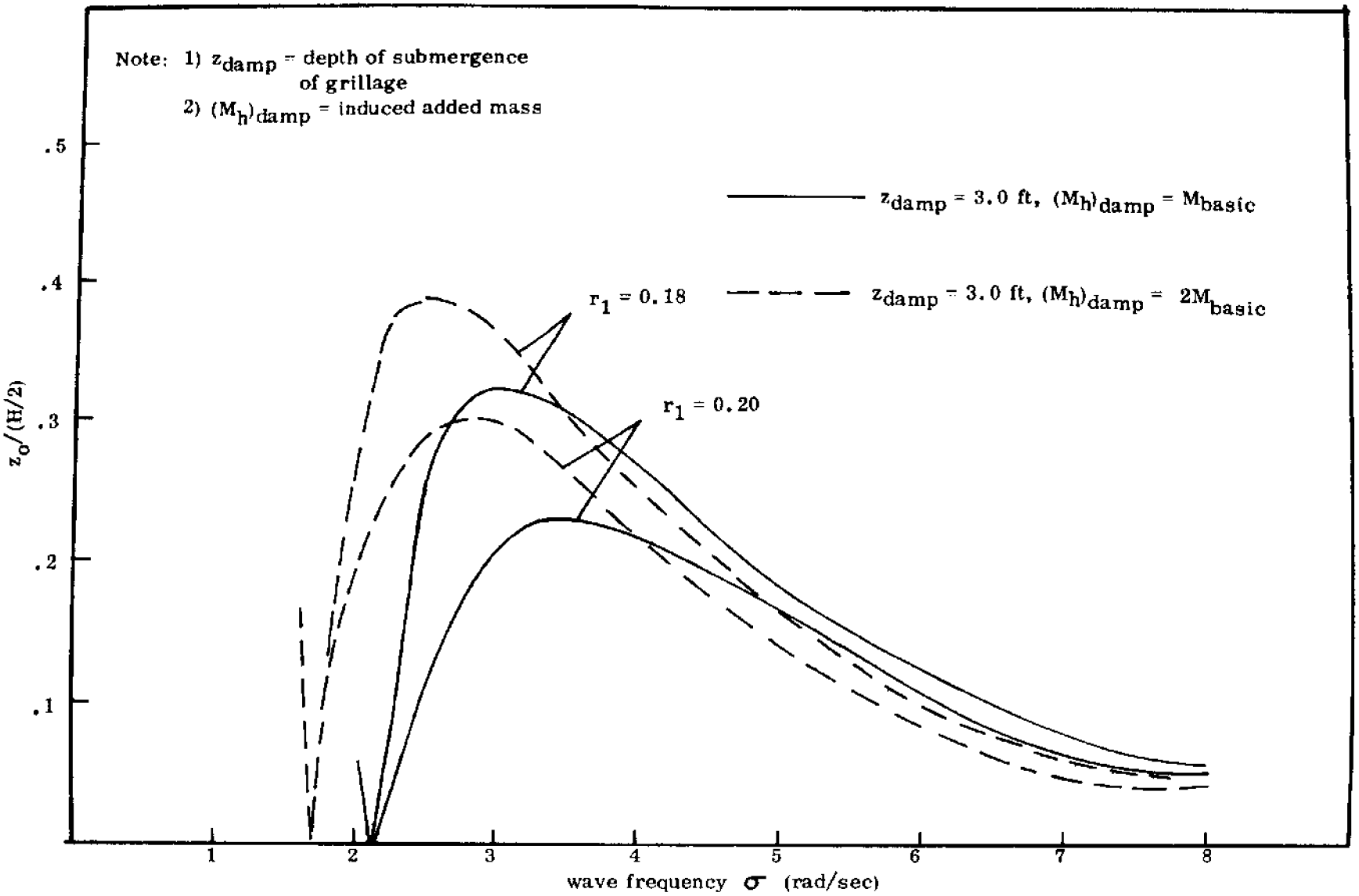

Fig. 22 Unit amplitude response in heave for artificially induced mass and increased upper cylinder diameter.

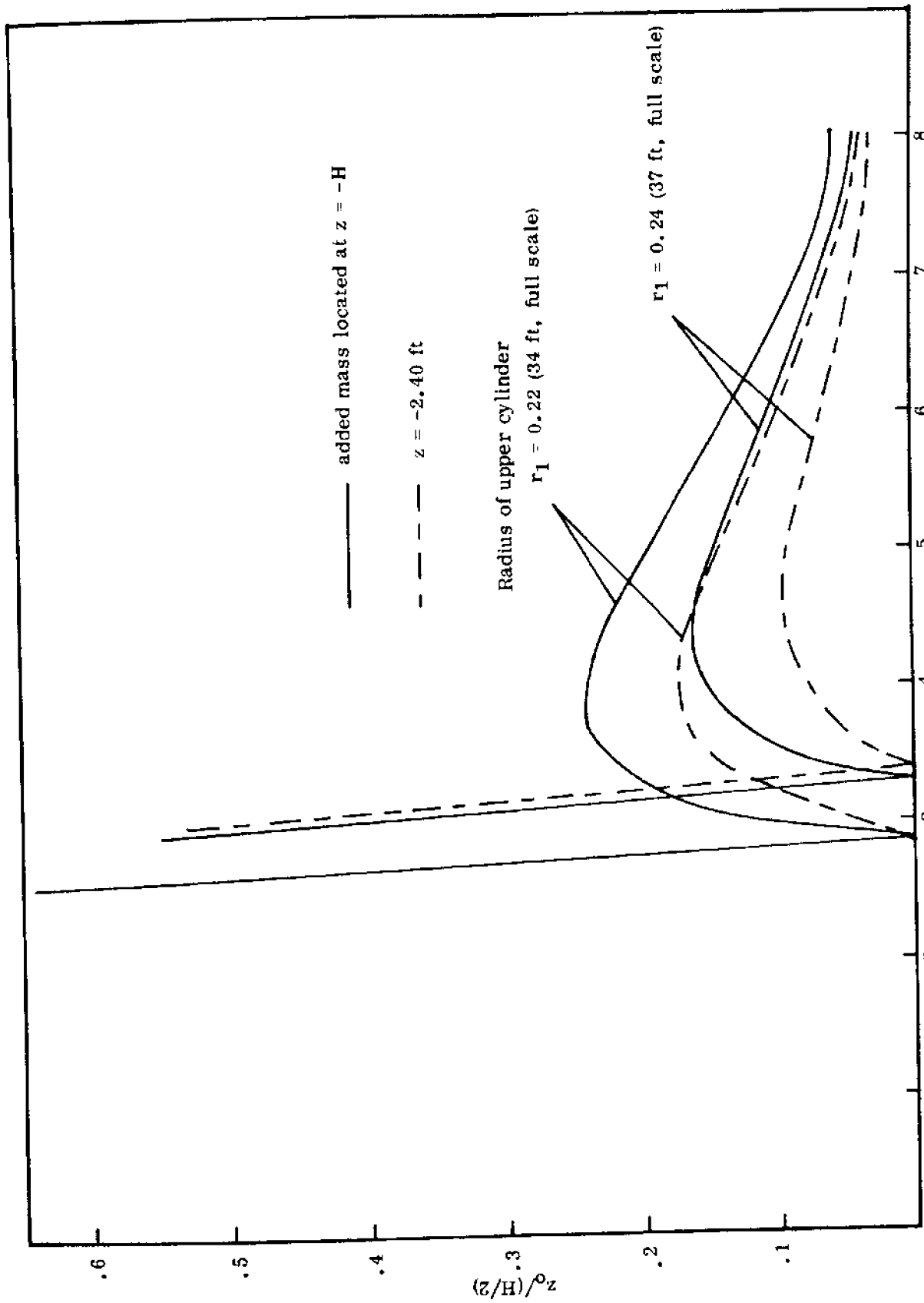

Fig. 23 Unit amplitude response in have for very large upper cylinder diameter and addition of artificially induced mass equal in quantity to basic mass.

V. MODULE

A. Hydrostatics

The hydrostatic calculations commonly used in naval architecture are carried out to obtain the required data for buoyancy and intact stability of a module. A list of the pertinent quantities and the corresponding formulas is given below.

The computer program developed to correspond to these formulas is labeled Program CB. The five major parts of a single column (h_1 through h_5 in Fig. 24) are each divided vertically into five sections, or water lines. All the various quantities in the stability calculations are then evaluated for the 25 water lines so obtained. Water line no. 21 is the design water line (DWL), and no. 1 is the base line.

The quantities for a single column are:

$\Delta z_i = z_i - z_{i-1}$ — distance between adjacent water lines

$A_{\omega,i} = r_i^2 \pi$ — water plane area

$\Delta V_i = (A_{\omega,i} + A_{\omega,i-1}) \cdot \Delta z_i$ — displaced volume (single column) between two water lines

$\Delta A_{c,i} = r_i \cdot \Delta z_i$ — cross-sectional area between two water lines

$\Delta D_i = \Delta V_i \cdot \rho g$ — corresponding displacement

$(D_i) = \sum \Delta D_i$ — displacement to WL - i

$V_i = \sum \Delta V_i$ — displacement volume up to WL - i

$A_{c,i} = \sum \Delta A_{c,i}$ — cross sectional area up to WL - i

$$KB_i = \sum_{n=1}^{i} (\Delta V_n)\left(\frac{z_n + z_{n-1}}{2}\right) / V_i$$

The quantities for a module are:

$L \equiv$ number of columns

$(D_i)_{tot} = L \cdot D_i$ — displacement to WL - i

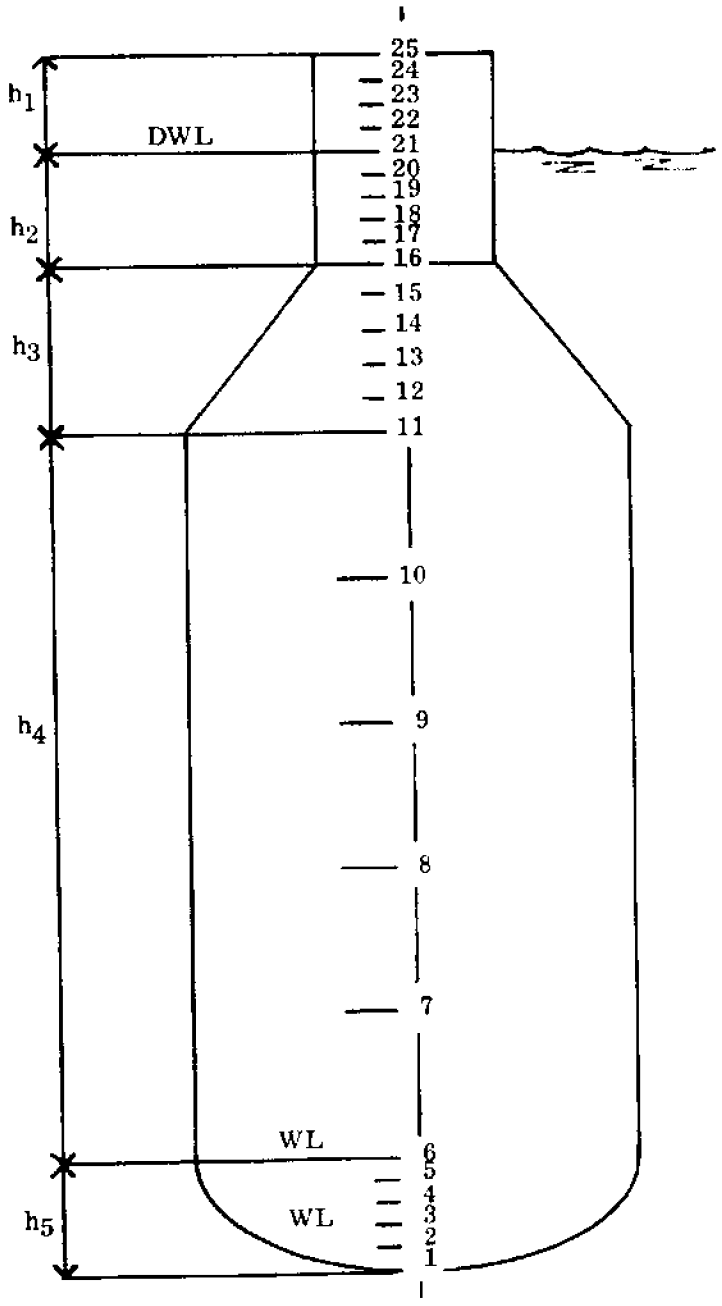

Fig. 24 Definition sketch for vertical subdivision (water lines) of a column.

$(V_i)_{tot} = L \cdot V_i$	displacement volume to WL
$(A_{\omega,i})_{tot} = L \cdot A_{\omega,i}$	water plane area
$(TPI_i)_{tot} = (A_{\omega,i})_{tot}/420.$	tons per inch at WL-i
$(C_{\omega,i})_L = A_{\omega,i}\left[\sum_{\ell=1}^{L} x_\ell\right]/(A_{\omega,i})_{tot}$	longitudinal center of flotation
$(C_{\omega,i})_T = A_{\omega,i}\left[\sum_{\ell=1}^{L} y_\ell\right]/(A_{\omega,i})_{tot}$	transverse center of flotation
$I_{xx,i} = A_{\omega,i} \sum_{\ell=1}^{L} x_\ell^2$	second central moment of water plane area about y-axis
$I_{yy,i} = A_{\omega,i} \sum_{\ell=1}^{L} y_\ell^2$	second central moment of water plane area about x-axis
$(I_{xx,i})_T = I_{xx,i} - (C_{\omega,i})_L^2 \cdot (A_{\omega,i})_{tot}$	corresponding second moments about axes through centers of flotation
$(I_{yy,i})_L = I_{yy,i} - (C_{\omega,i})_T^2 \cdot (A_{\omega,i})_{tot}$	
$(BM_i)_T = (I_{xx,i})_T/(V_i)_{tot}$	distance between center of buoyancy and metacenter
$(BM_i)_L = (I_{yy,i})_L/(V_i)_{tot}$	
$(\overline{KM}_i)_T = \overline{KB}_i + (\overline{BM}_i)_T$	height of metacenter above base line
$(\overline{KM}_i)_L = \overline{KB}_i + (\overline{BM}_i)_L$	
$(R_i)_T = (D_i)_{tot} \cdot \overline{BM}_T \cdot \sin 1^o$	moment to trim 1 degree (if CG and CB coincide)
$(R_i)_L = (D_i)_{tot} \cdot \overline{BM}_L \cdot \sin 1^o$	
$(MTI_i)_T = (D_i)_{tot} \cdot (\overline{BM}_i)_T \cdot \frac{1}{12\ell_T}$	moment to trim 1 inch at outer perimeter
$(MTI_i)_L = (D_i)_{tot} \cdot (\overline{BM}_i)_L \cdot \frac{1}{12\ell_L}$	
ℓ_T	length of platform (between perpendiculars)
ℓ_L	"beam" of platform (between perpendiculars)

B. Response Operators in Six Degrees of Freedom

The equations of motion of a platform comprised of an arbitrary number of columns are derived next. The algorithm for calculating the response operators of such a platform will be general and can be used for the calculation of a single module, a cluster of modules, or the complete core-ring. The platform is thereby assumed to be a rigid body. The linearized equations of motion in six degrees of freedom can be obtained by formally extending those of the linear oscillator of one degree of freedom to six degrees of freedom. The equations, written in matrix notation, are then

$$[a]\{\ddot{x}\} + [b]\{\dot{x}\} + [c]\{x\} = \{f(t)\}$$

where

$[a]$ = inertial matrix

$[b]$ = matrix of damping coefficients

$[c]$ = matrix of restoring coefficients

$\{x\}$ = displacement vector

$\{f(t)\}$ = wave force vector

The elements of the matrixes (6 x 6) and of the wave force vectors are described by Ochi and Vuolo.[1] The matrix of the restoring coefficients includes those due to elastic restoration from a mooring system, if any.

Assuming steady state response

$$\{x\} = \{H(j\sigma)\}\, e^{j\sigma t}$$

to sinusoidal waves

$$\xi(t) = \frac{H}{2} e^{j[k(x\cos\chi - y\sin\chi) - \sigma t]}$$

---

[1] M.K. Ochi and R.M. Vuolo, "Seakeeping Characteristics of a Multi-Unit Ocean Platform." Presented at Spring Meeting of Society of Naval Architects and Marine Engineers, Honolulu, Hawaii, May 25-28, 1971.

we obtain after substitution:

$$\left[-\sigma^2\,[a] + j\,[b] + [c]\right]\left\{H(j\sigma)\right\} = \left\{Q(j\sigma)\right\}$$

or

$$[\alpha]\left\{H(j\sigma)\right\} \qquad \left\{Q(j\sigma)\right\}$$

Hence the complex frequency response operators in all six degrees of freedom are obtained as

$$\left\{H(j\sigma)\right\} = [\alpha]^{-1}\left\{Q(j\sigma)\right\}$$

The unit amplitude responses are then

$$\left\{x_o\right\} = \left\{|H(j\sigma)|\right\}$$

and the phase response operators are

$$\left\{\epsilon\right\} = \left\{\arctan \frac{I_m\,[H(j\sigma)]}{Re\,[H(j\sigma)]}\right\}$$

The computer program corresponding to this procedure of solution is labeled PLATF. The response operators are plotted in Figs. 25 through 29, for a module without horizontal connecting cylinders, and in Figs. 30 through 34 for a module with horizontal cylinders. In the corresponding calculations, a water depth of 14 ft is assumed because of the limited water depth at the available model testing facility. The influence of the limited water depth on the motions of the module is felt only for waves with frequencies less than 3 rad/sec. The effect is to reduce heaving motion and increase surging motion.

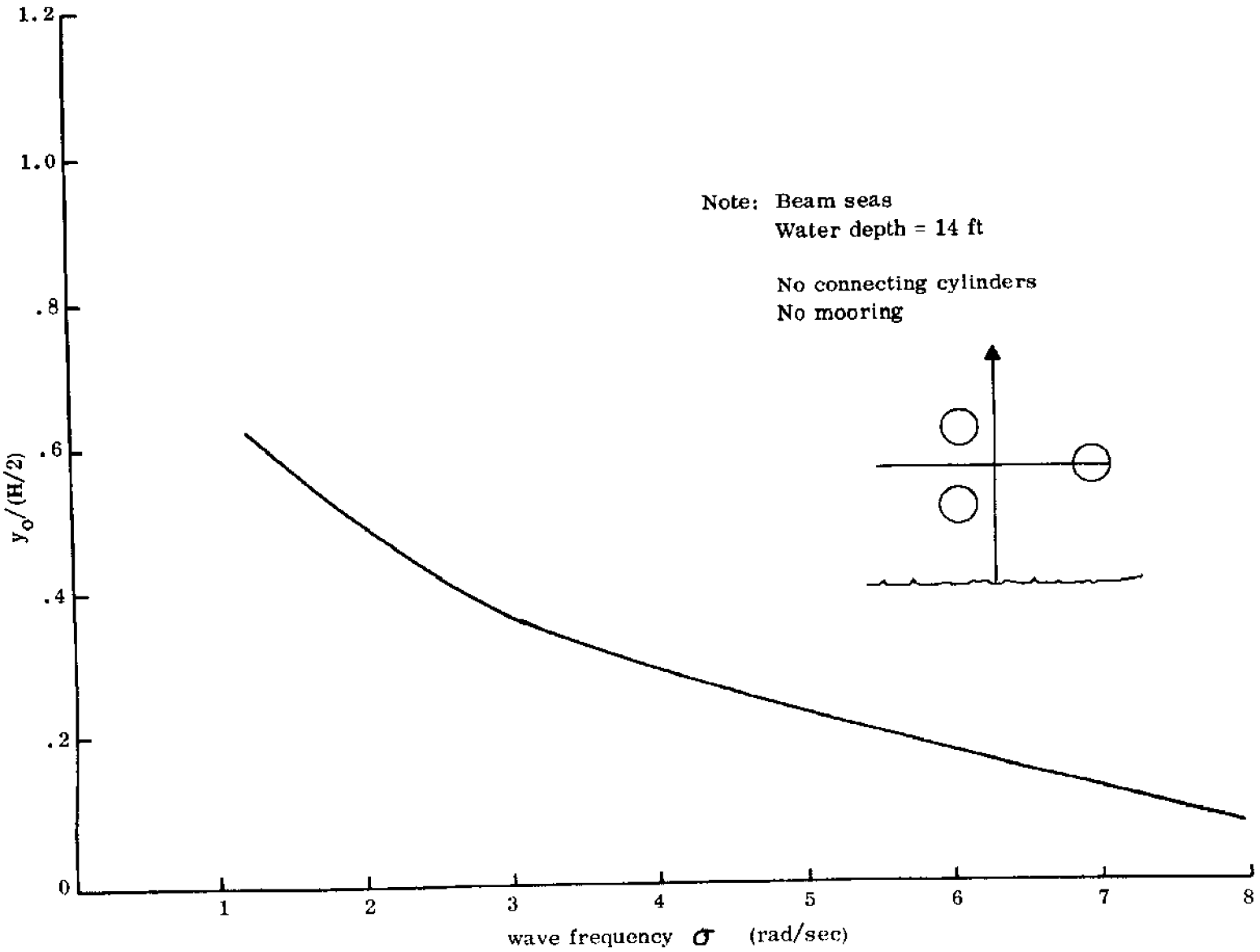

Fig. 25 Unit amplitude response in sway.

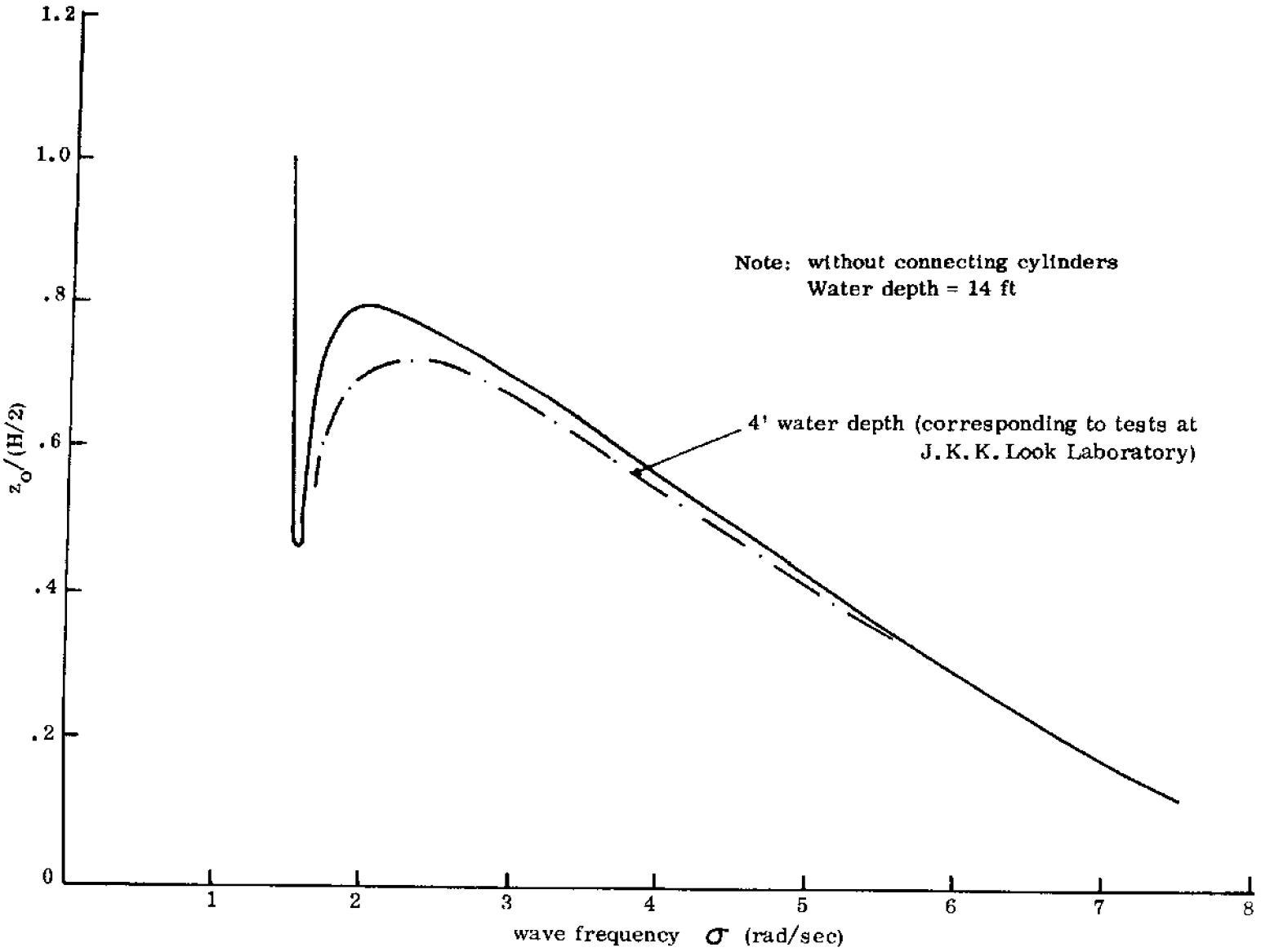

Fig. 26 Unit amplitude response in heave.

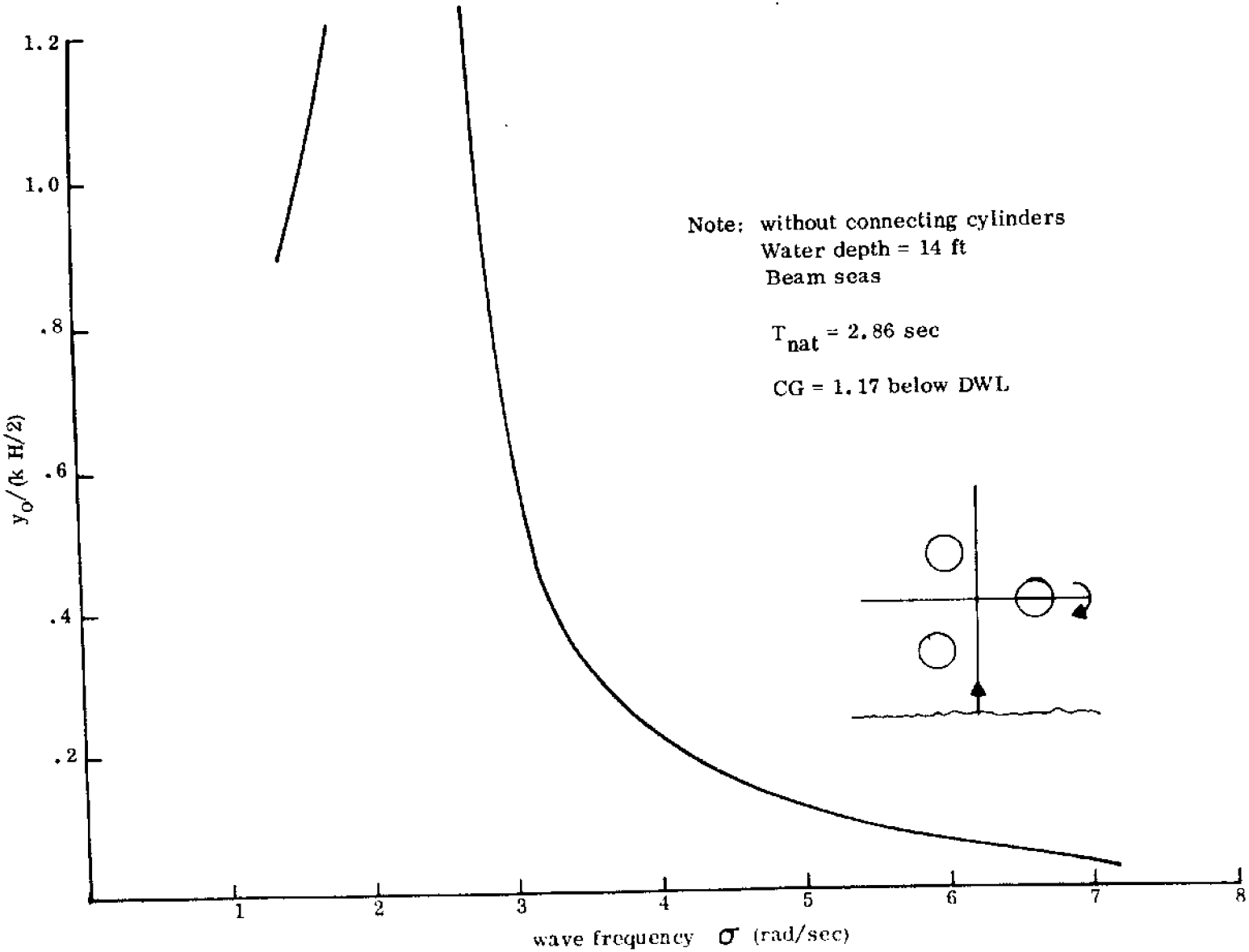

Fig. 27 Unit amplitude response in roll (normalized by wave slope, k H/2)

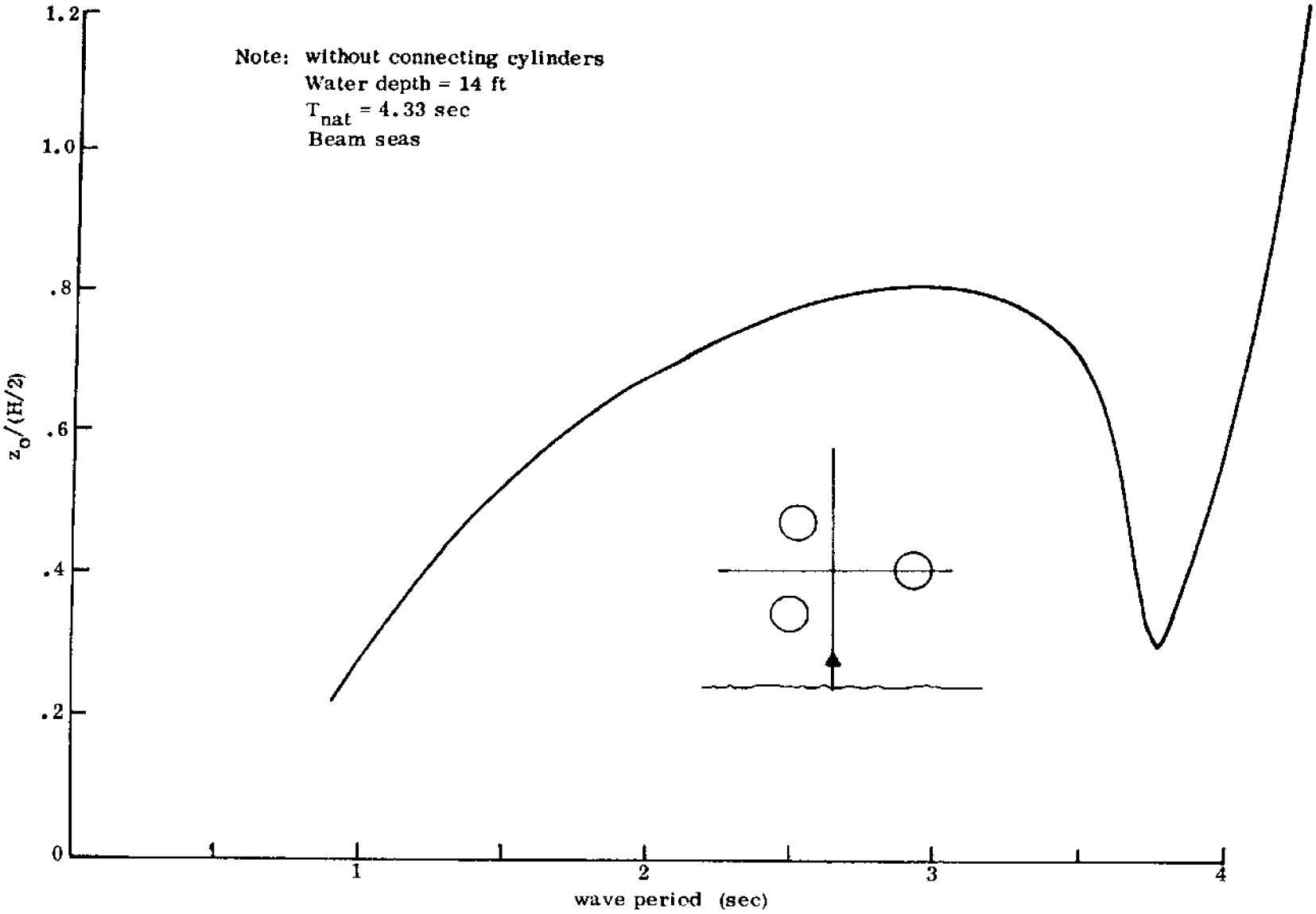

Fig. 28 Unit amplitude response in heave.

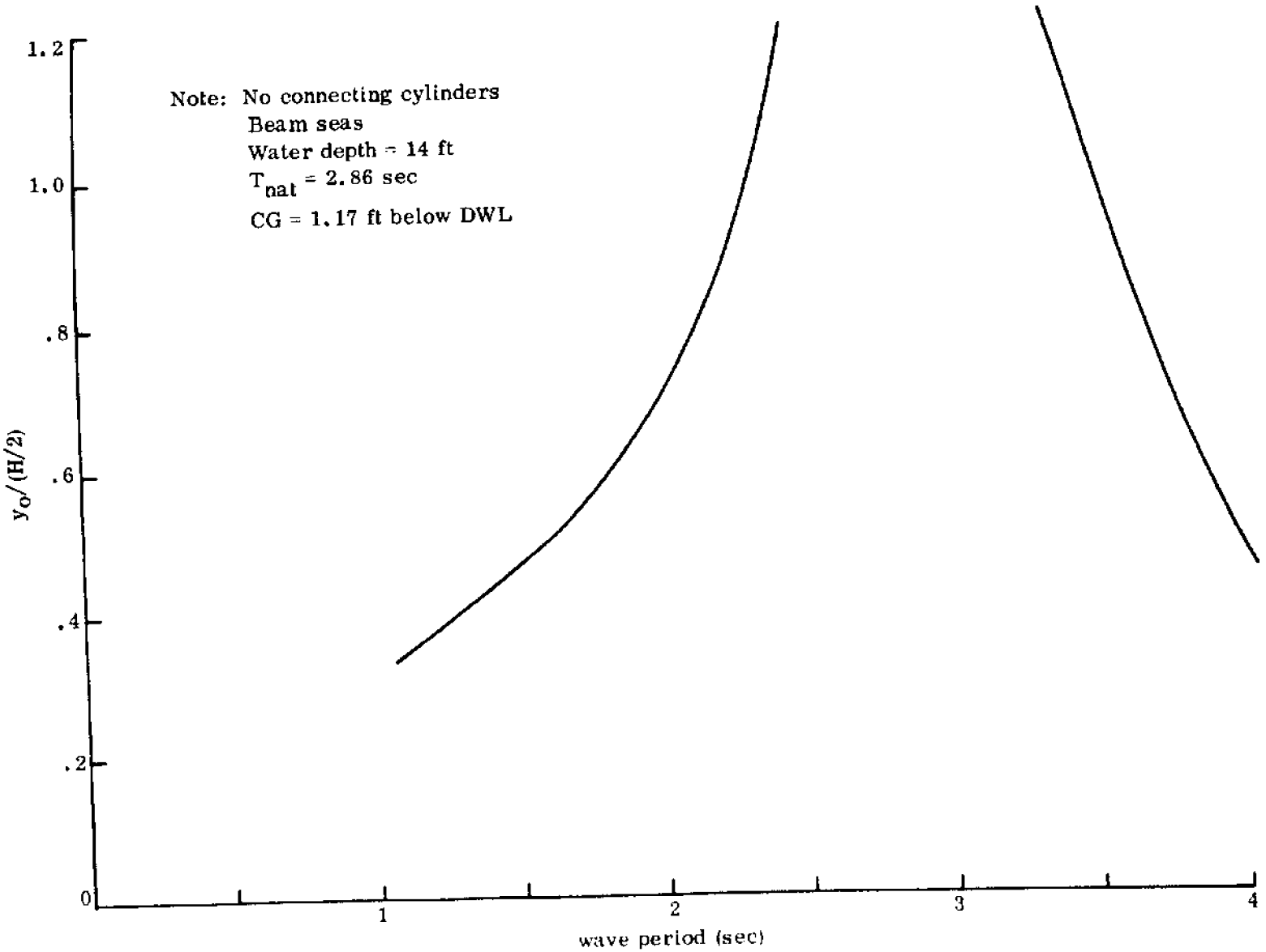

Fig. 29 Unit amplitude response in roll

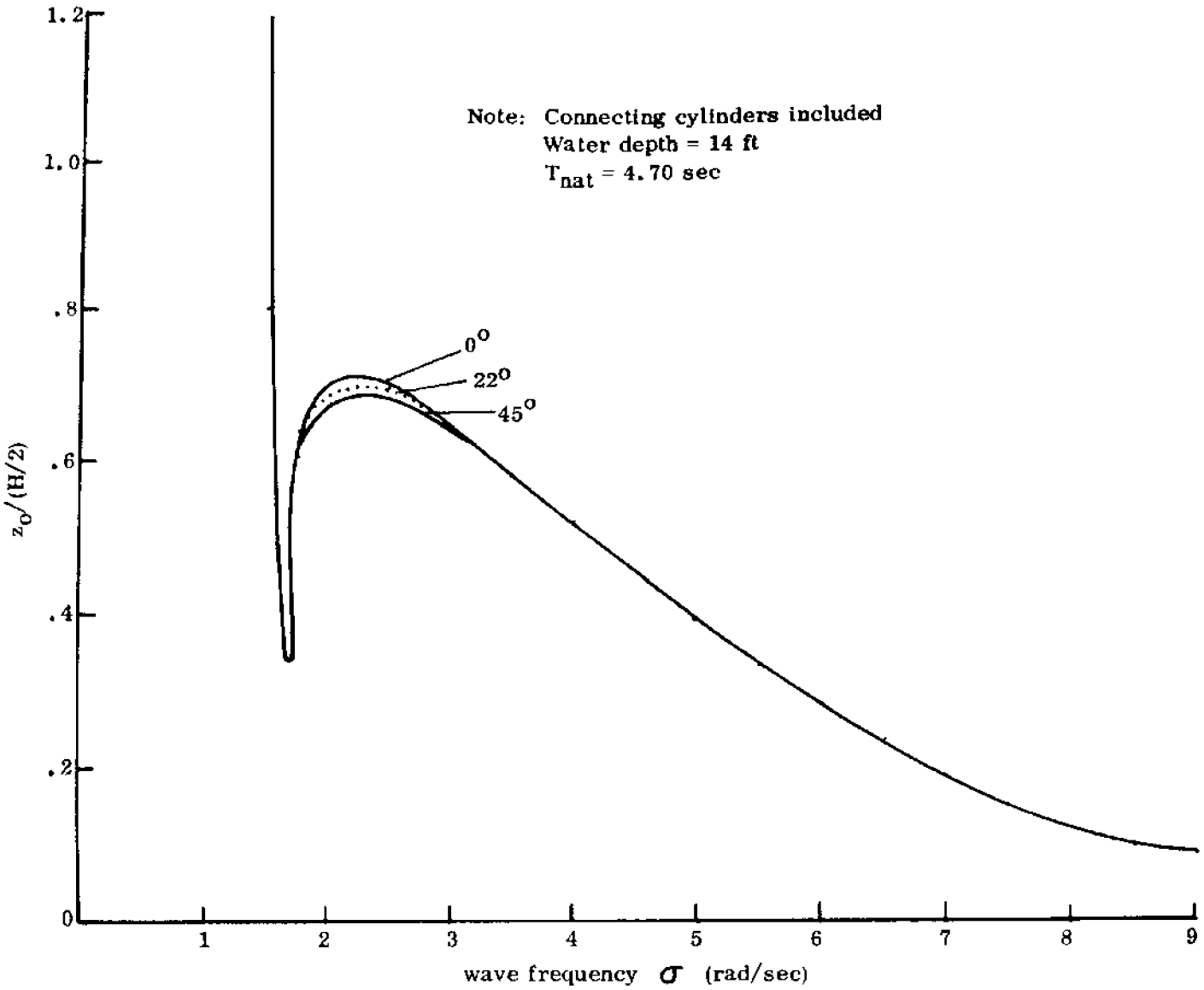

Fig. 30 Unit amplitude response of a module in heave.

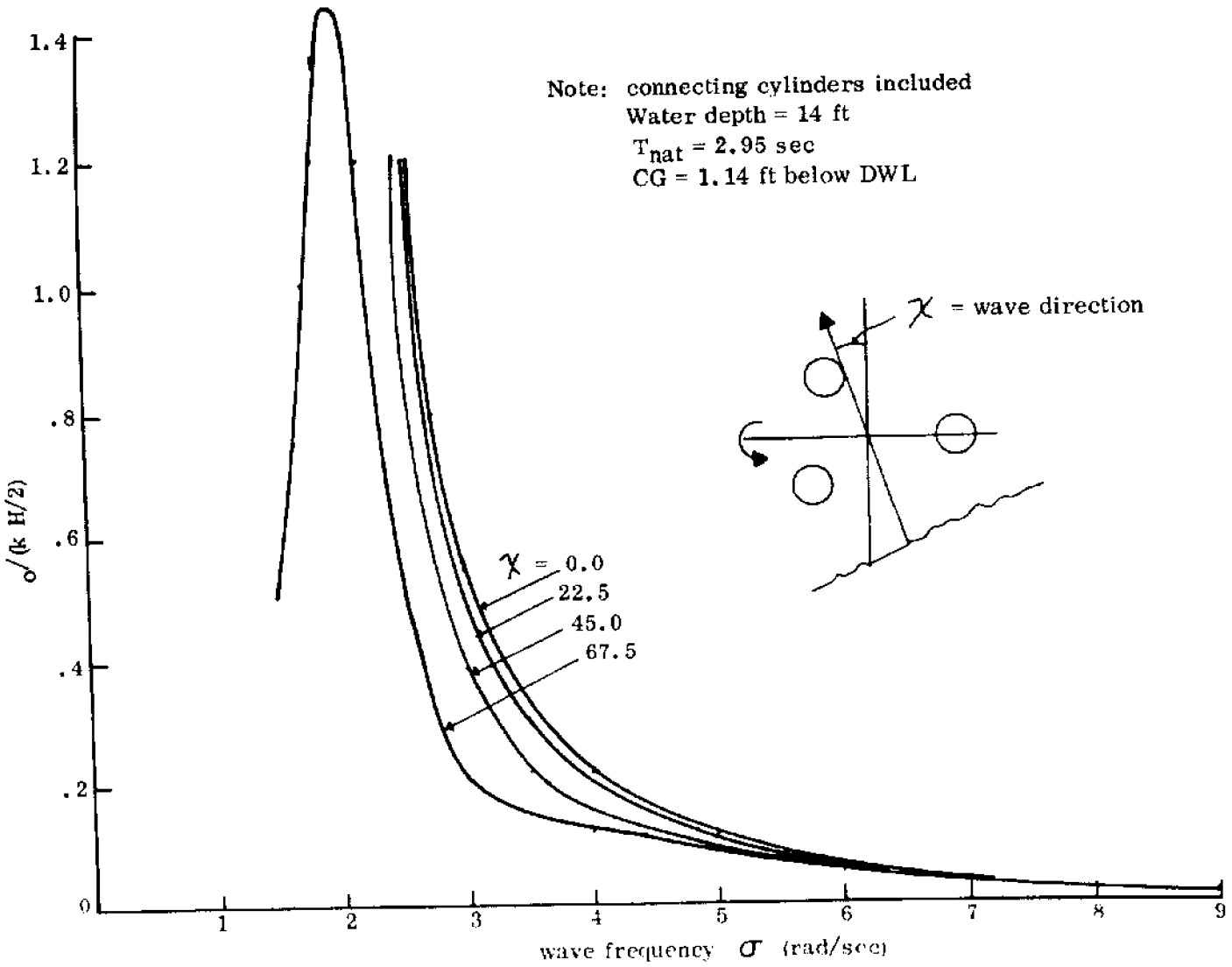

Fig. 31 Unit amplitude response of a module in roll.

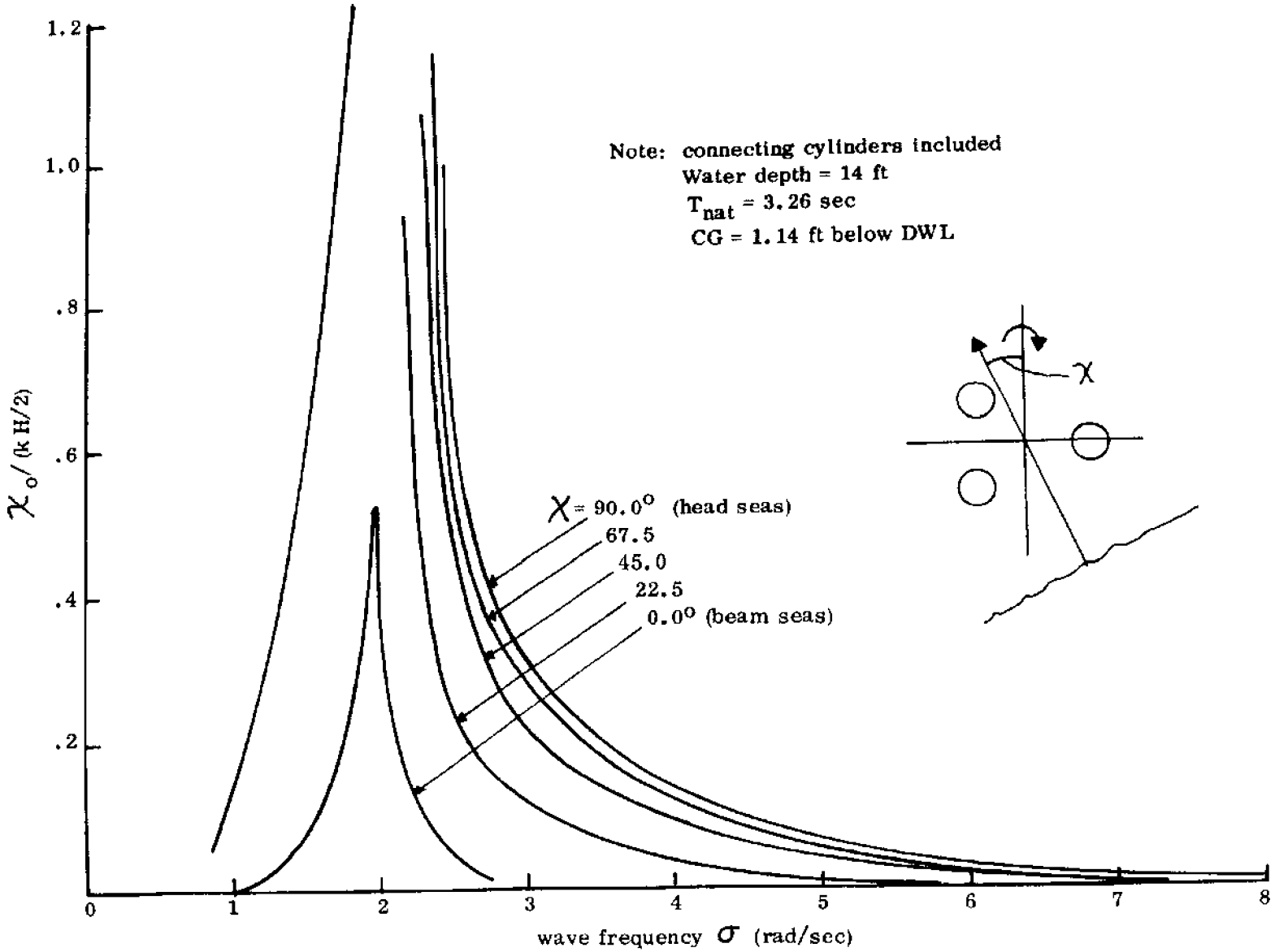

Fig. 32 Unit amplitude response of a module in pitch.

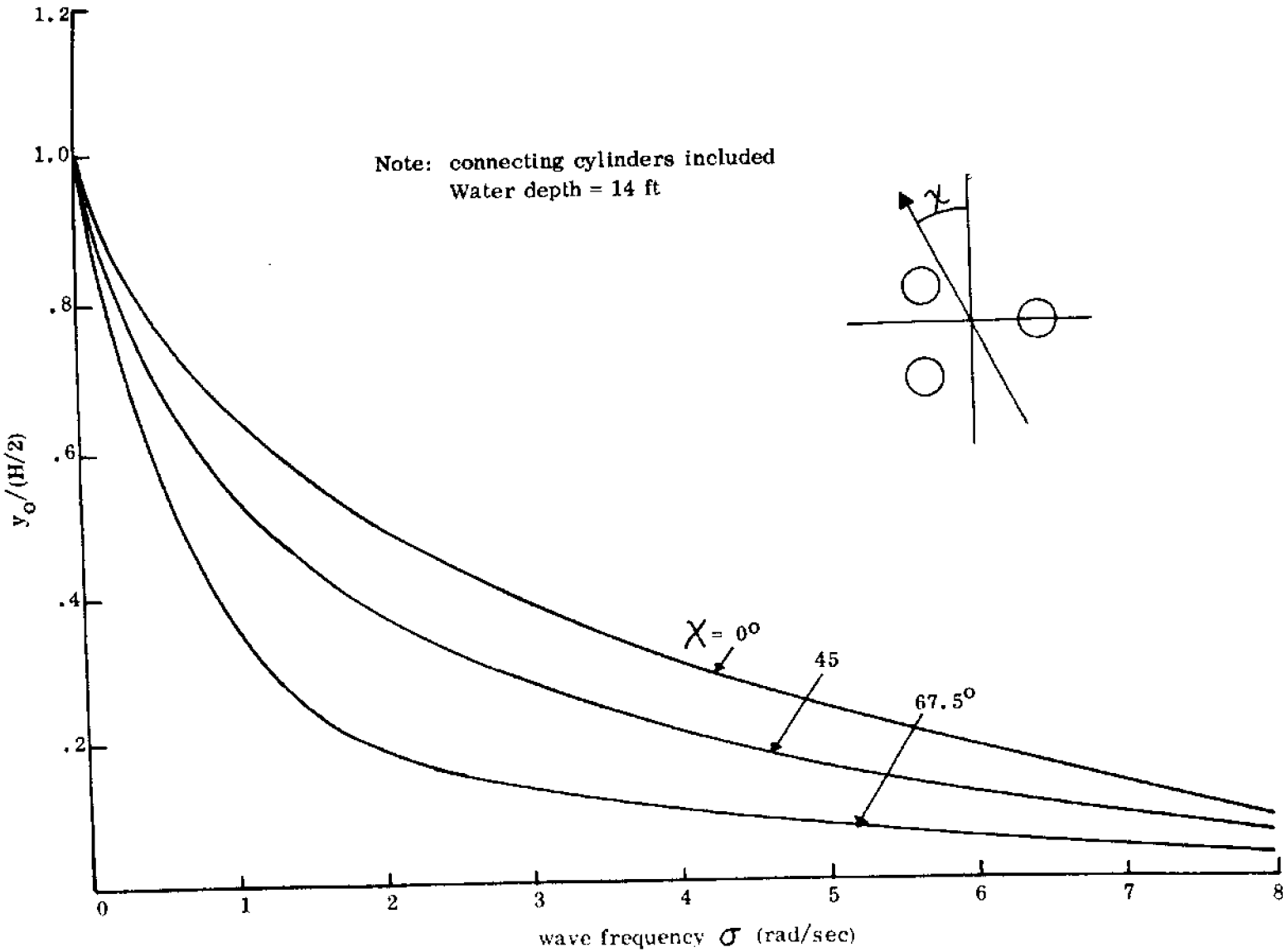

Fig. 33 Unit amplitude response of a module in sway.

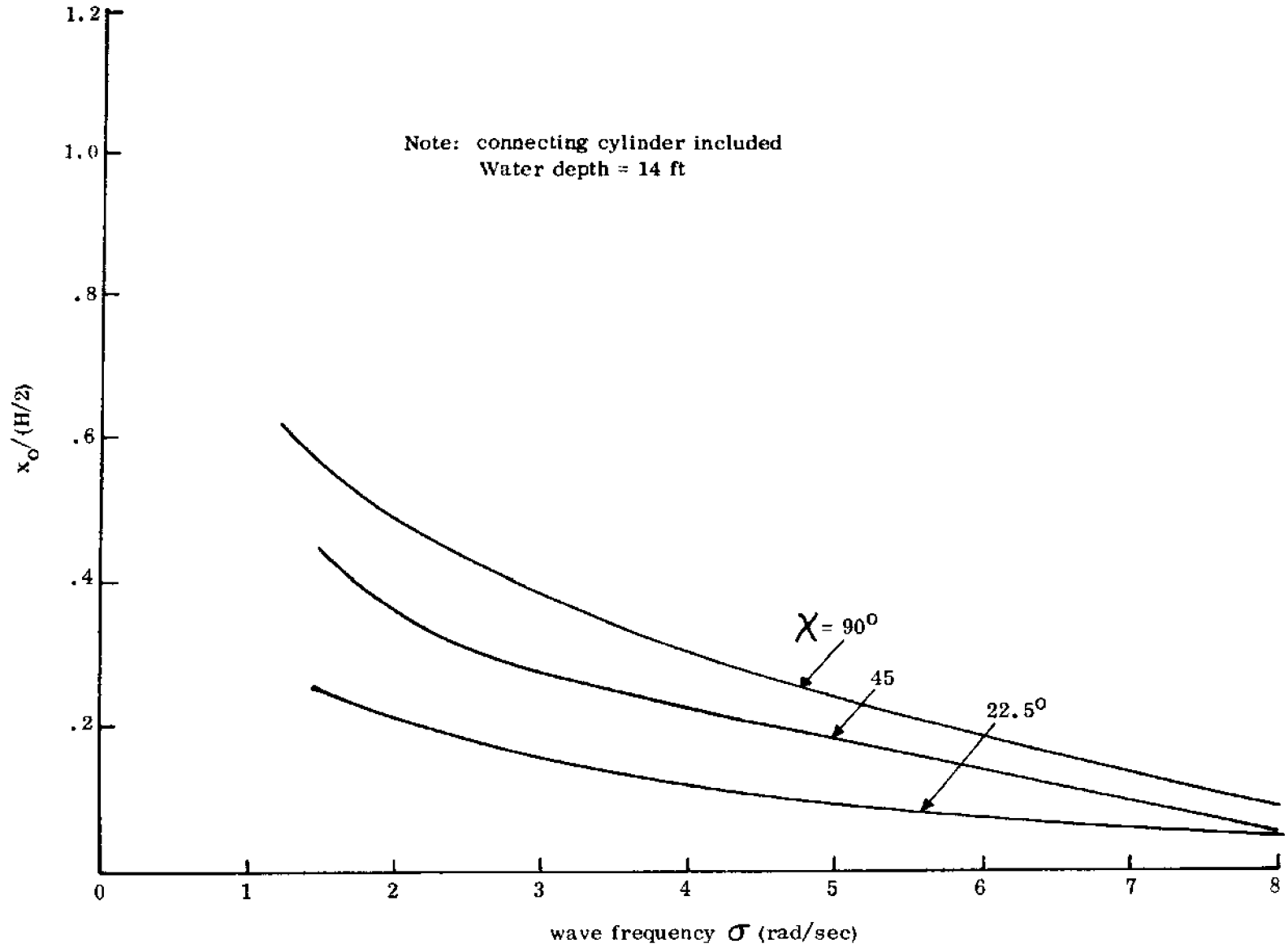

Fig. 34 Unit amplitude response of a module in surge.

VI. CORE-RING

A. Hydrostatics

The same quantities as those described in Section V.A for the module were evaluated for the core-ring using the computer and Program CB. Calculations were carried out for a large number of column configuration, but the locations of the columns in the core-ring were not altered. The calculations were carried out for 24 configurations corresponding to the following parameters:

Diameter of upper cylinder (single column): 30.0, 36.0, 42.0, 48.0, 54.0, 60.0, 66.0, 72.0 ft.

Design draft: 180.0, 224.0, 268.0 ft.

The results are contained in a volume of tables. For convenience, the parameters TPI, Δ, CB, A_c have been plotted for the following cases (Figs. 35-43):

draft	180.0			224.0			268.0		
upper diameter	30.0	48.0	72.0	30.0	48.0	72.0	30.0	48.0	72.0

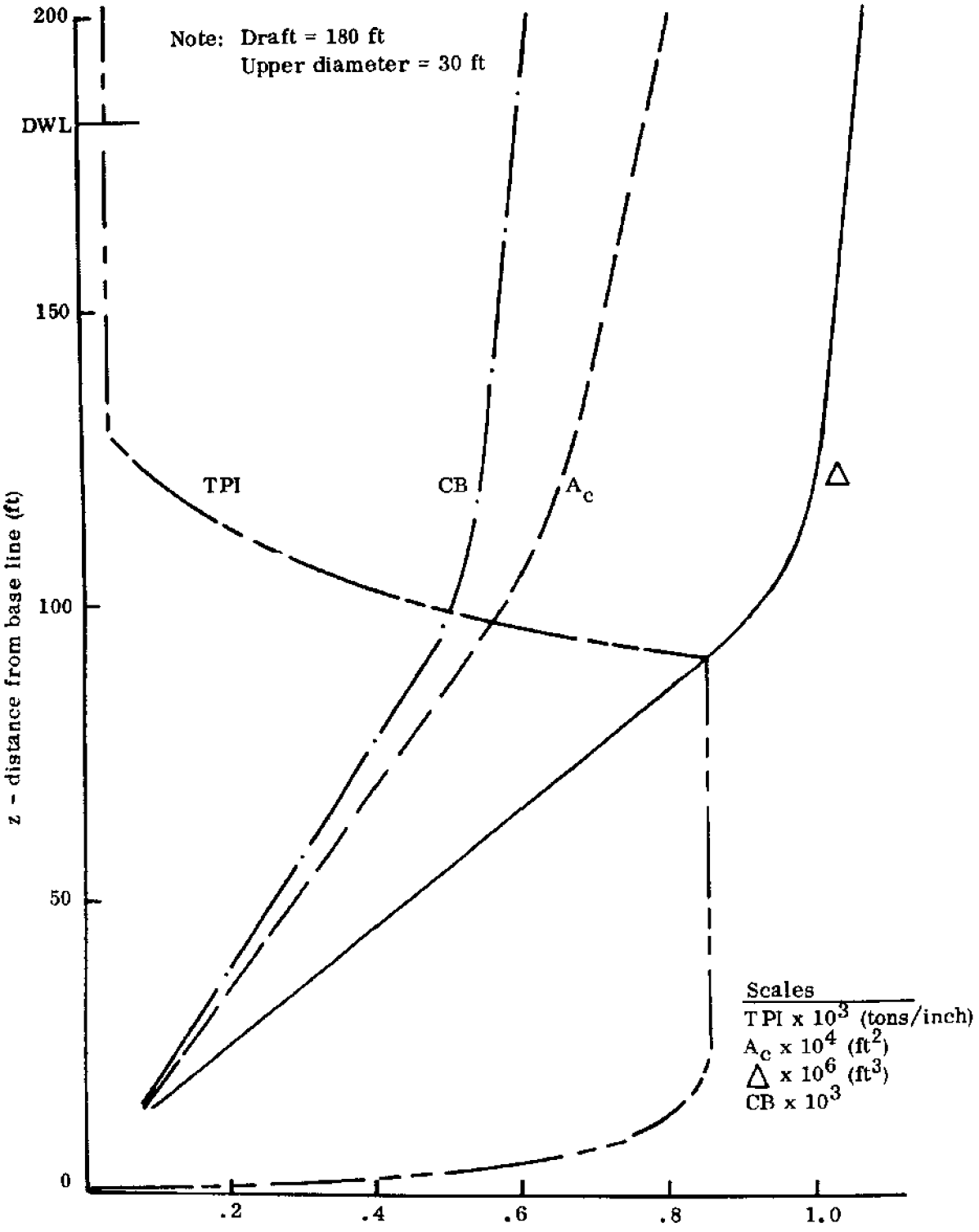

Fig. 35 Curves of form.

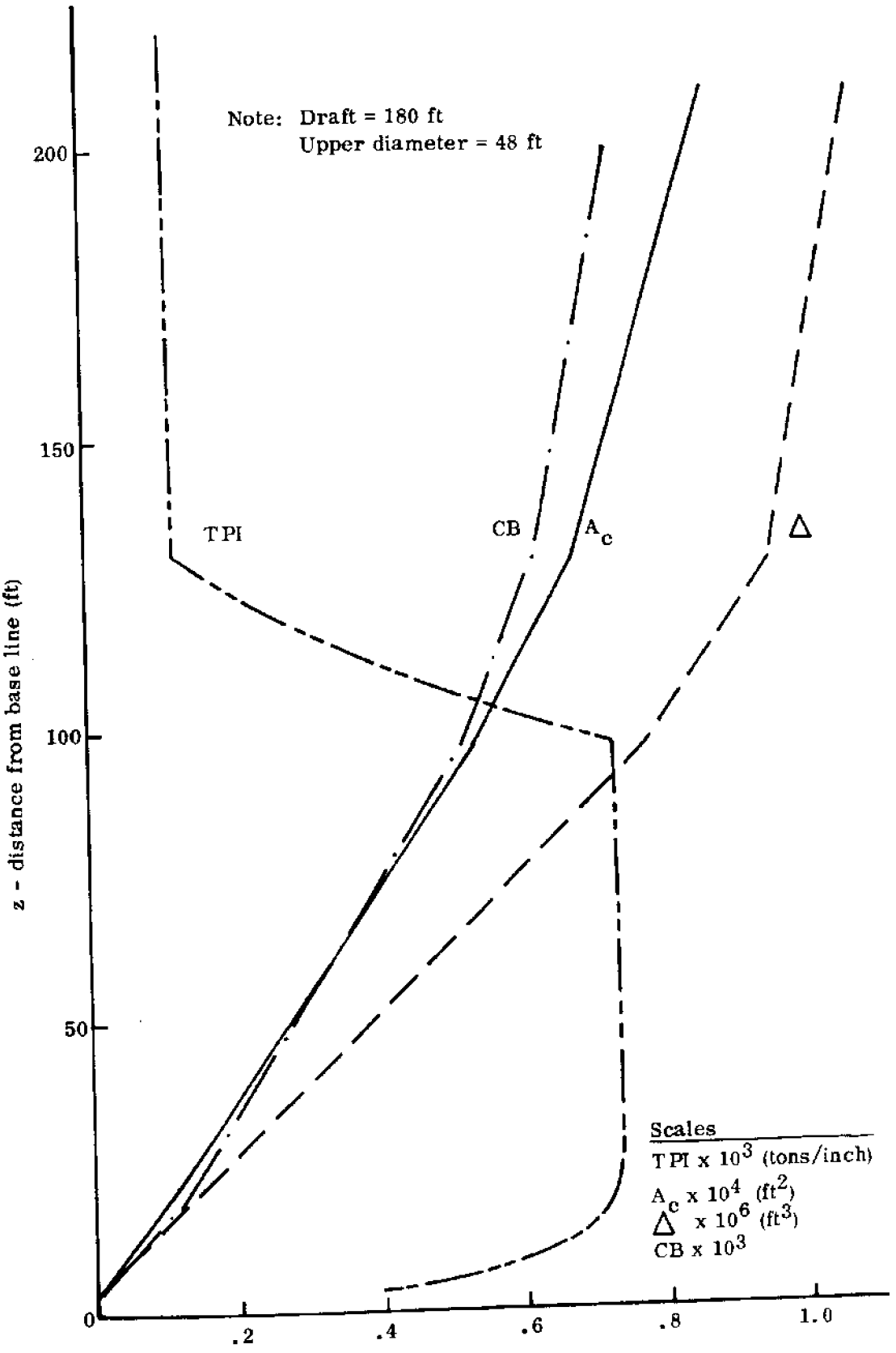

Fig. 36 Curves of form.

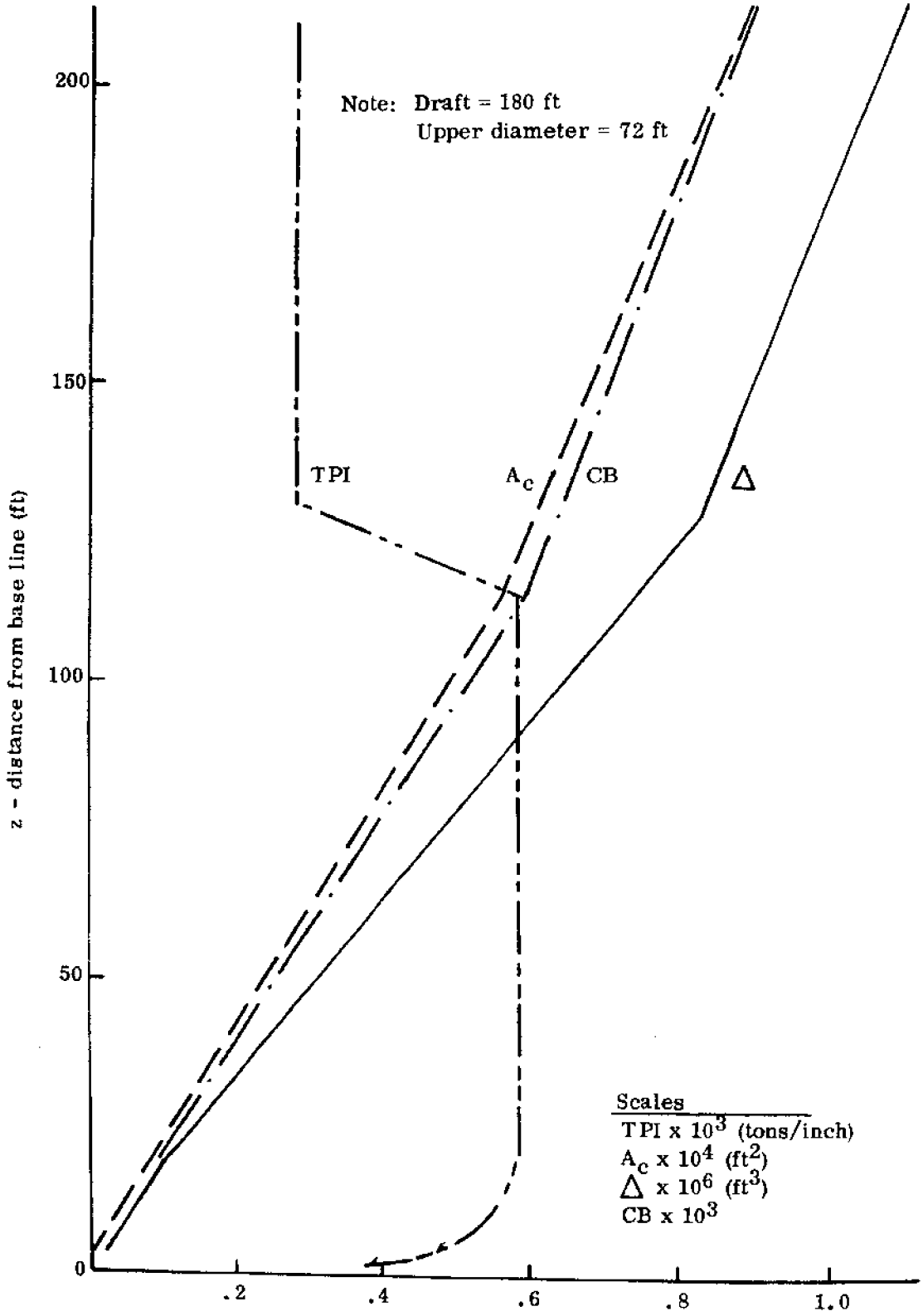

Fig. 37 Curves of form.

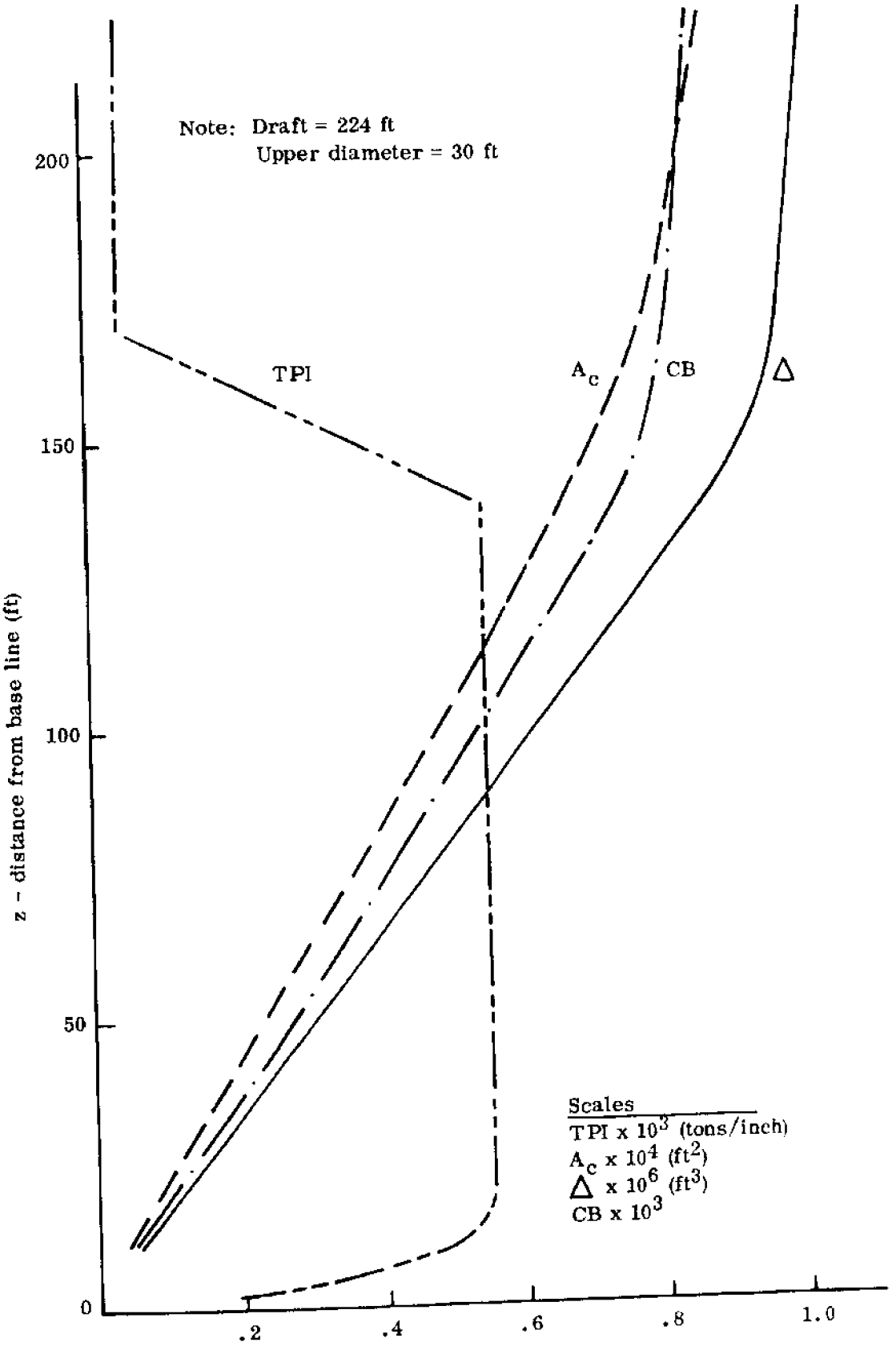

Fig. 38 Curves of form

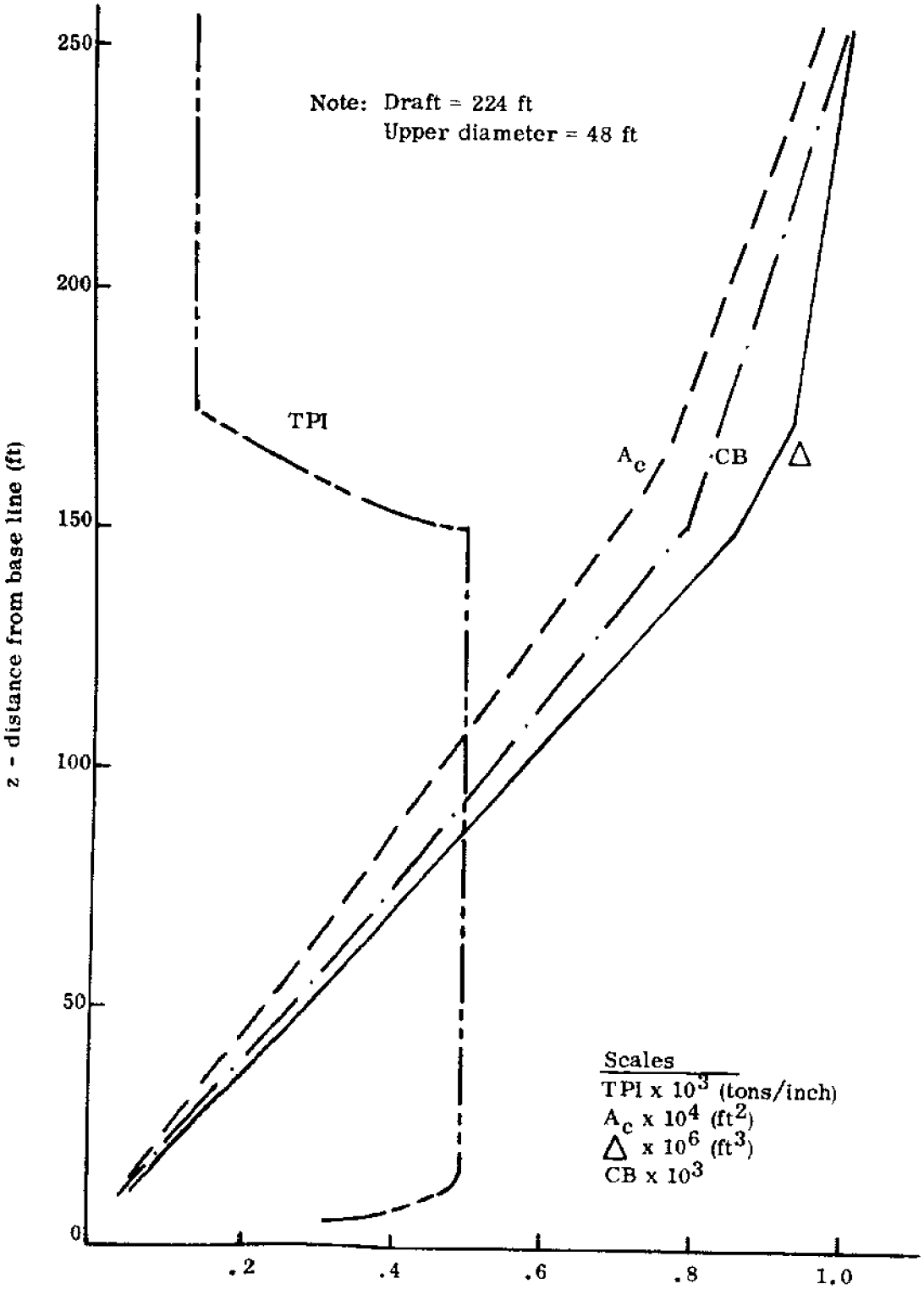

Fig. 39 Curves of form.

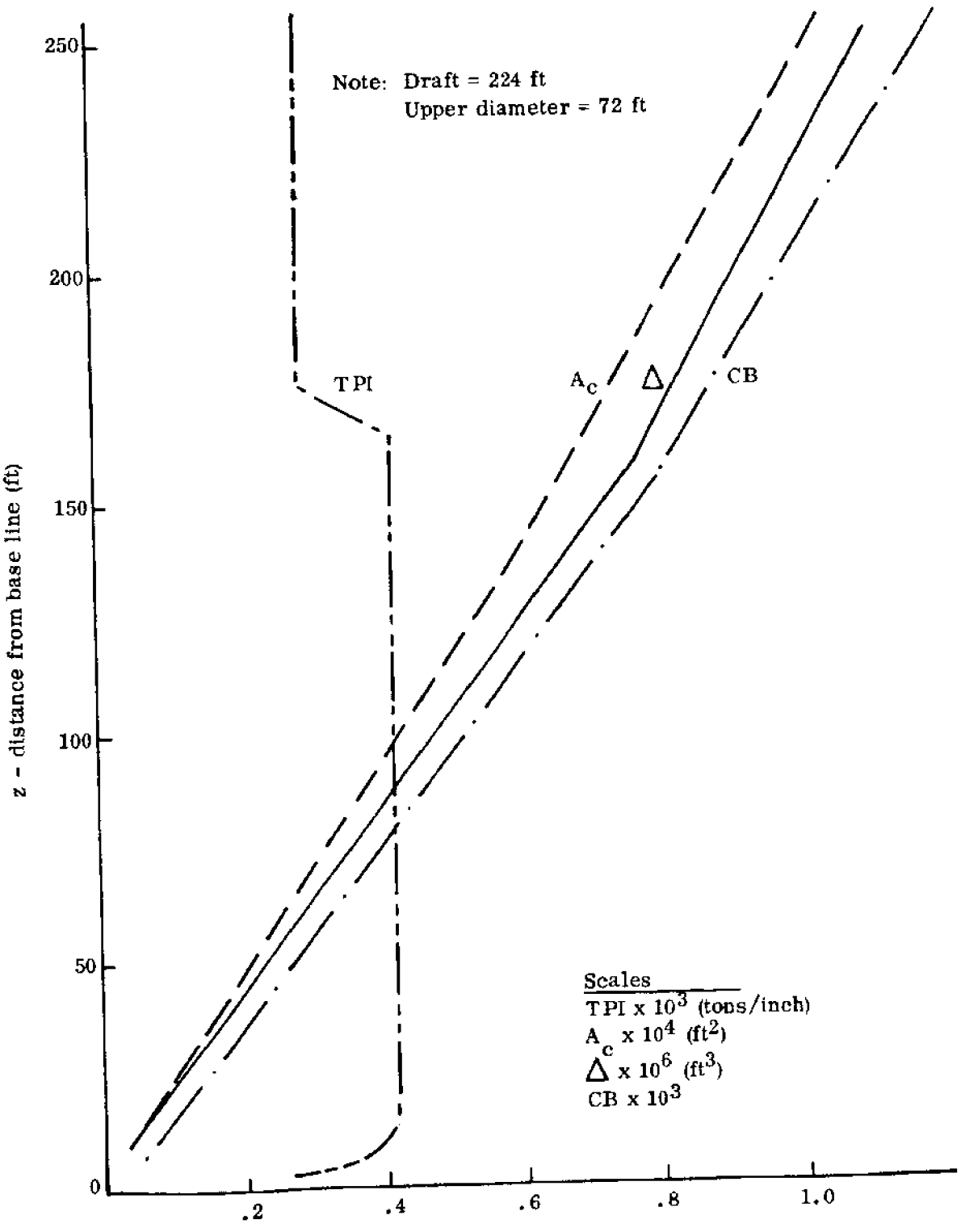

Fig. 40 Curves of form.

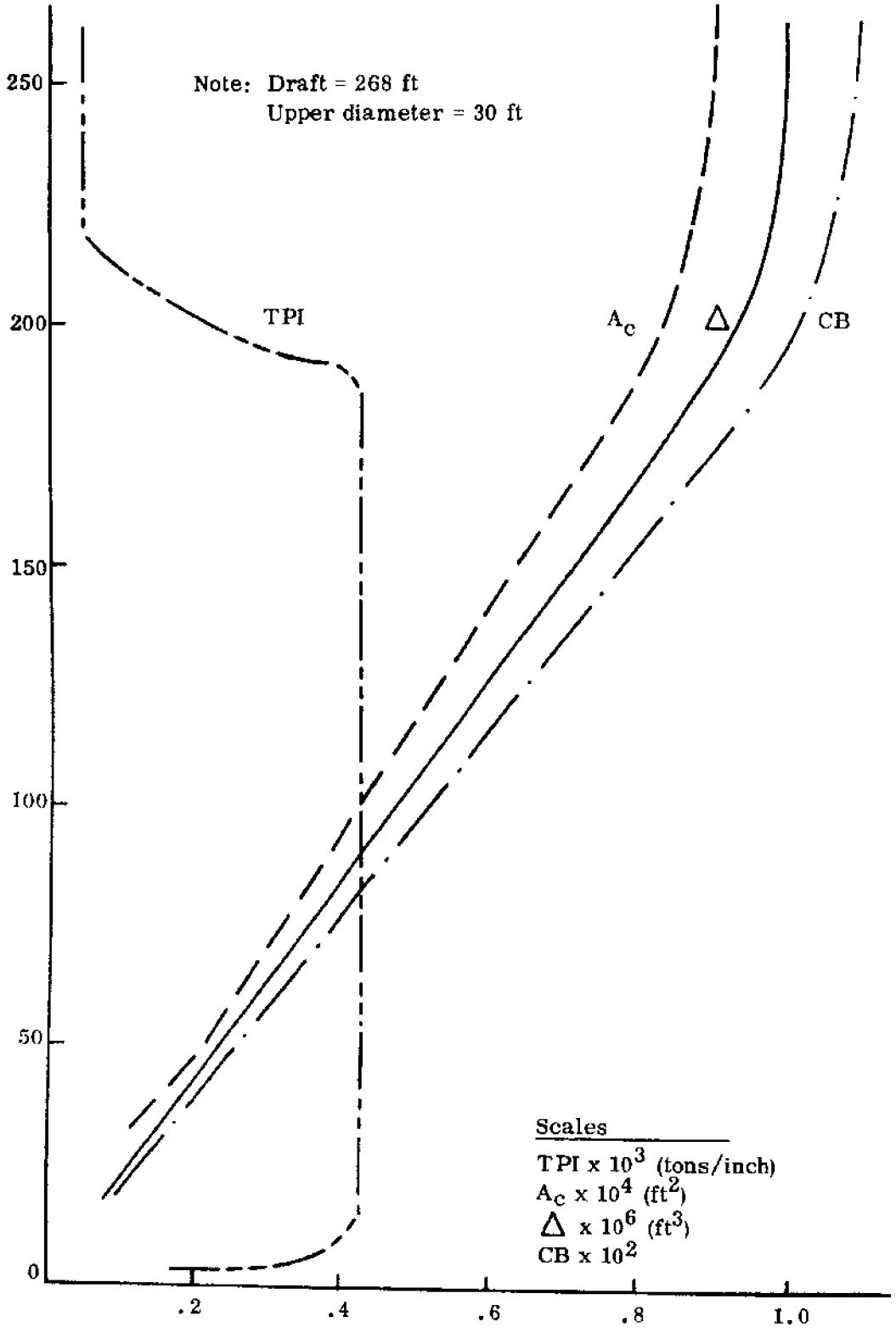

Fig. 41 Curves of form

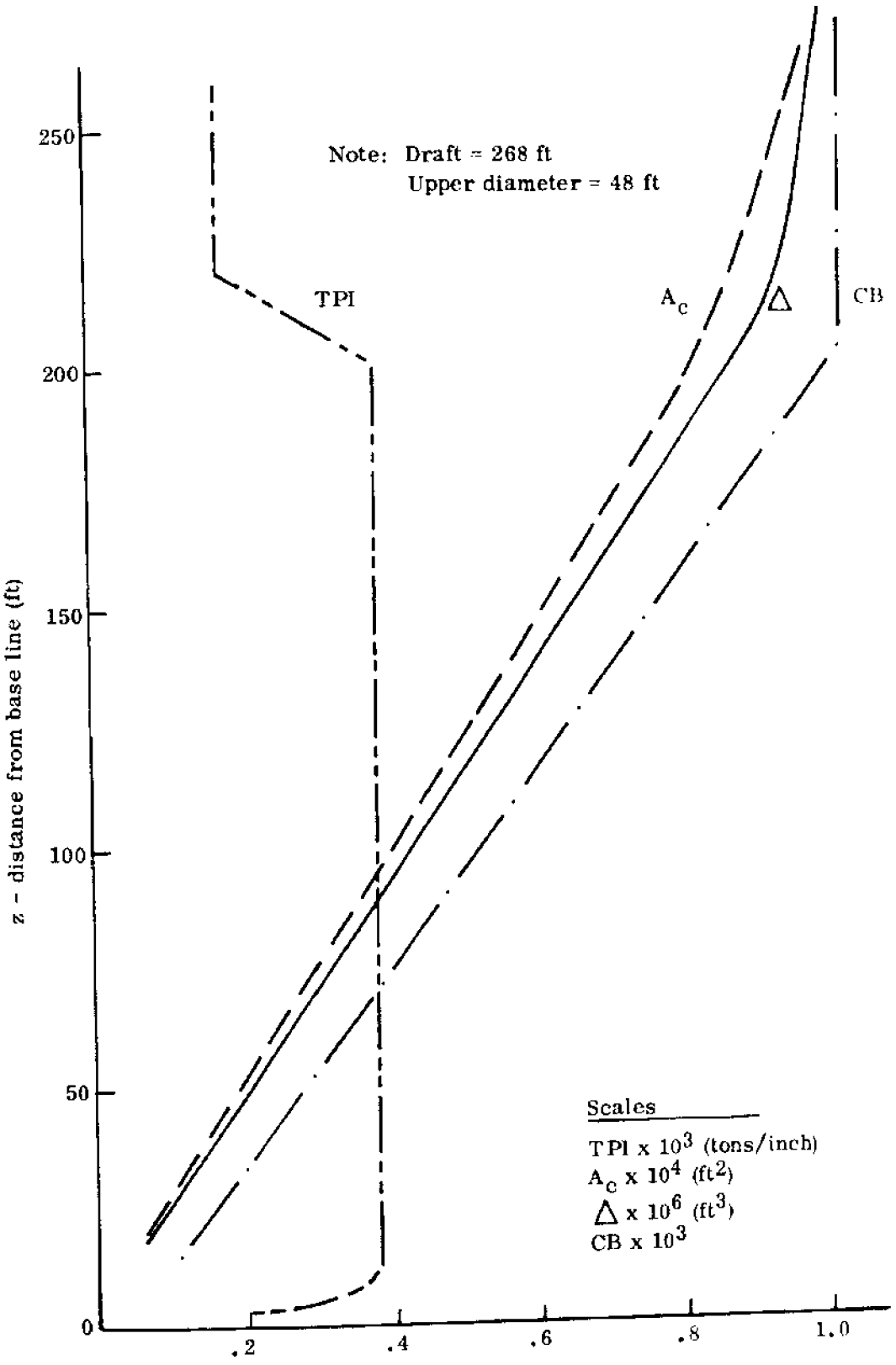

Fig. 42 Curves of form.

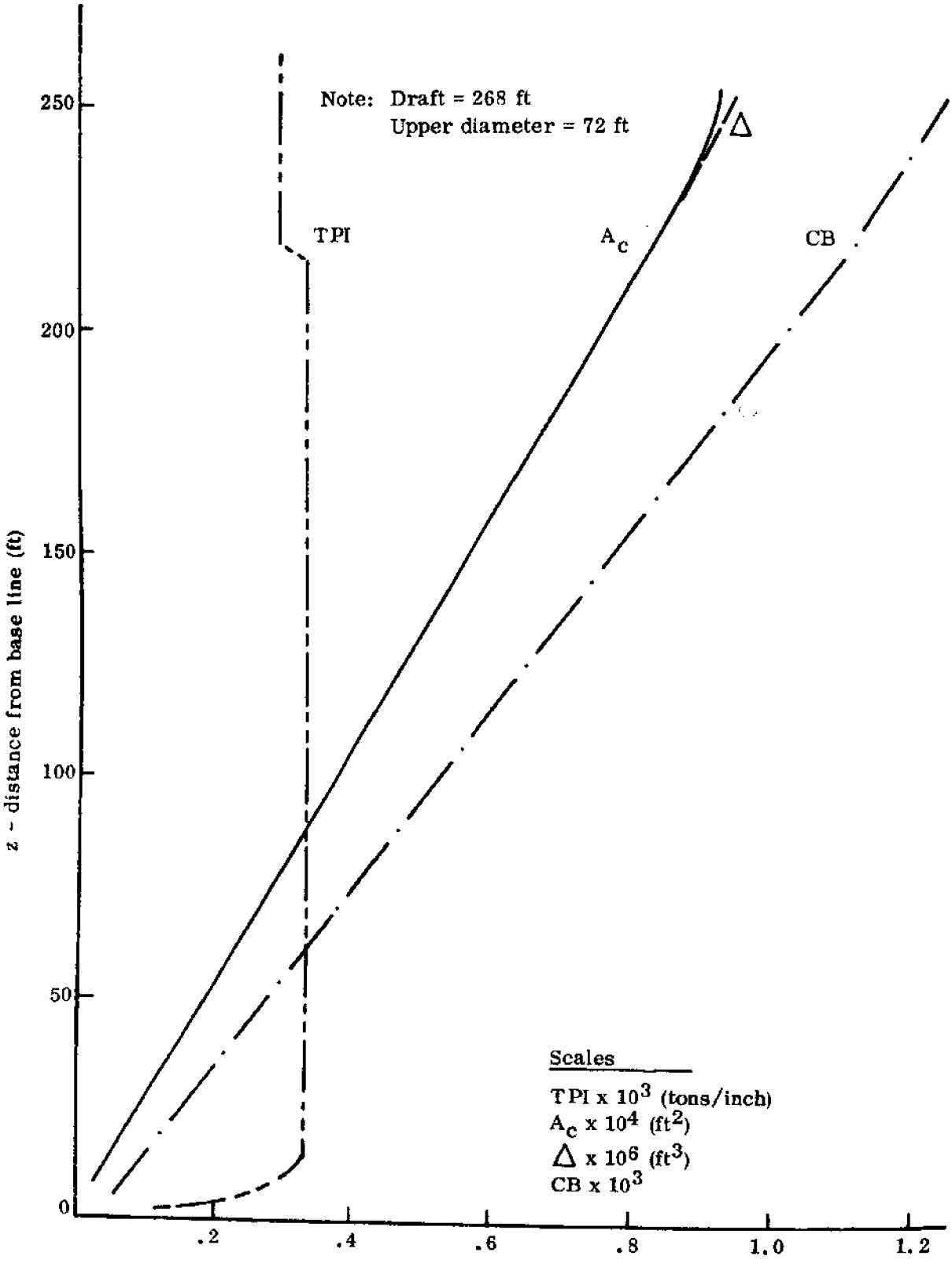

Fig. 43 Curves of form.

B. Response Operators

The theory and procedure for obtaining the response of the complete core-ring is the same as that developed for the module. There are, however, some minor modifications on account of the large lateral extent of this platform. It is necessary to calculate the relative displacements in x, y, and z directions at the location of each of the 30 columns and iterate the calculation of the response operators until convergence on these quantities is achieved. The numerical effort for this procedure is considerable, while the affected drag forces are almost negligible, as pointed out earlier. For wave frequencies larger than the zero motion frequency, the linearization procedure for the damping coefficients has therefore been omitted, and a linear damping coefficient assumed. The computer program developed for the inner ring is labeled RING.

The calculations were carried out for the full-scale dimensions of the platform. The response operators are plotted versus the actual wave periods to make the diagrams more readily accessible. Water depth was assumed to be 1800 ft, the water depth at the location of the planned city.

C. Response Operators for Existing Configuration

As discussed in Section I, the dynamic analysis began with a more or less intuitively conceived column configuration. Based on this configuration, the 1:20 model was built and will provide useful data for calibrating the computer model. These data and their comparison with theoretically derived results will be reviewed in Technical Report No. 3.

The Unit amplitude response in heave for the existing configuration is plotted in Fig. 44. The two wave periods at which no heaving occurs are those for which the wave forces acting along the platform cancel each other. The zero-motion wave period which arises due to cancelling force on one column alone (as discussed in Section IV) falls outside this diagram and should not be confused with the zero-motion points here. It is seen that a maximum heave response of 0.58 occurs near 30-second wave periods. There is no heaving motion due to waves shorter than 7.5 second. Because of the circular arrangement of the columns, the heaving response of the whole ring is independent of wave direction.

Figure 45 shows the surging response of the freely floating ring (no mooring system, no positioning system acting). Because of the arrangement of the ring, sway and surge responses are equal for incident waves shifted in direction by 90 degrees. The same holds true for pitch and roll (Fig. 46).

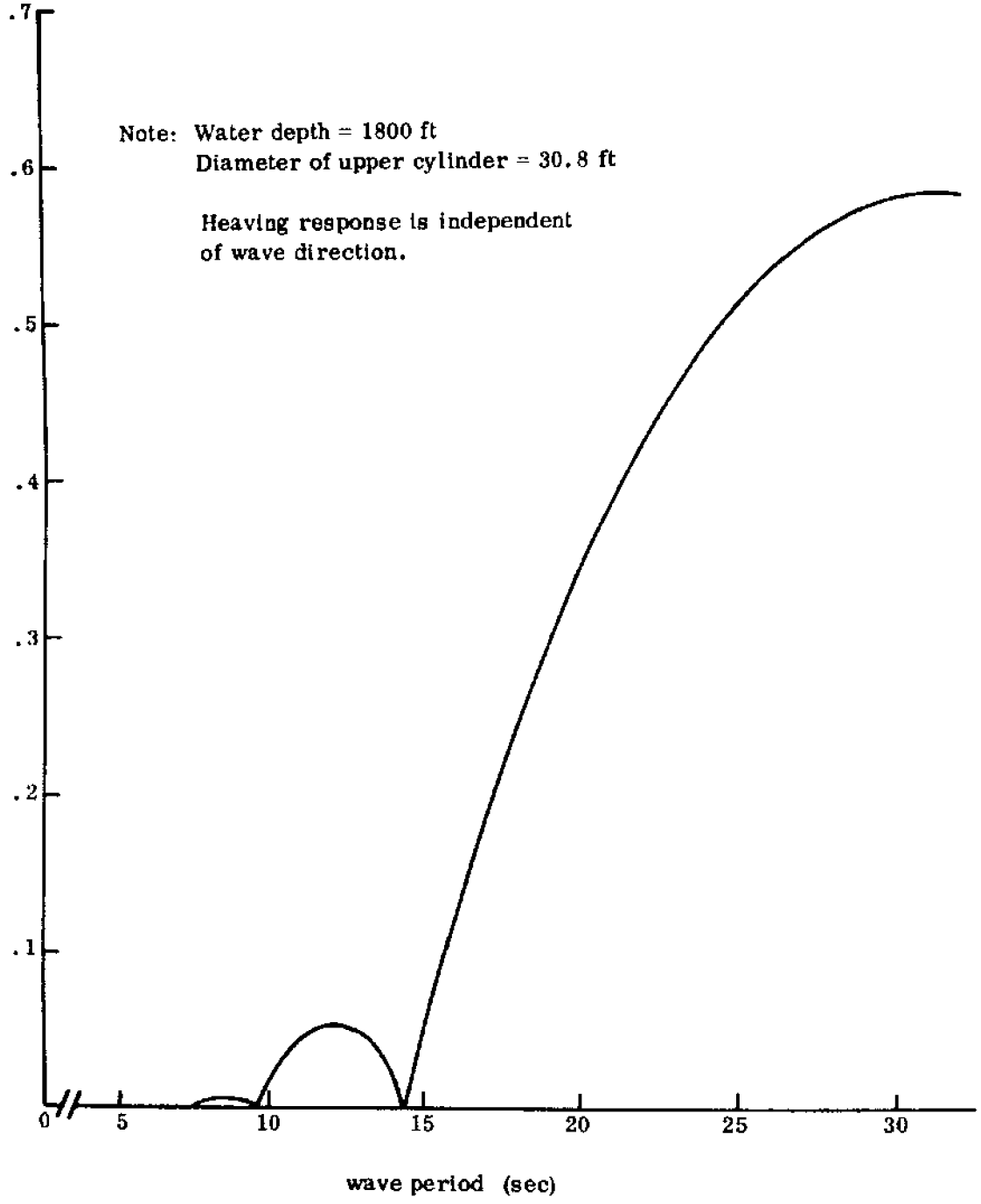

Fig. 44 Unit amplitude response in heave (core-ring).

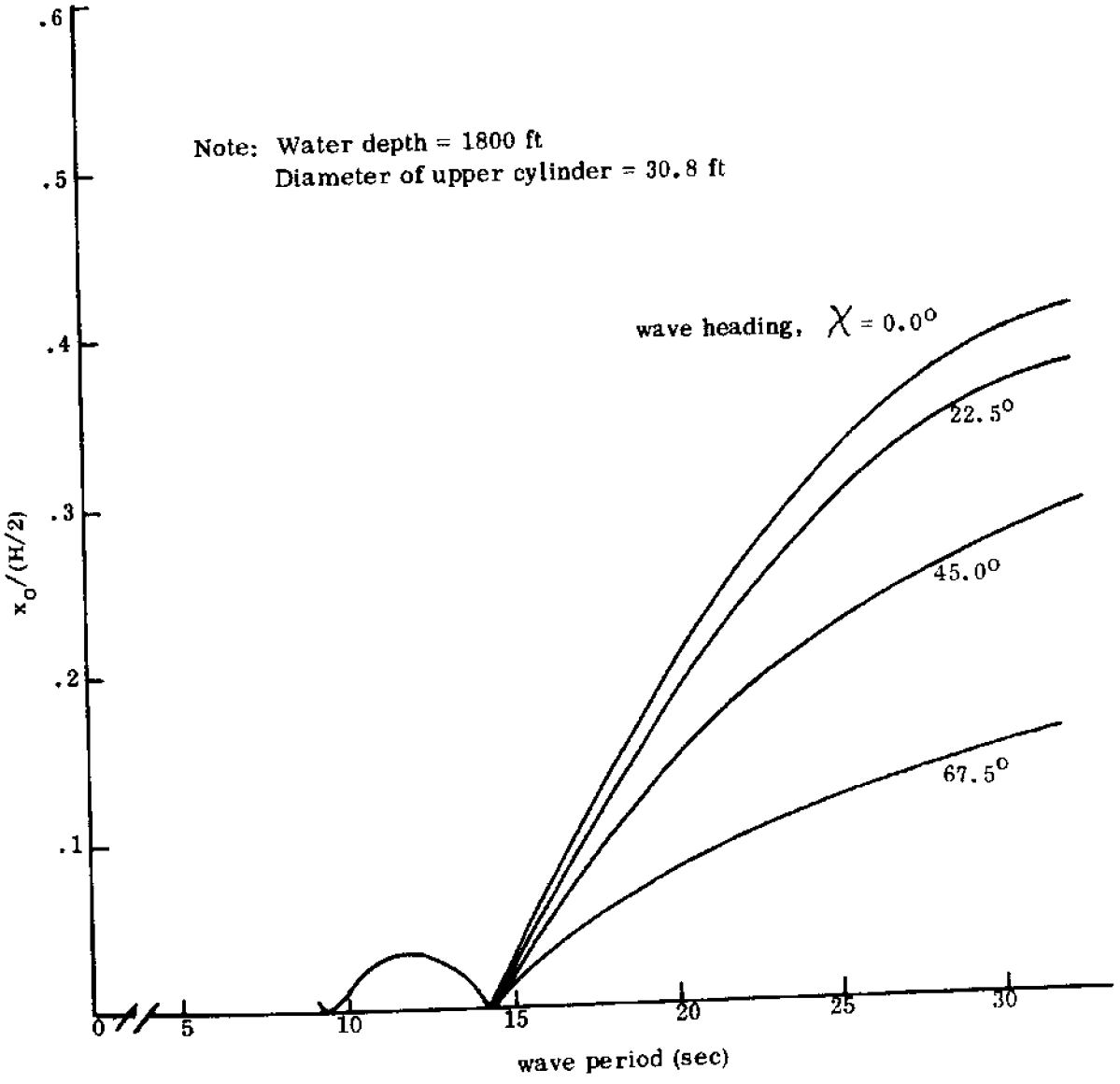

Fig. 45 Unit amplitude response in surge (core-ring).

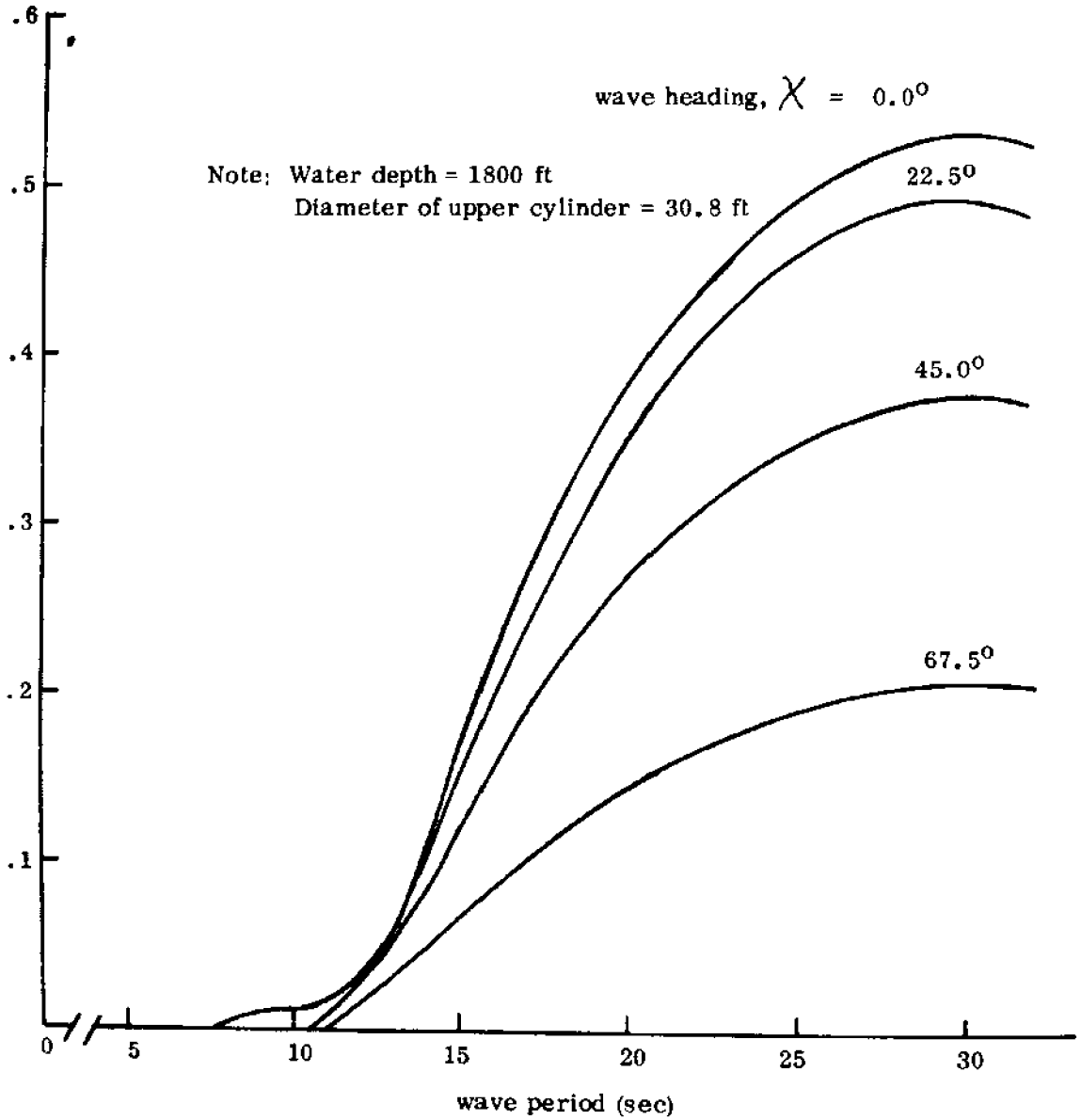

Fig. 46 Unit amplitude response in pitch (core-ring).

In other words, there is always an axis about which the rotation, as given by the pitching response operator, is greatest for $\chi = 0$ degrees. The ordinate of this diagram is normalized by the wave steepness. It is seen that a maximum response of 0.53 times the wave steepness is given at 30-second waves. There is zero yawing response due to the circular arrangement.

D. Response Operators of Alternate Column Configurations

In the preceding diagrms, considerable response is still shown at wave periods greater than 15 seconds. As a result of the single column calculations, it was found that with an increase in the upper cylinder diameter, the inertial force could be reduced and also the net wave displacement force (in heave). The upper cylinder diameter was therefore varied (as shown in Fig. 47). Figures 48 and 49 depict the resulting response operators in surge and heave. The small peak in response at 12-second waves was unaffected, but the response to wave periods greater than 15 seconds has been reduced significantly. Because of the reduction in the natural heaving period, resonance conditions now affect the cases with the two largest upper diameters. Here the importance of exact environmental prediction becomes evident. For waves of less than 24 seconds, the platform with the largest upper diameter would have by far the least response. Unfortunately, waves of greater than 24 seconds do exist. The platform with a 48 ft upper diameter appears to avoid resonance conditions, assuming that waves of 30 seconds have very little energy and seldom occur. Swells of 25 seconds have been reported, however. In this case, the initial configuration with a 30 ft upper diameter would show only a 23% response, hence showing only half the response of the initial configuration. In other words, the initial configuration of 30 ft diameter would heave twice as much as the 48 ft diameter configuration.

Almost the same result is obtained for the pitching response, as depicted in Fig. 50. In this diagram, the effect of variation of the vertical location of the center of gravity (CG) is also depicted. For the 48 ft diameter case, for instance, locating the CG 120 ft below the design water line, or 36.9 ft above the BG would result in minimum pitching motions. When choosing the location of CG, however, static stability criteria must also be considered. Figure 51 gives the pitching response with wave heading as a parameter. However, as mentioned before, there is always an axis about which the maximum response (corresponding to $\chi = 0$) will occur.

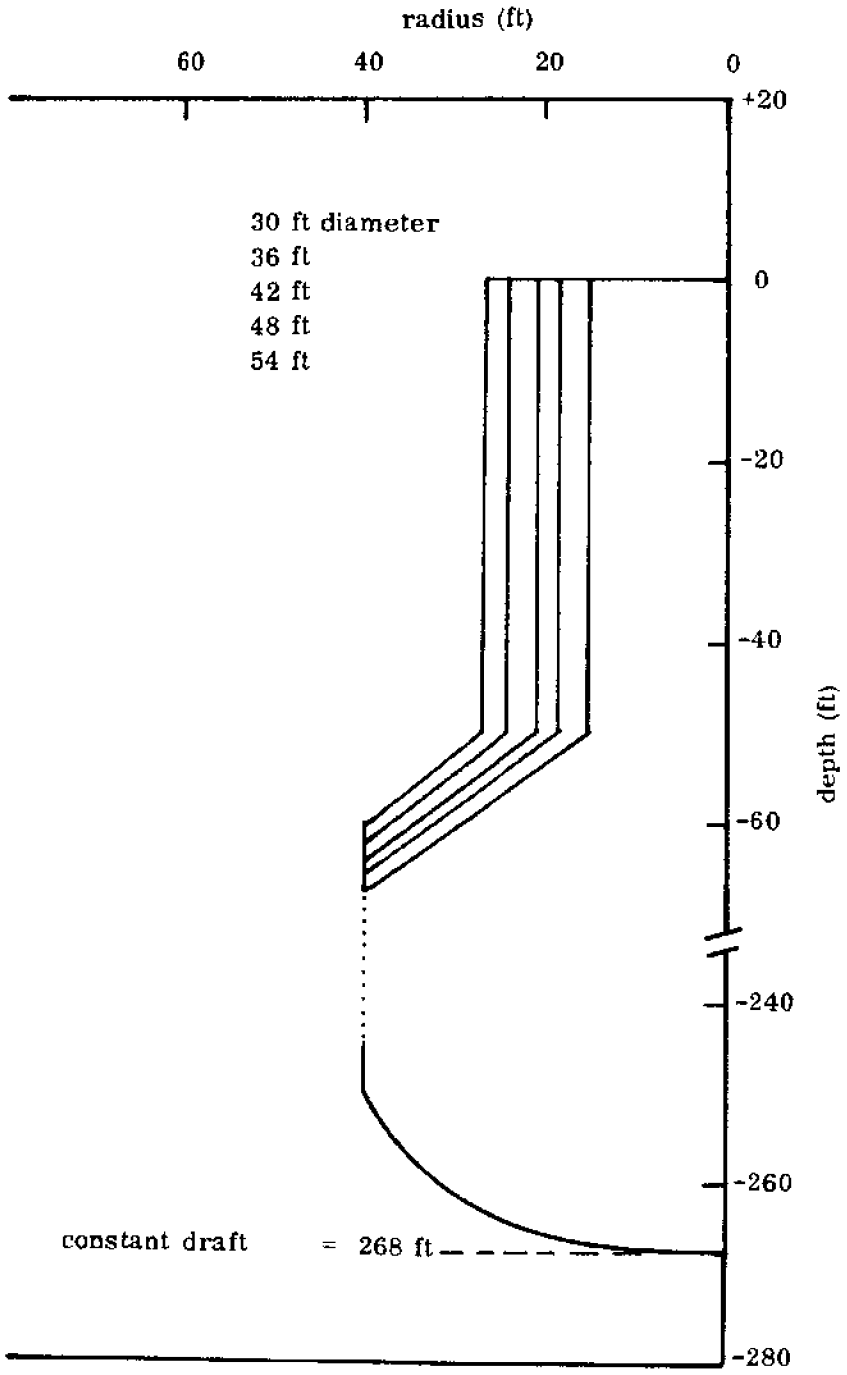

Fig. 47 Variation of diameter of upper cylinder.

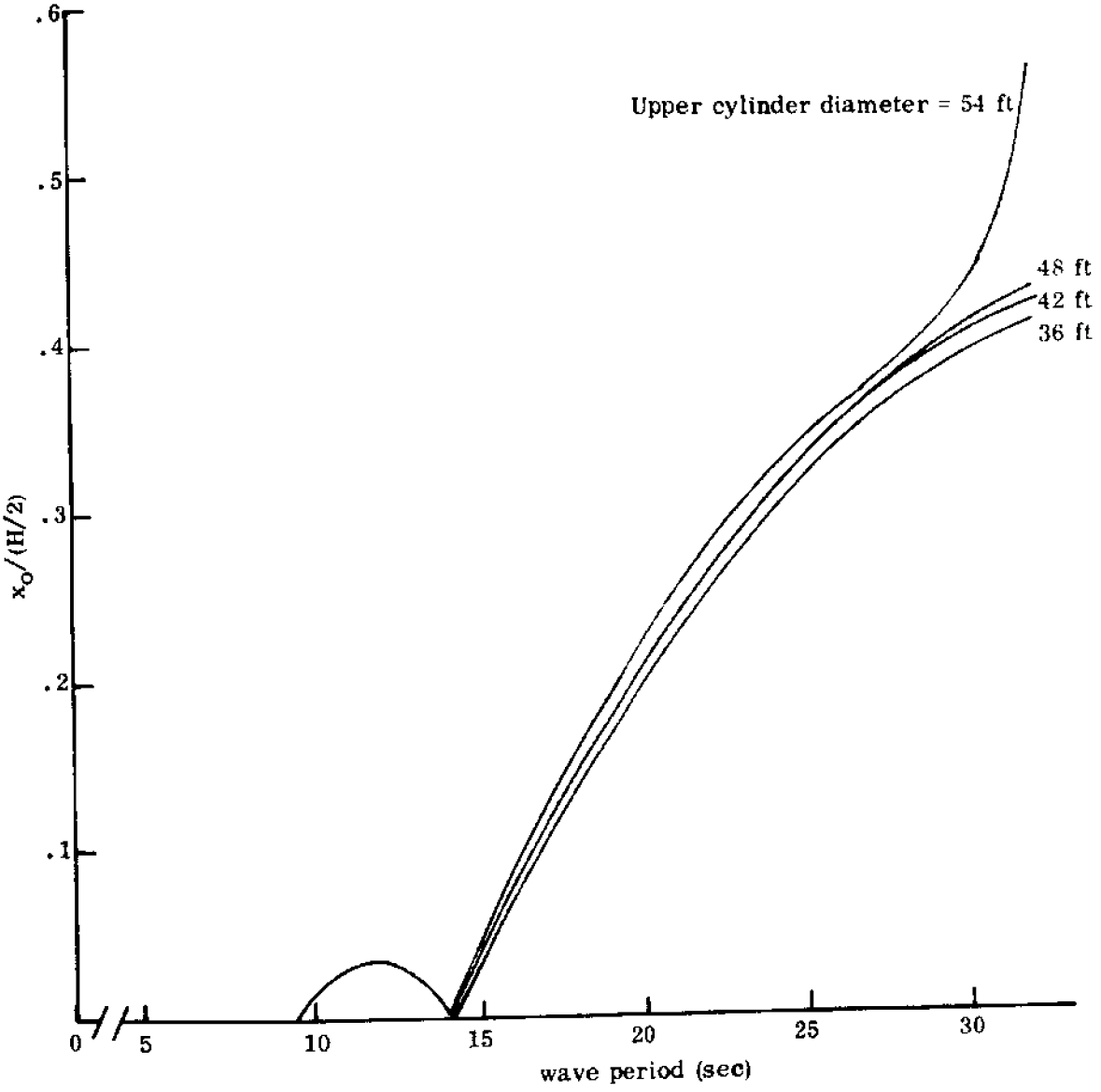

Fig. 48 Unit amplitude response in surge with variation of upper cylinder diameter.

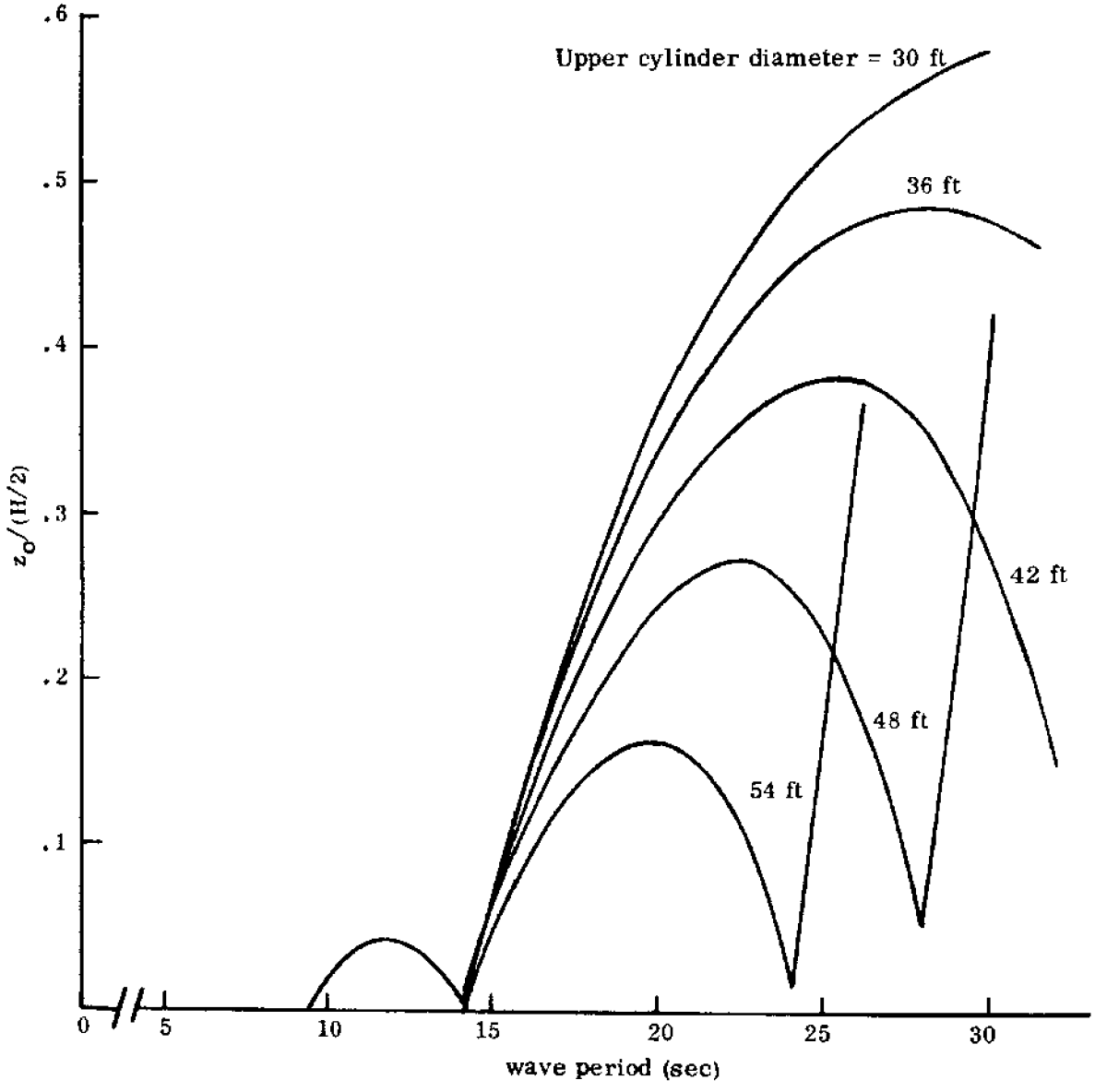

Fig. 49 Unit amplitude response in heave with variation of upper cylinder diameter.

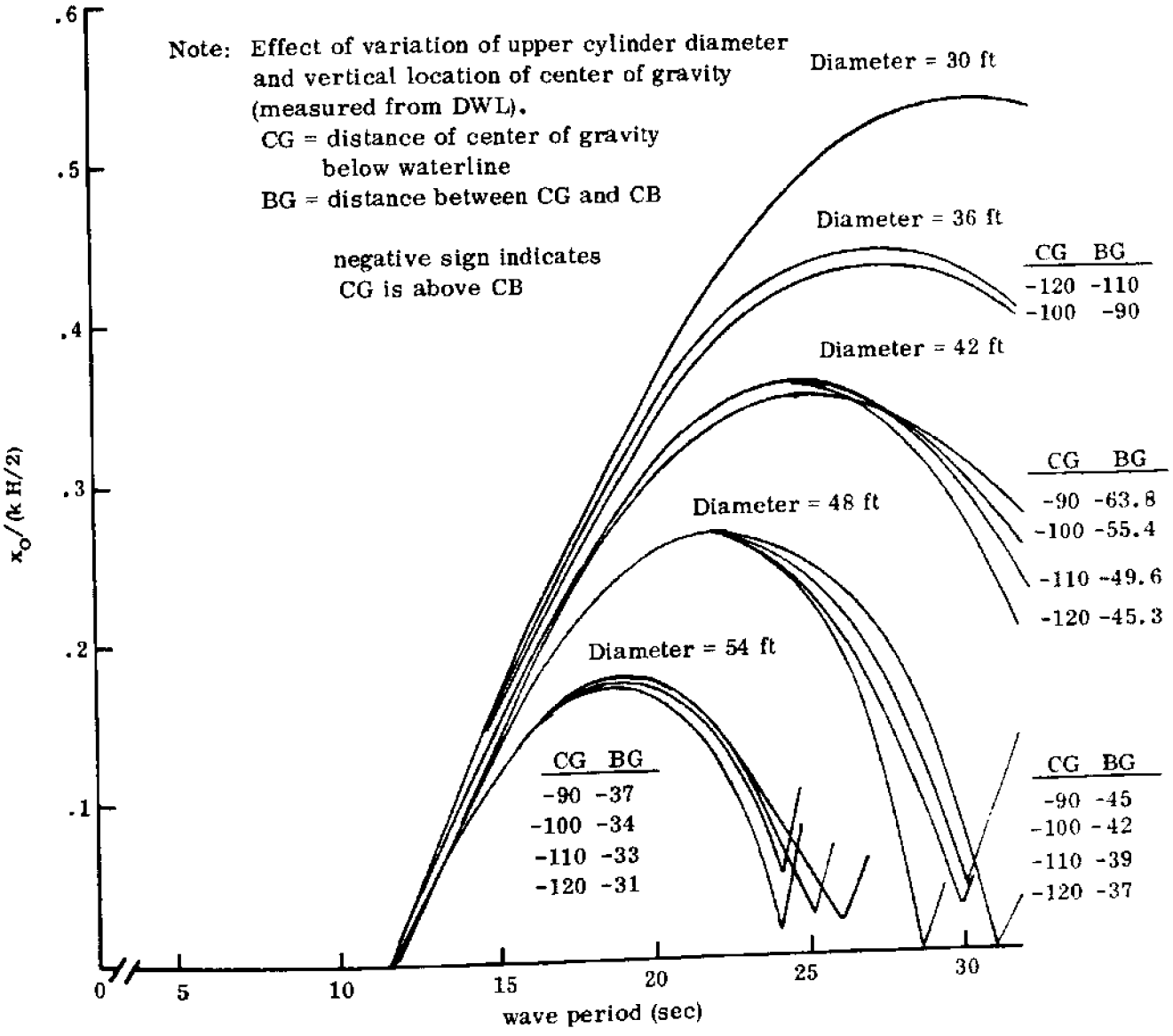

Fig. 50 Unit amplitude response in pitch (normalized by wave slope).

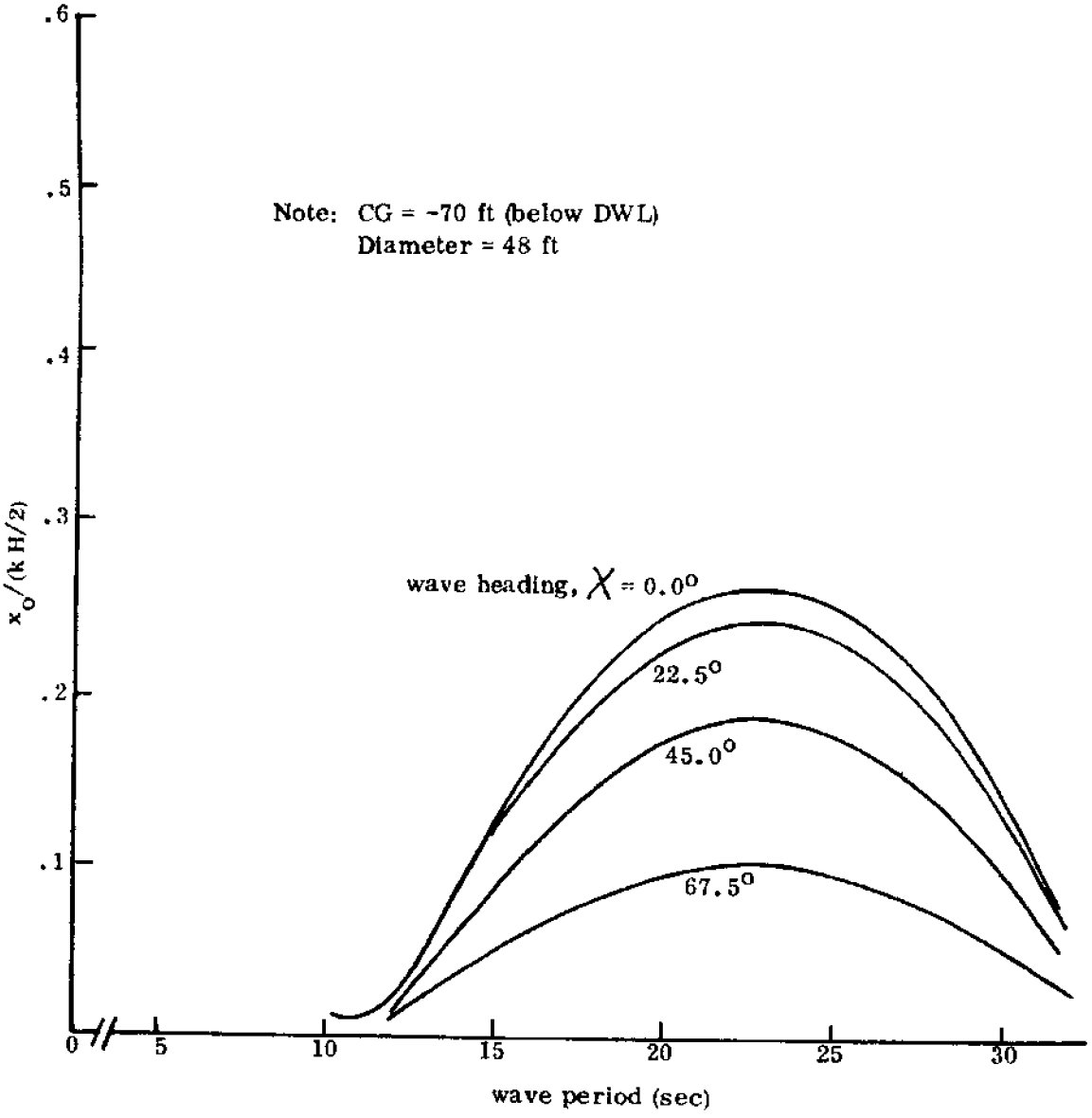

Fig. 51 Unit amplitude response in pitch (normalized by wave slope).

E. Motions in Irregular Seas

The response operators developed in the previous sections pertain to regular wave input. Since regular waves are seldom found in an actual seaway, one must resort to statistical descriptions of the seaway and the resulting motion of the platform. Instead of using response operators, one now looks for statistical averages of double amplitudes of motion. The method generally used for describing the seaway is by means of ocean wave spectra, for which empirical formulations have been developed by various authors. The platform motion in actual sea conditions can also be described by a motion spectrum, from which in turn, such statistical averages as the significant double amplitudes of motion can be calculated.

1. Ocean Wave Spectra

Of the many forms of ocean wave spectra proposed by various authors, one that is easy to use and conforms readily to the parameters of the sea state, i.e., significant wave height and significant wave period, is that given by Bretschneider (1959).[1] It is of the same form as the spectrum by Moskowitz (1964)[2] and Pierson-Moskowitz (1964)[3]. In the present study a recently revised form of the Bretschneider spectrum (1970)[4] is used.

---

[1]Bretschneider, C.L. "Wave Variability and Wave Spectra for Wind Generated Gravity Waves." Beach Erosion Board, T.M.118, U.S.Army Corps of Engineers.

[2]Moskowitz, L. "Estimates of the Power Spectrum for Fully Developed Seas for Wind Speeds of 20 to 40 Knots." J. Geophys. Res., Vol.69, No.24, Dec. 1964.

[3]Pierson, W.J. and L. Moskowitz. "A Proposed Spectral Form for Fully Developed Wind Seas Based on Similarity Theory of S.A. Kitaigoroskii". J. Geophys. Res., Vol. 69, No. 24, Dec. 15, 1964.

[4]Bretschneider, C.L. "Forecasting Relations for Wave Generation." Look Lab Hawaii, Vol. 1, No. 3, July 1970. (Quarterly publication of J.K.K. Look Laboratory of Oceanographic Engineering, Dept. of Ocean Engineering, University of Hawaii).

a. Non-Dimensional Wave Spectrum

The Bretschneider frequency spectrum is given in non-dimensional form by

$$S(\nu) = 4\nu^{-5} \exp(-\nu^{-4})$$

where

$$\nu = \frac{T_s}{T} = \frac{T_s}{2\pi} \cdot \sigma$$

and T_s = significant wave period

T = wave period (generic)

The significant wave period can be obtained from the average wave period, $\overline{T}$, as

$$T_s = \frac{\overline{T}}{0.906}$$

or alternatively from the modal period T_0 of the spectrum as

$$T_s = T_0 \sqrt[4]{4/3}$$

The frequency spectrum is then obtained as

$$S(\sigma) = \frac{1}{2\pi} H_s^2 \cdot T_s \cdot S(\nu)$$

Substitution of the non-dimensional spectrum and setting

$$\sigma_s = \frac{2\pi}{T_s} = \text{significant frequency of the sea state}$$

yields

$$S(\sigma) = 4 H_s^2 \sigma_s^4 \sigma^{-5} \left[\exp - \left(\frac{\sigma}{\sigma_s}\right)^{-4}\right]$$

Note that this spectrum is a wave height spectrum, and the area under the spectrum correspond to the square of the significant wave height.

b. Two-Dimensional Wave Spectrum

Waves in an actual sea condition are not uni-directional as assumed in the above wave spectrum. This can be taken into account by introducing an angular dispersion factor. Several expressions have been proposed, but it appears that until further data are available, the angular dispersion factor can be satisfactorily expressed as

$$\frac{2}{\pi} \cos^2 \theta$$

where θ is the angular deviation of the direction of propagation of a particular wave from the principal wave heading.

Taking this spreading factor into account, the Bretschneider-spectrum can be written in the two-dimensional form as

$$S_{\eta\eta}(\sigma, \theta) = \frac{8}{\pi} H_s^2 \sigma_s^4 \sigma^{-5} \exp\left[-\left(\frac{\sigma}{\sigma_s}\right)^{-4}\right] \cos^2\theta \quad -\frac{\pi}{2} \leq \theta \leq \frac{\pi}{2}$$

The significant wave height (i.e., the average of the one-third highest wave) is then readily obtained, namely

$$H_{sig} = \int_{\sigma_1}^{\sigma_2} \int_{-\pi/2}^{\pi/2} S_{\eta\eta}(\sigma, \nu) \, d\nu \, d\sigma$$

2. Statistical Analysis

Knowing the complex frequency response operators $H_i(j\sigma)$ for all modes of motion, the corresponding significant double amplitudes of motion are obtained by integrating the motion spectra over the range of frequencies.

The platform motion spectra due to a two-dimensional wave spectrum are obtained from

$$S_{x_i x_i}(\sigma, \chi) = \int_{-\pi/2}^{\pi/2} S_{\eta\eta}(\sigma, \nu) \left| H_i(j\sigma, \chi + \nu) \right|^2 d\nu$$

where χ = angle between direction of principal wave heading and the longitudinal axis of the platform.

The significant double amplitude for a particular principal wave heading is then given by

$$[X_i(\chi)]_{sig} = \sqrt{\int_{\sigma_{min}}^{\sigma_{max}} S_{x_i x_i}(\sigma, \chi)\, d\sigma}$$

3. Results

a. Existing Configuration

The significant double amplitudes of platform motion are plotted in Figs. 52 through 54. The abscissa in these diagrams is the significant wave period corresponding to actual wind wave spectra as defined above. The corresponding significant wave heights for sea states 3 to 7 are listed in the table below.

Sea State	Significant Wave Period (sec)	Significant Wave Height (ft)
3	6.9	3.3
4	7.8	7.0
5	9.0	10.0
6	10.5	18.0
7	13.6	30.0

The conditions for sea state 7 were reached in Hawaiian waters during the hurricanes "Nina" (1957) and "Dot"(1959). The surging motion at sea state 7 appears to be about 50% of the heaving motion. The pitching motion in terms of angular displacement at this sea state is only about 1 degree in double amplitude, but the double amplitude of vertical motion (due to pitching alone) of a point on the periphery of the city is about 8.0 ft. In the worst case, the full heaving double amplitude would have to be added, so that a total maximum significant double amplitude of vertical motion on the periphery of the platform could reach 11.0 ft.

Possible sea states of longer significant wave period, but of significant wave height less than that of a fully developed sea, are discussed in the next section.

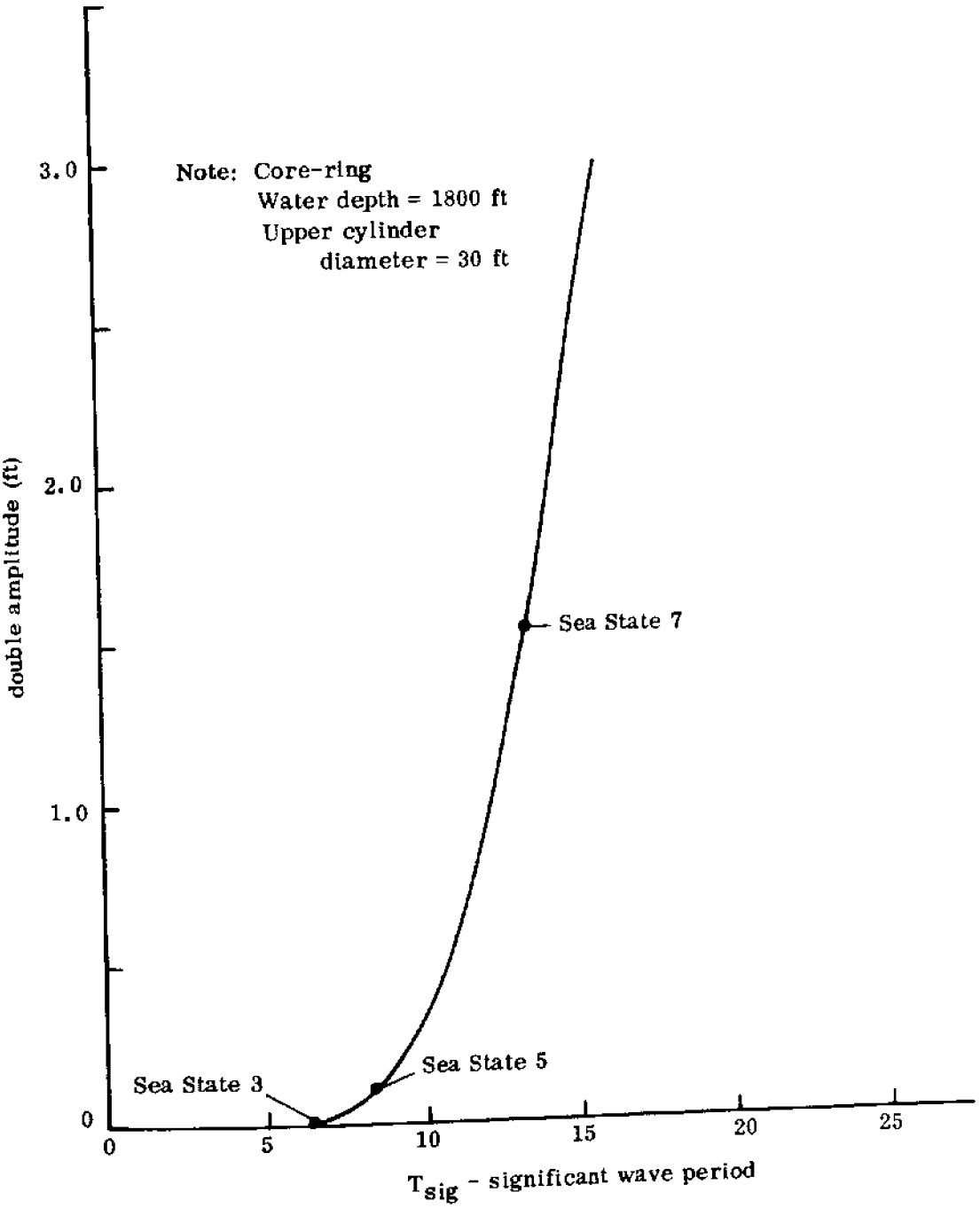

Fig. 52 Significant double amplitude of surging motion, (core-ring, d = 30 ft).

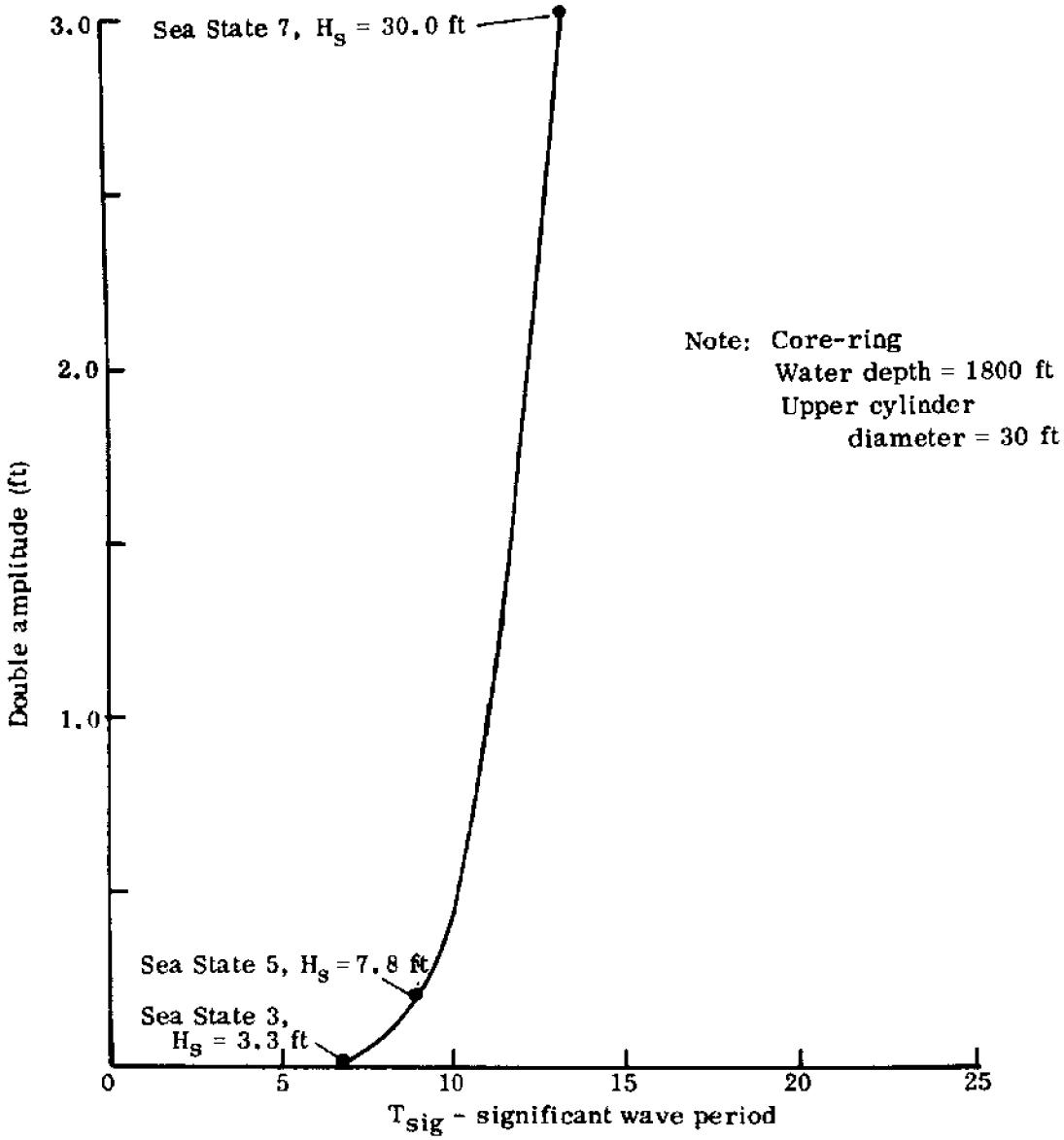

Fig. 53 Significant double amplitude of heaving motion.

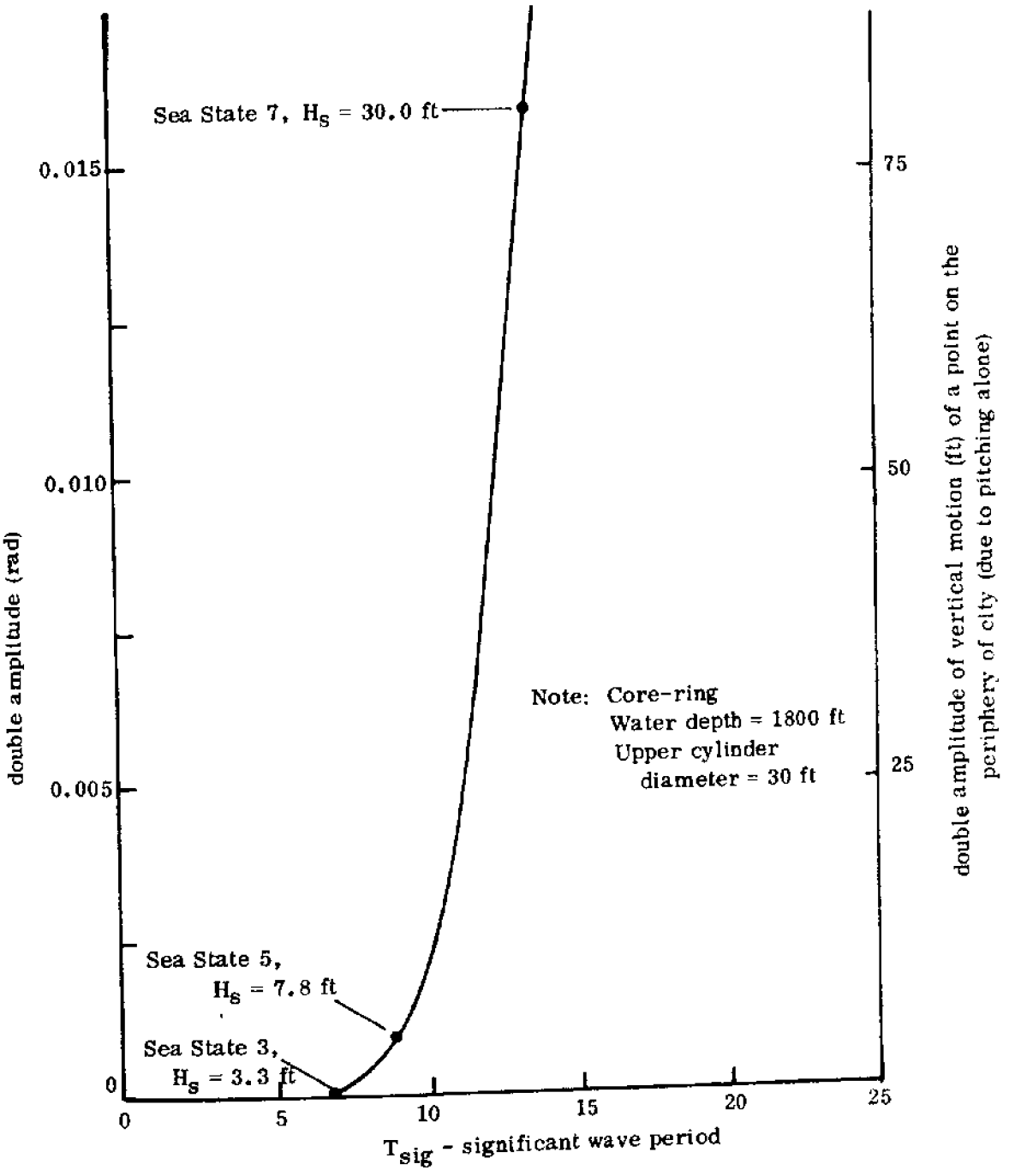

Fig. 54 Significant double amplitude of pitching motion.

b. Alternative Configuration

From the heaving response operators of a single column (as plotted in Fig. 14) and the response operators of the total platform (as depicted in Figs. 49 and 50), the model configuration with an upper cylinder diameter of 0.32 ft (48 ft full size) was somewhat arbitrarily chosen for further analysis because of its minimum motion response.

Figures 55 through 57 depict the significant double amplitudes in surge, heave and pitch for this particular configuration. Because of the rotational symmetry of the platform, the modes of motion of surge and sway are synonymous, as are roll and pitch. If the motions are defined with respect to a particular axis, and the predominant wave direction is measured from this axis, the resulting pitching motions are as indicated in Fig. 57. It should be remembered, however, that there is always an axis about which the maximum shown pitching motion occurs.

Figure 58 depicts the spectral energy density distribution of heaving motion for sea state 7. The area under this curve is proportional to the square of the heaving motion. This diagram is shown as a sample, because it demonstrates the frequency bands from which the motion energy is derived. It can be clearly seen that a major contribution of energy stems from long period waves, even though these have already relatively low height, as the peak of the spectrum lies at about 14 seconds, or $\sigma = 0.45$. This period, fortunately, is one at which the heave forces on the platform cancel because of the large lateral extent of the platform. At this sea state ($T_{sig} = 13.6$ sec) the advantage of the zero-force period of 28 sec does not come into bearing, as no energy exists in waves of this length. Increasing the upper cylinder diameter to 54 ft would be advantageous. At the planned location of the floating city, however, the presence of extremely long swells becomes important.

To investigate this situation, diagrams of energy density spectra corresponding to unit amplitude significant waves were developed (Fig. 59). The corresponding significant double amplitude of motion was termed significant double amplitude ratio and plotted in Fig. 60 for heaving motion. The actual double amplitude of motion is readily obtained by multiplying the value of this ratio by the significant wave height. This wave height can be the reported height of long period swells in lieu of anything better. The longest reported swell of any height known to the author has a period of 24 sec and a height of 8.5 ft. The resulting double amplitude of heaving motion would be 2.9 ft. The corresponding accelerations, however, would be extremely gentle. Sea state 7, giving the same amplitude of heaving motion, would yield $(24/13.6)^2 = 3$ times higher accelerations.

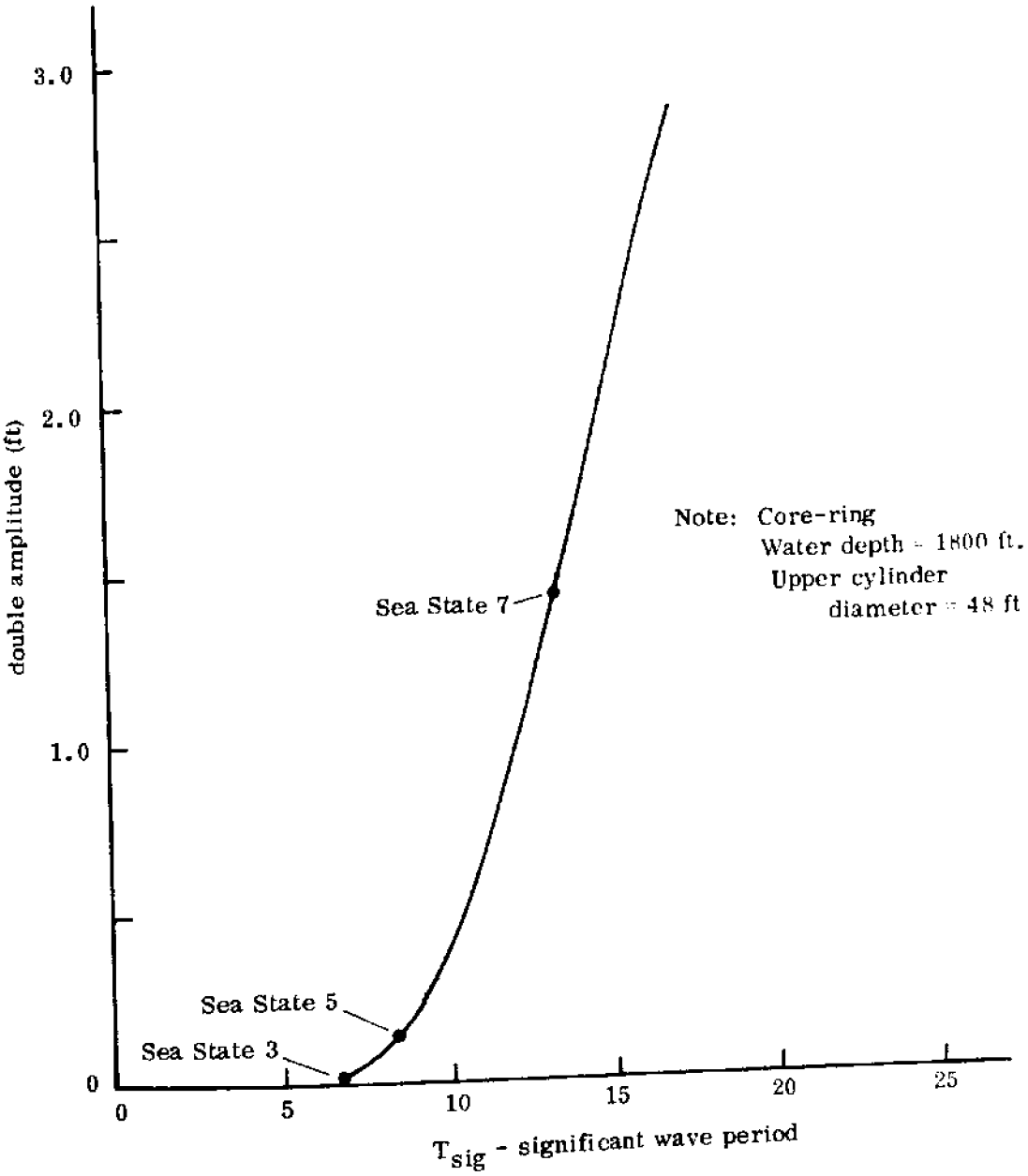

Fig. 55 Significant double amplitude of surging motion.

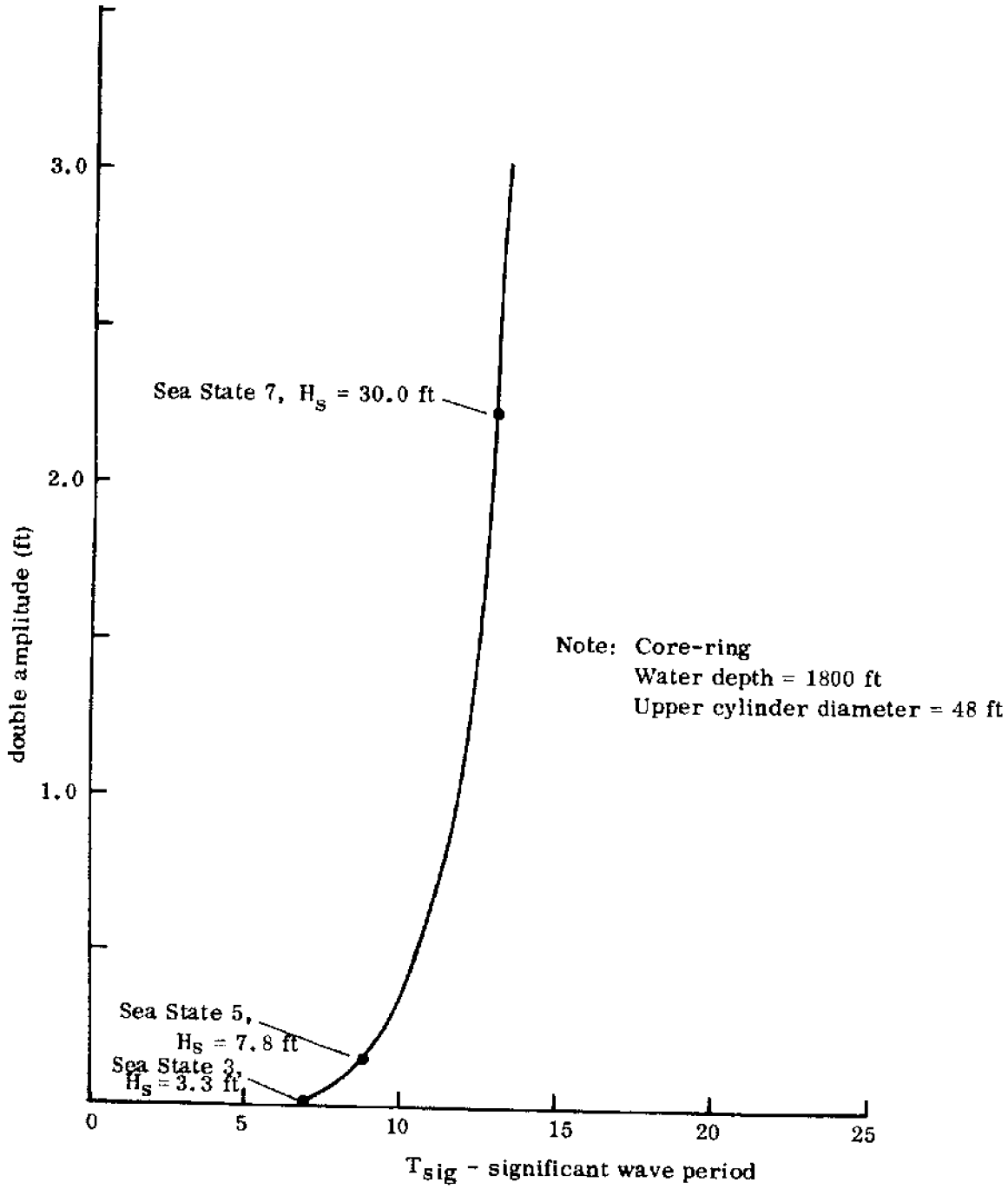

Fig. 56 Significant double amplitude of heaving motion.

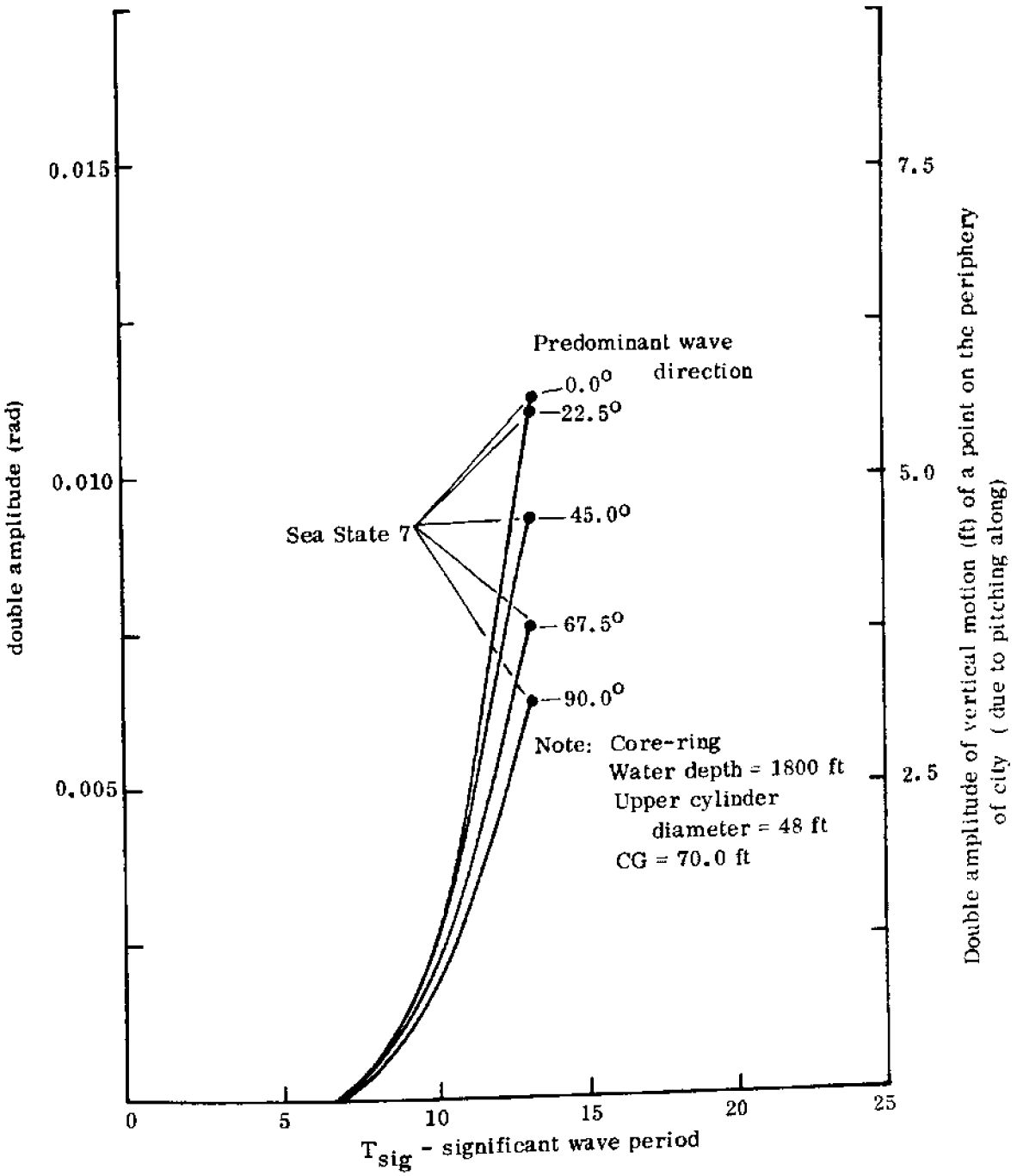

Fig. 57 Significant double amplitude of pitching motion.

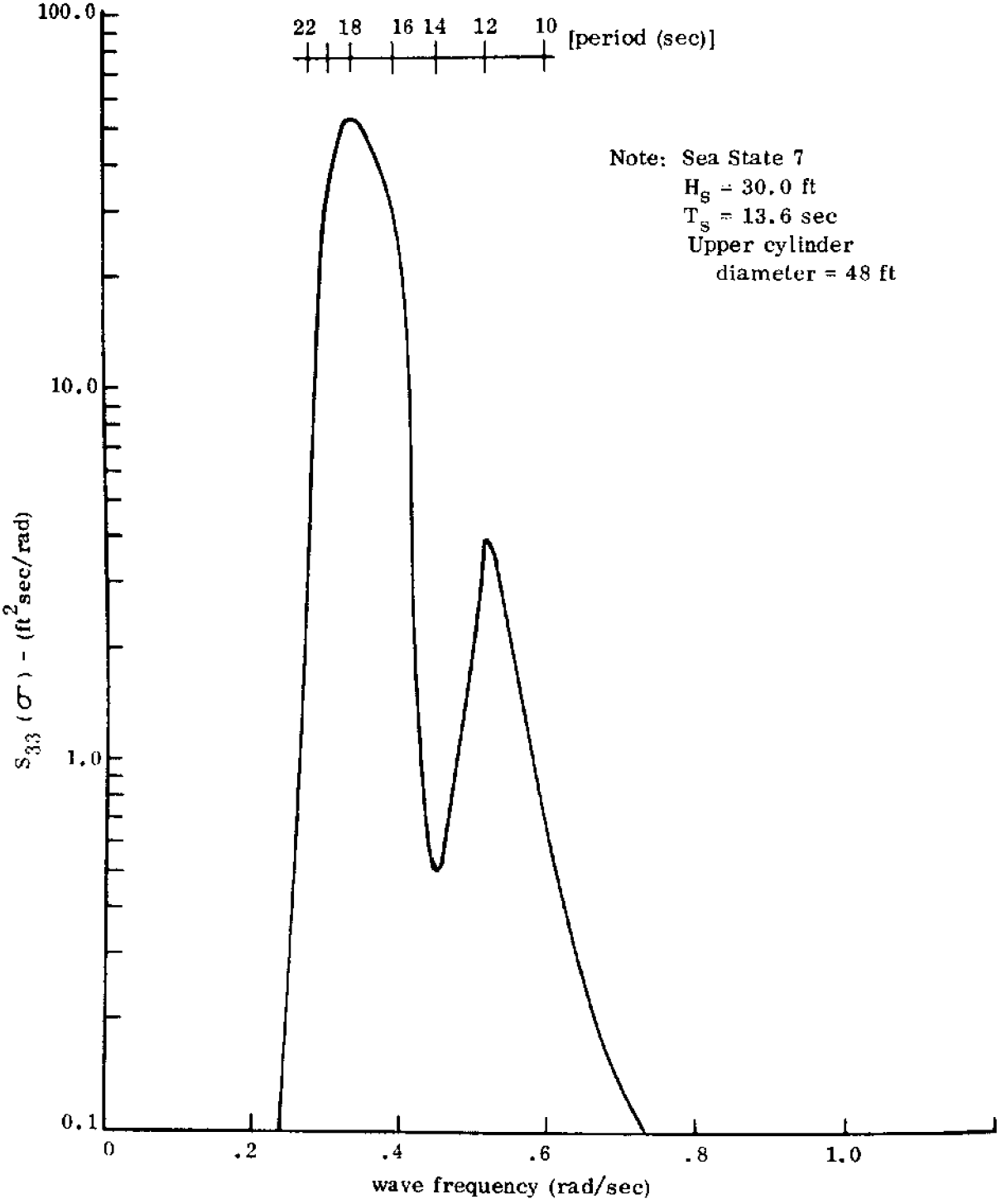

Fig. 58 Spectral energy density distribution of heaving motion.

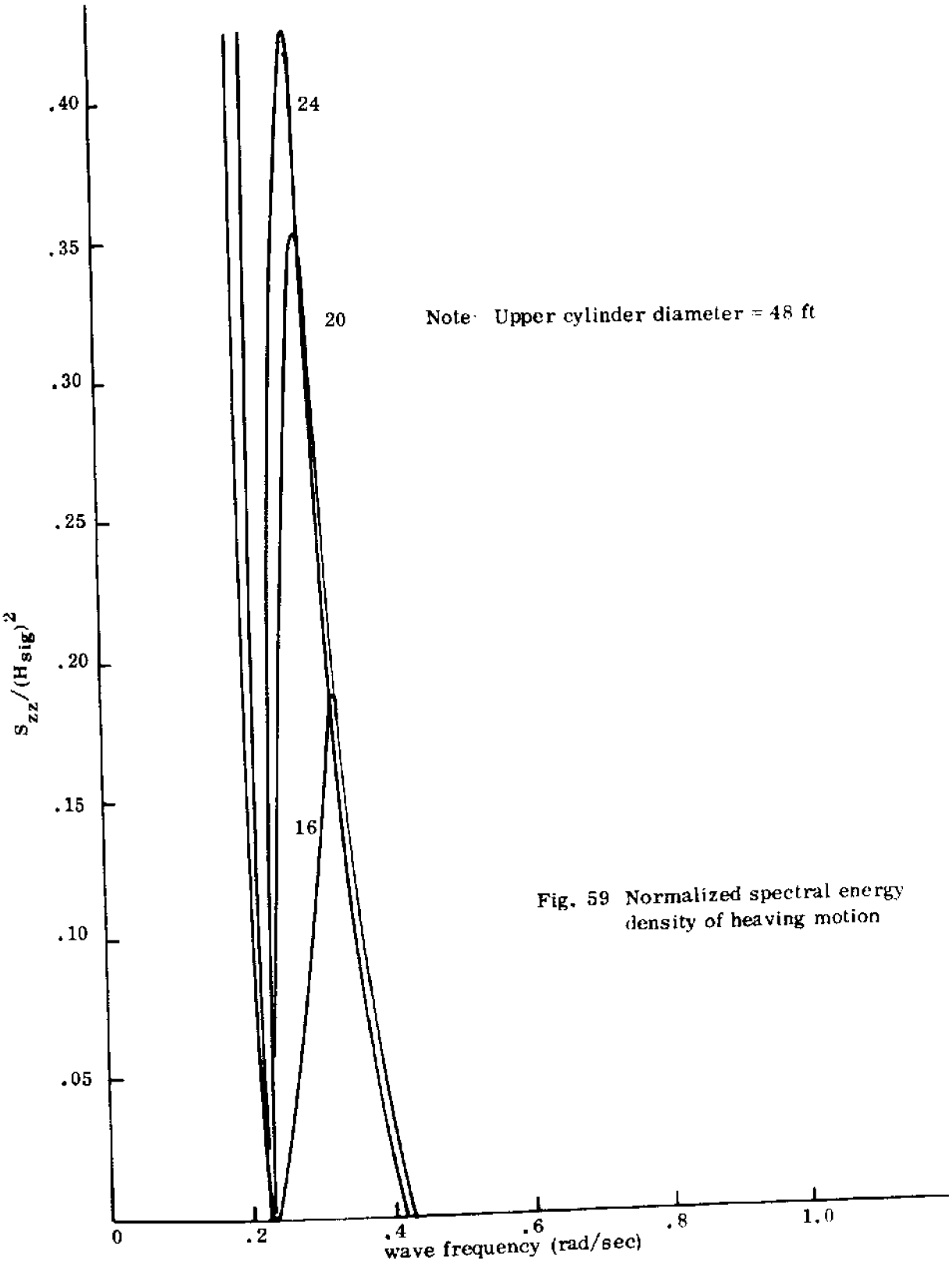

Fig. 59 Normalized spectral energy density of heaving motion

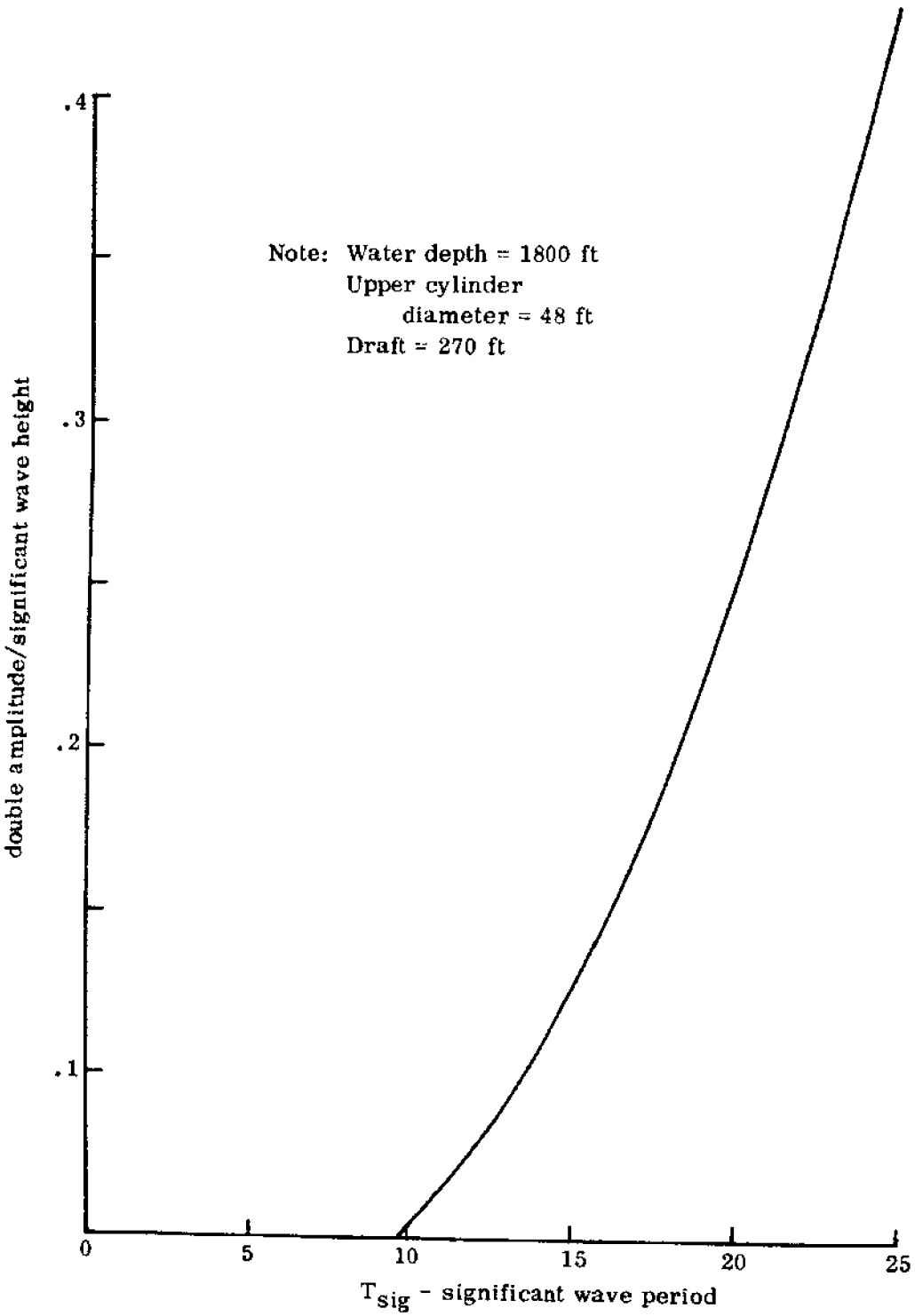

Fig. 60 Significant amplitude ratio in heave.

F. Limits of Perceptibility of Motion

The physiological response of human beings to periodic vertical oscillations can be described by defining certain regions in terms of the normalized acceleration factor (z_m/g) as depicted in Fig. 61. The lowest curve in this diagram defines the limiting acceleration factor (f_L) for imperceptible vertical accelerations. It is seen that f_L varies slightly with the period of oscillation (wave period). From this limiting acceleration factor, one can calculate the corresponding amplitudes of harmonic motion, namely

$$z_m = \left(\frac{\ddot{z}_m}{g}\right) \; g/\sigma^2$$

with

$$f_L = \left(\frac{\ddot{z}_m}{g}\right)_L$$

we obtain

$$z_m = f_L \frac{g}{\sigma^2} = f_L \frac{g}{(2\;)^2} T^2$$

or $z_m = 0.82\, f_L\, T^2$ (ft)

Making a further conservative assumption by using only the lowest value of f_L, i.e.

$$f_L = 0.015$$

we obtain the maximum double amplitude for imperceptible motion as

$$2\, z_m = 0.024\, T^2$$

which is plotted in Fig. 62. This curve can be superimposed on the diagrams for significant double amplitudes of heaving motion in the preceding section. It is seen that in spite of the conservative assumption of f_L, the motion amplitudes are always less than the limit for perceptibility.

In attempting to predict the physiological response from the unit amplitude operators in heave (without having to resort to the significant double amplitudes in irregular waves), one can proceed as follows:

Assuming a realistic value for wave heights of long waves, e.g.

$$H_{max} = 1.1\sqrt{L} = 2.5\ T \text{ (in deep water}$$

we can define a limiting value for the unit amplitude response operator in heave as

$$\left(\frac{z_m}{H/2}\right)_L = f_L \frac{g}{(2\ )^2} T^2 \frac{2}{2.5\ T}$$

$$\text{or} \left(\frac{z_m}{H/2}\right)_L = 0.65\ f_L\ T$$

Using for f_L the constant value of 0.015, we obtain

$$\left(\frac{z_m}{H/2}\right)_L = 0.01\ T$$

which is plotted in Fig. 62. All unit amplitude responses less than this limit will correspond to imperceptible motion under any condition.

This curve can be superimposed on the diagrams of unit amplitude response in heave in previous sections. In particular, Fig. 49 is of interest. It is seen that our curve will intersect the response operators at periods of about 16 seconds. The particular environmental conditions at the planned location of this platform must be taken into account. At a wave period of 16 seconds, the limiting response operator assumes a wave height of $H = 2.5 \times 16 = 40$ ft, a wave height which has never been observed in this area. The fact that the response operators are larger than permissible is therefore of no importance. The reported wave heights decrease rapidly toward longer wave periods.

Under resonance conditions, assuming a unit amplitude response of 2 or 3 at resonance and assuming a wave height of 8.5 ft at a 24 second period (the highest long swell reported in this general area), we obtain motion double amplitudes up to 25 feet. This amount, however, is still less than the perceptible minimum motion as seen from Fig. 62. One can therefore conclude that it appears justifiable from the motion perceptibility point of view to allow natural heaving periods of the platform as low as 24 seconds. This statement holds only for the symmetric core-ring type platform.

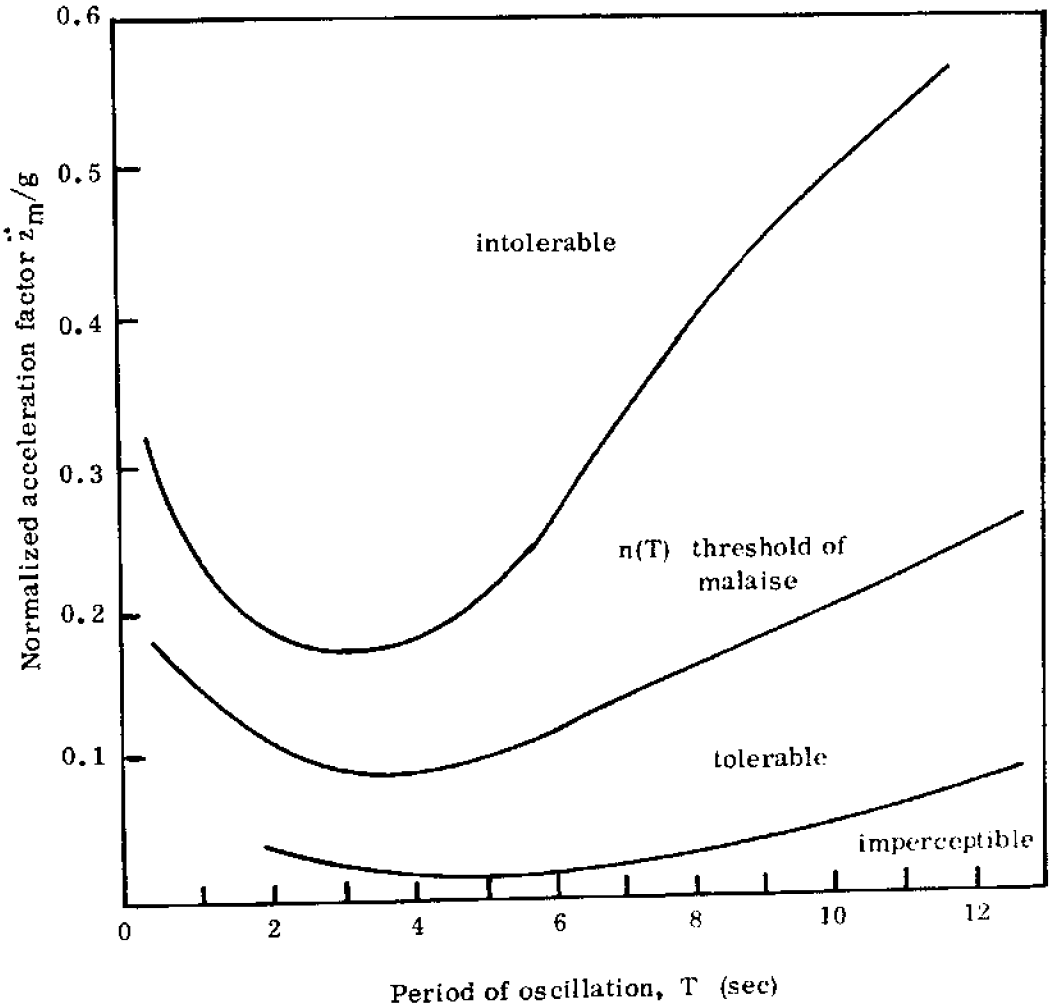

Fig. 61 Physiological response to periodic vertical oscillations (Source: M. St. Denis, Technical Report No. 1)

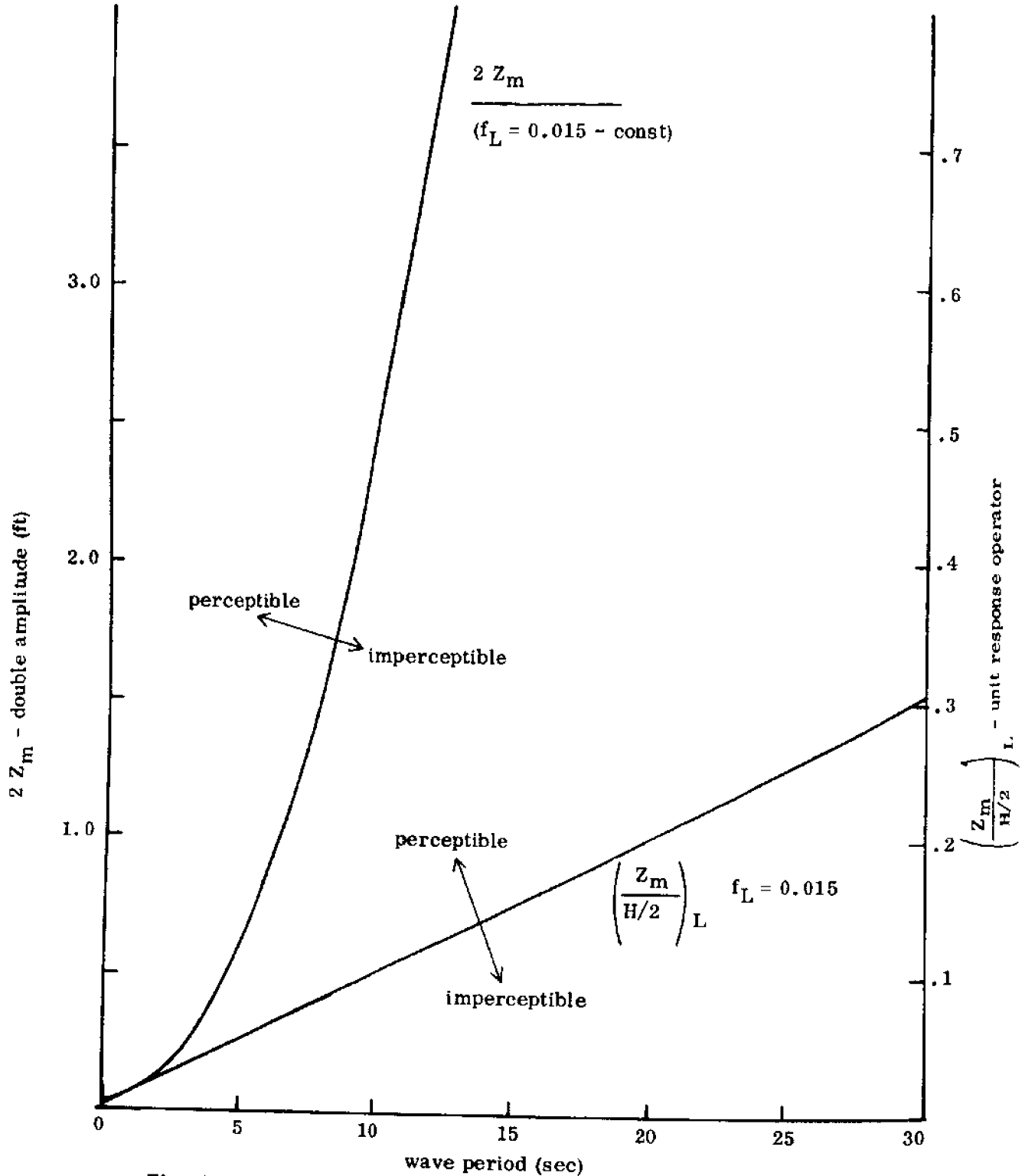

Fig. 62 Envelopes of double amplitudes and unit response operators for motion perceptibility.

G. Response Operators for the 1:20 Scale Model

The response operators of the 1:20 scale model in all six degrees of freedom were obtained by inputting the correct model dimensions into computer program RING. The pertinent model dimensions for a single column are given in Fig. 63. The arrangement plan of the whole ring is shown in Fig. 64.

A correction was made, however, for the effect of liquid ballast. Because of the free surface of the ballast water (with the lower cylinder only partially filled), the weight of the ballast cannot be treated as a fixed weight. The free surface makes the weight of the ballast water appear to be centered at the metacenter of the ballast water (see Fig. 65).

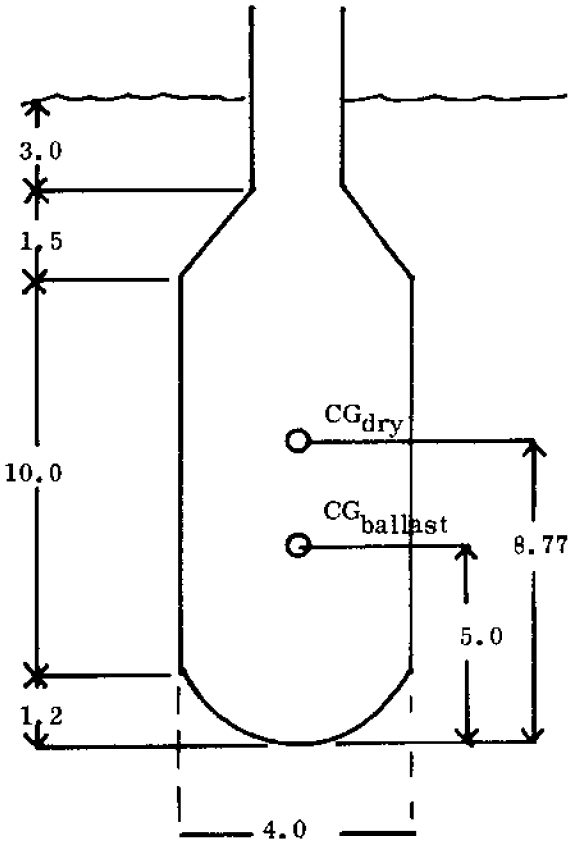

Fig. 63 Dimension sketch and location of CG

Denoting:

s = center of gravity of ballast in upright position
s = center of gravity of ballast in heeled position
m = metacenter of ballast liquid
b_v = half-breadth of cross section

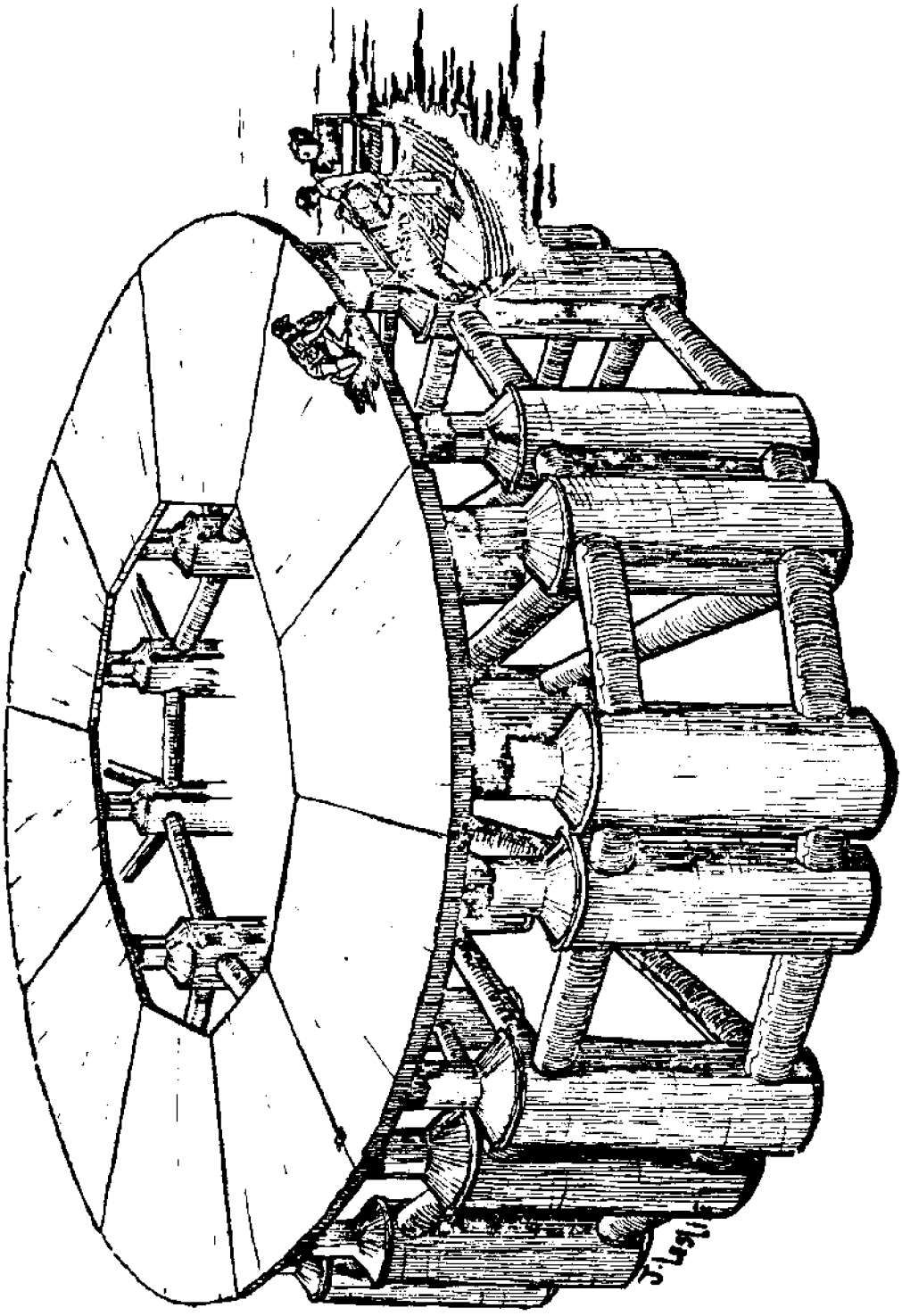

Fig. 64 Arrangement of columns for core-ring (1:20 model).

we can write

$$\overline{sm} = \frac{i_v}{v} = h$$

where

$$i_v = 2/3 \int_0 b_v^3 \, d\ell$$

v = volume of ballast water

Referring to Fig. 65, h is the vertical distance between the effective CG of the ballast liquid (m) and the CG of the ballast if it were fixed (s).

In our case we have

$$b_v = \sqrt{R^2 - \ell^2}$$

where R = inner radius of lower cylinder

hence

$$i_v = 2/3 \int_0^R (R^2 - \ell^2)^{3/2} \, d\ell$$

with R = 2.0 ft and $i_v = 12.57$ ft^4

Weight of ballast = 6500 lbs (given)

hence v = 6500.0/64.0 = 102 ft^3

and

$$h = \frac{12.57}{102} = 0.123 \text{ ft}$$

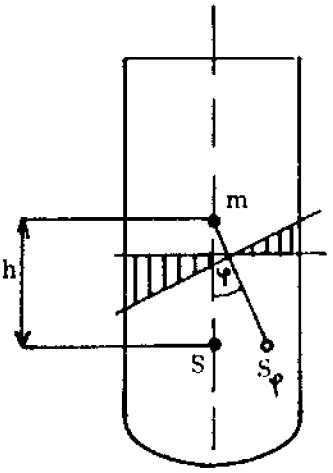

Fig. 65 Effect of free surface of ballast water.

Taking this correction into account, the effective center of gravity of a column in ballasted condition is $\overline{CG}$ = 10.1 ft below DWL.

Results - Single Column

Figure 66 depicts the unit amplitude response in heave for a single column. The results are also directly applicable for the response of a single module for wave periods larger than 5 seconds. In this diagram the phase lag

between heaving motion and wave elevation at the center of the buoy is shown as a dotted line. Positive phave lag indicates that the buoy is at its highest point at a time interval $\Delta t = \epsilon / \sigma$ after the wave crest has passed the buoy. Figure 67 depicts the variation of amplitude of the various wave force components, i.e., wave displacement force, wave inertia force, and wave drag force, with time. The total wave force amplitude and phase lag between wave force and wave crest is also given. The results for these two diagrams were obtained from computer program HEAV3.

Results - Core-Ring

Figure 68 gives the unit amplitude response in surge of the complete core-ring. The response operators were calculated for a water depth of d = 40 ft, as given at the test site. To illustrate the influence of limiting water depth, the responses were calculated also for 130 ft water depth. Figure 69 depicts the unit amplitude response in heave for water depths of 40 and 130 ft, respectively. The values near resonance take damping into account and were obtained from computer program HEAV3. The remainder of the curves were calculated by program RING.

The unit amplitude response in pitch is shown in Fig. 70. The scale on the left side is given in radians per foot of wave amplitude, the scale on the right margin is in degrees per foot, while the scale to the left of the latter is in inches of heaving motion at the outer ring of the columns per foot of wave amplitude. This scale has been included for convenience of visual observation at the test site. A dimensionless form of the pitch response operator is shown in Fig. 71. Here the unit amplitude in pitch as normalized by the wave slope [i.e. $\psi_o/(k\ H/2)$] has been plotted. This form is useful in comparing with other scale models. Figures 68-71 were computed by program RING.

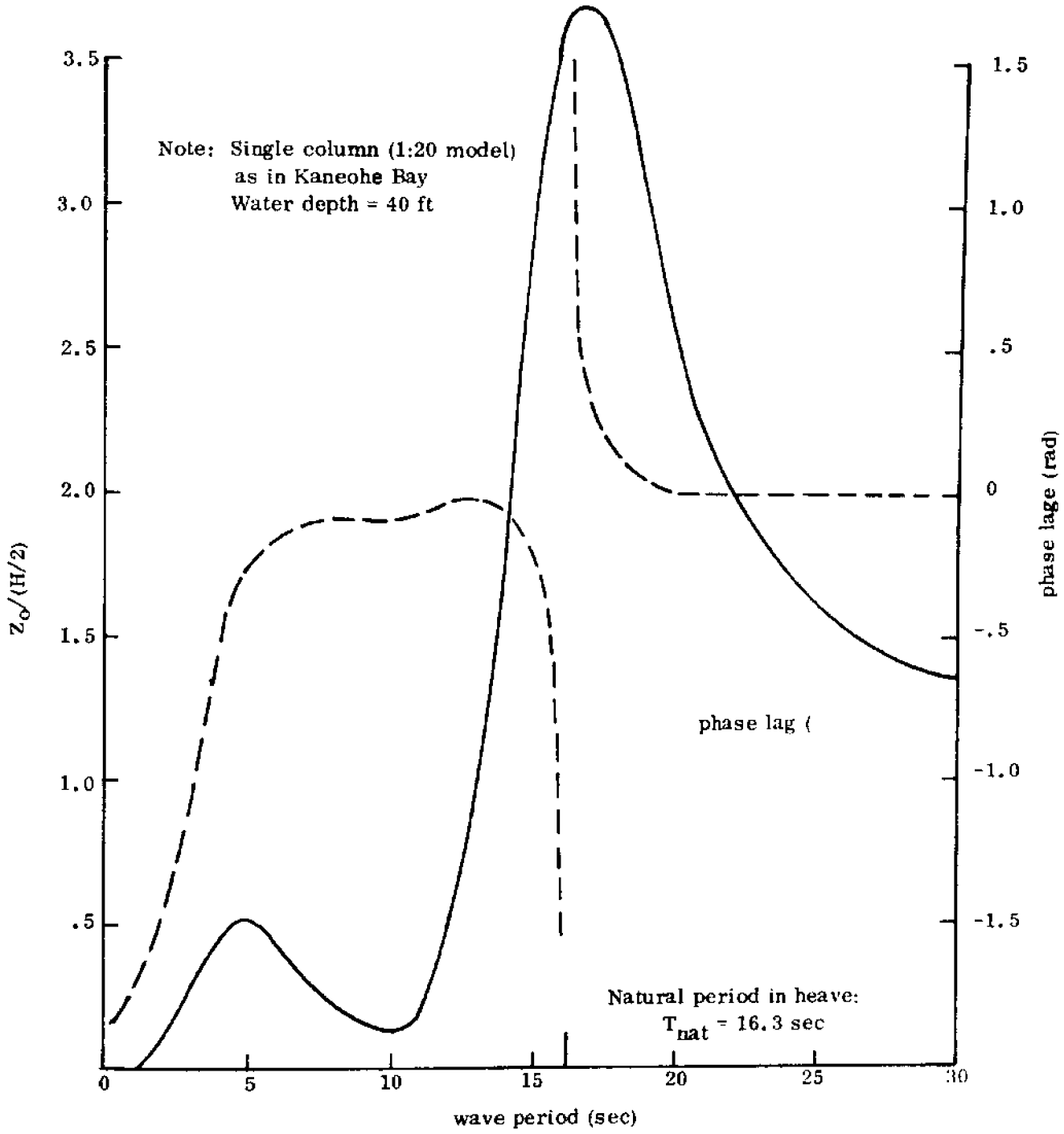

Fig. 66 Unit amplitude response in heave.

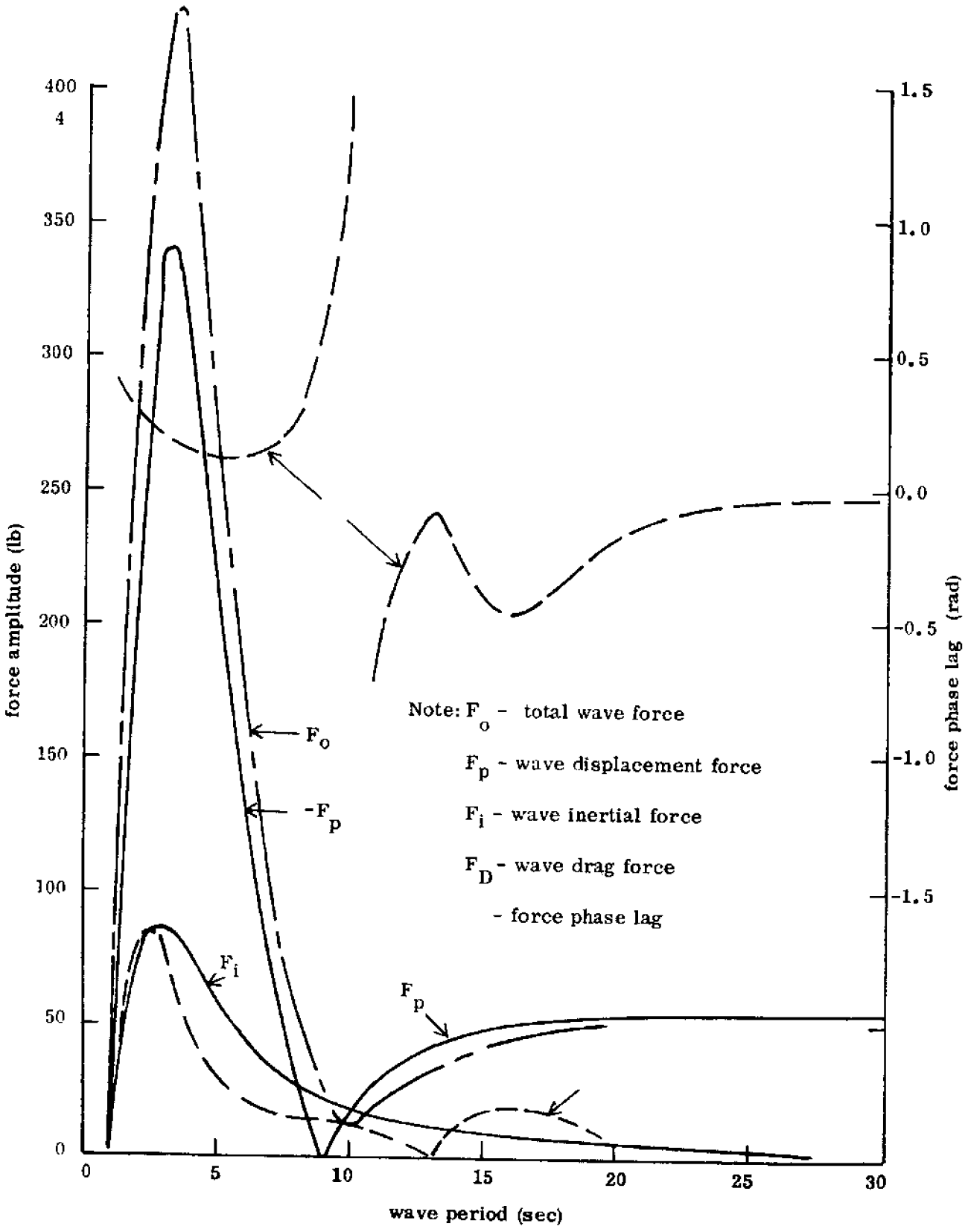

Fig. 67 Wave forces in heave (single column). Dimensions as in Kaneohe Bay (1:20 model)

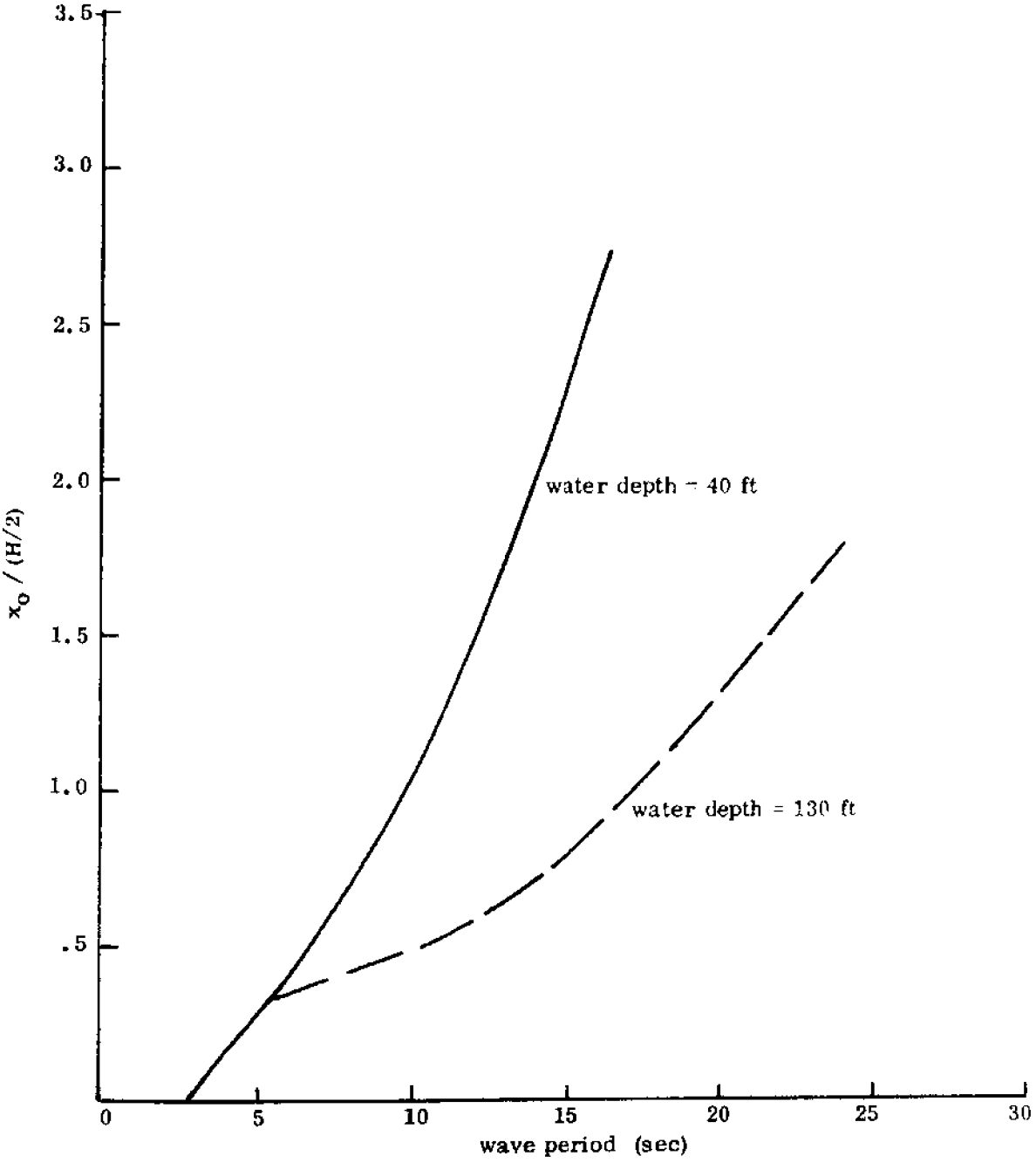

Fig. 68 Unit amplitude response in surge. Core-ring (1:20 model)

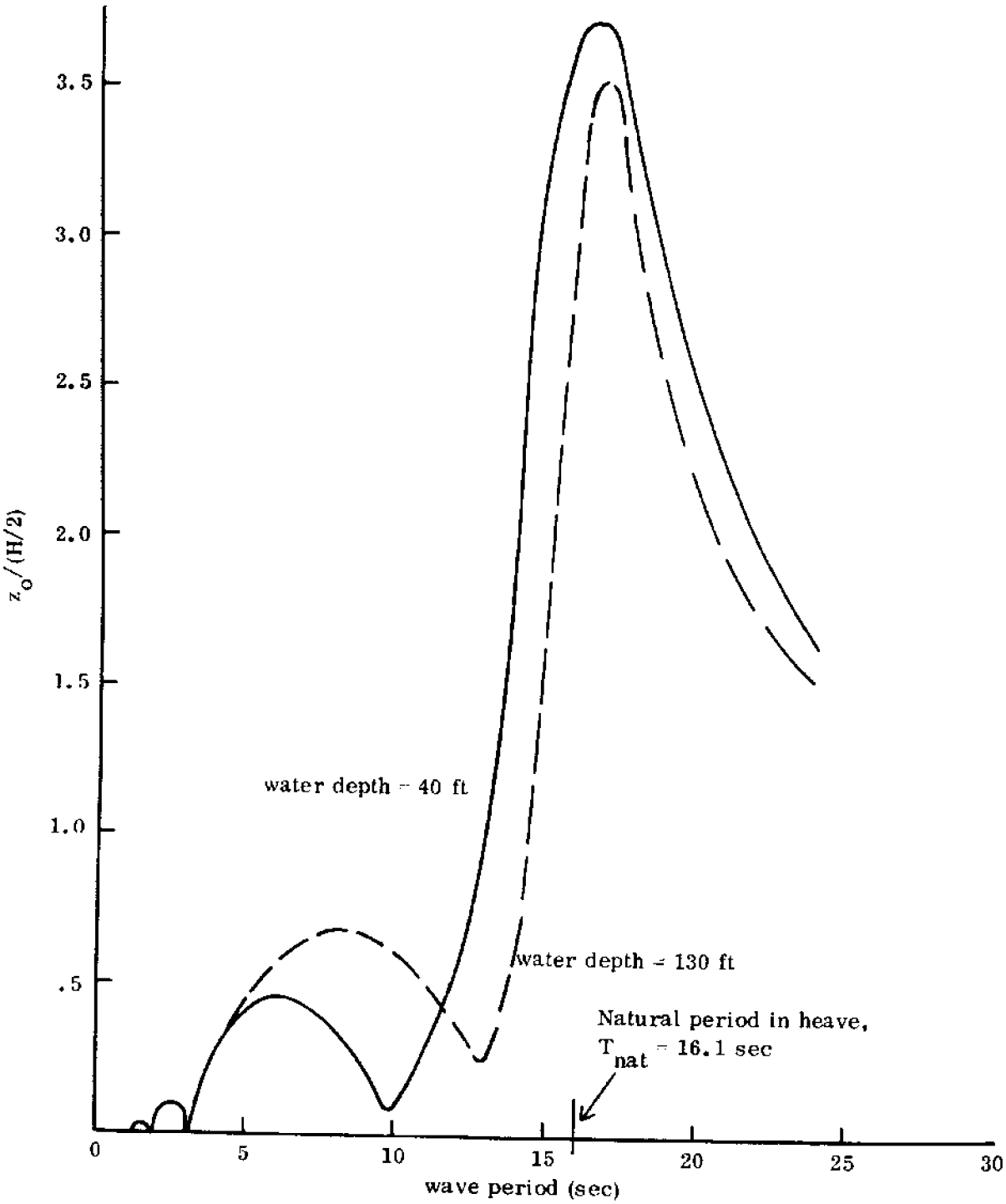

Fig. 69 Unit amplitude response in heave. Core-ring (1:20 model)

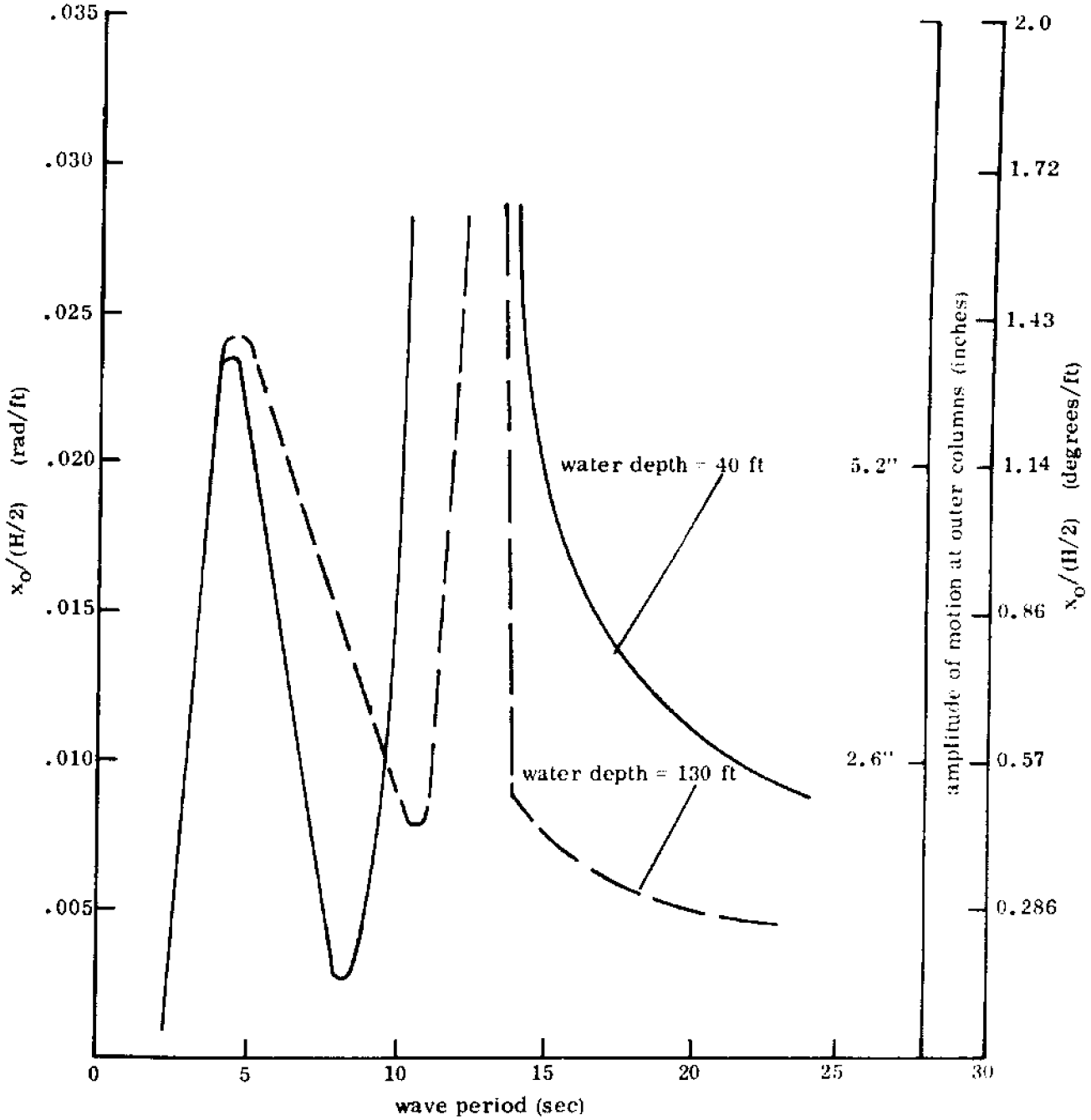

Fig. 70 Unit amplitude response in pitch. Core-ring (1:20 model)

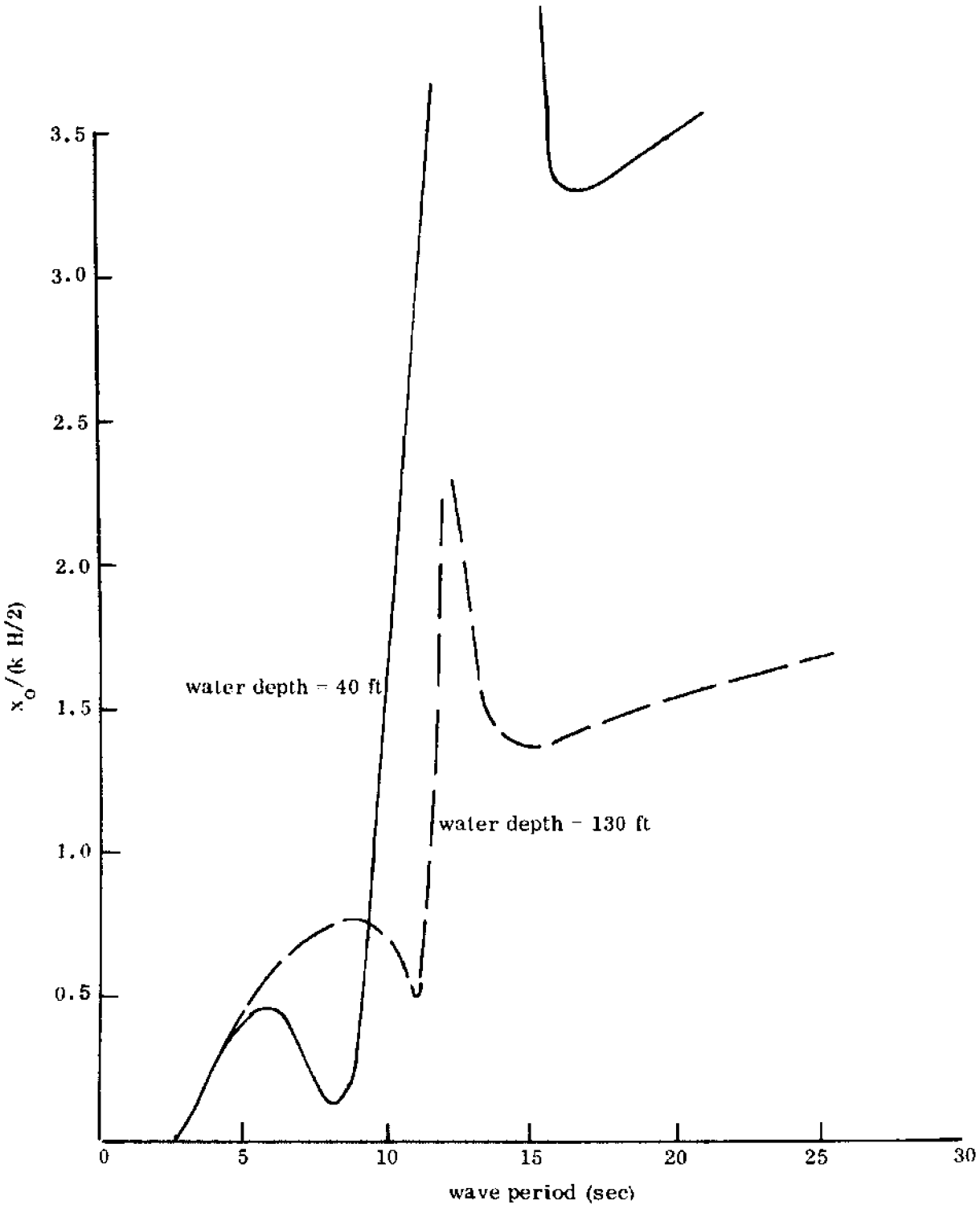

Fig. 71 Unit amplitude in pitch, normalized by wave slope. Core-ring (1:20 model).

VII. FINDINGS AND CONCLUSIONS

Figures 49 and 50 give the response operators for the heaving and pitching motion of the platform. The diagrams show a considerable reduction in motion as the diameter of the upper cylinder (the surface-piercing one) is increased from the original d = 30 ft. The 48 ft diameter upper cylinder configuration appears to be the optimum configuration, yielding minimum response in both heave and pitch. The 54 ft diameter configuration would yield even less response up to a wave period of 25 seconds. For longer waves, resonance conditions come into play. A precise environmental prediction of wave height at these periods would be of paramount importance if this configuration should be considered. Because of the lack of such data, the 48 ft diameter upper cylinder configuration can be assumed optimum.

Applying the results from Fig. 62, in particular the envelope curve for response operators, it is seen that the motion of this platform will be imperceptible at any wave period. The motion derived from response operators would correspond to regular ocean swells. Comparing the envelope curve of imperceptible significant double amplitudes (Fig. 62) with the double amplitudes as derived in Section VI. E on platform motion in irregular seas, we see that these average motions are also always less than the limit for perceptibility.

This means that somewhat longer motion could be allowed without creating the risk of occasional widespread seasickness among the city's inhabitants.

Reduction of platform draft is assumed to result in reduced construction cost at the expense of increased motion in a seaway. The objective then becomes to design the cheapest platform that will have responses that are imperceptible to the inhabitants. From Fig. 20, a draft of d = 180 to 220 ft might suffice in this respect. The shallower draft might be beneficial for the usage of the volume inside the larger cylinders.

VIII. RECOMMENDATIONS FOR FUTURE RESEARCH

As became apparent in the preceding section, the optimum configuration with respect to minimum response over the whole range of wave periods could be established only approximately, pending better wave data. Also the envelope curves for imperceptible motions, i.e., the human response to accelerations, must be more clearly established.

Having good environmental data and good human response data, we would indeed be in a position to design a platform of minimum cost to fulfill the requirement of imperceptible motion in any expected seaway.

Design Alternatives

The shallow draft configuration (180 ft draft) of the platform yields lower cylinders that virtually touch each other. This configuration therefore comes close to a so-called semi-submersible platform, i.e., a platform with a long cylindrical underbody with columns reaching through the surface to carry the upper platform. Such structures are being used in large oil-drilling platforms designed for work in extremely rough ocean environments. The platform for the MOHOLE project was another prominent example. It might turn out that the resistance to currents of such a hull design would be considerably less than that of a column-stabilized platform (present configuration).

If we were to consider even larger floating cities, a barge-type of platform might become more practical. It would therefore be interesting to determine the thresholds at which these transitions would be most likely to occur. Even for smaller platforms, such as the present configuration, three, four or multiple submerged hulls connected in parallel to each other might be the most useful as far as utilization of the submerged space is concerned; certainly the drag resistance to currents of such a hull design could be an order of magnitude less than the present configuration and an enclosed harbor for cargo barges could be included as well.

Summary

The following items should be covered in future research. They are listed in order of urgency and pertinence to the present project.

1. Maximum wave heights of long period ocean swells at the platform's location.
2. Frequency of occurrence and directionality of such swells.
3. Design storms, i.e., wave height and periods, wind velocities, currents.
4. Envelope of human response to motion. Limits for imperceptible vertical, horizontal and rotational accelerations as a function of period, in particular at periods between 20 and 30 seconds.
5. Optimization of present platform with respect to results from points 1-4.
6. Analysis of alternative configurations: semi-submersible type, multi-hulled low waterplane platform, barge type.
7. Dynamic positioning: optimization of platform with respect to horsepower requirements.
8. Articulated modules.
9. Possibilities for construction of the various alternatives of hull forms.